EARTHQUAKES AND SEISMOGRAPHIC MONITORING IN MONTANA

Michael C. Stickney

Montana Bureau of Mines and Geology, Butte, Montana

INTRODUCTION

Since the 1860s when settlers began writing about their experiences, numerous accounts of earthquakes document Montana as a seismically active region. Most—but not all—earthquakes occur in western Montana. All of Montana's largest earthquakes occurred prior to 1960, before local seismic monitoring networks existed. Except for earthquakes in 1897 in southwest Montana and in 1909 in northeast Montana, all major historical earthquakes have rudimentary instrumental epicenters determined principally from data recorded by seismograph stations at regional and teleseismic distances. Thus, there is limited information on the instrumentally determined hypocenters of Montana's most important earthquakes. Focal depths were not routinely computed before the mid-1960s. Seismic monitoring gradually began to improve in the 1960s, and by the 1980s, continuous monitoring from an evolving permanent seismograph network in western Montana revealed new details about seismicity in the Northern Rocky Mountain region.

The Intermountain Seismic Belt (ISB; Smith and Arabasz, 1991, and references therein) is a first-order feature of western U.S. seismicity. The ISB is a 1,500-km-long (932-mi-long) belt of shallow seismicity that extends from northwest Montana to northwest Arizona, and includes a branch—the Centennial Tectonic Belt (Stickney and Bartholomew, 1987)—extending westward from Yellowstone National Park through southwest Montana into central Idaho (fig. 1). In western Montana, the northern ISB is a ~100-km-wide (62-mi-wide) zone of shallow seismicity traversing western Montana from Yellowstone National Park to the northwest corner of the State. The W-trending Centennial Tectonic Belt parallels the northern flank of the Snake River Plain. Widely scattered seismicity occurs outside the ISB, including the 1909 northeast Montana earthquake. With the exception of the 1909 earthquake, all historical earthquakes of magnitude 5 or larger have occurred within the ISB. Most Montana earthquakes are not spatially associated with recognized faults, and thus earthquake catalogs are a critical component for understanding and characterizing Montana's seismic hazards (Wong and others, 2005). Only the 1959 M7.3 Hebgen Lake earthquake generated surface fault rupture, but ~80 late Quaternary faults in western Montana (Stickney and others, 2000) attest to numerous major prehistoric earthquakes accompanied by surface rupture.

This chapter reviews the most significant historical earthquakes in Montana and attempts to characterize them in the context of our current understanding of active tectonics. Several early earthquakes with magnitudes larger than 5.5 have revised locations and magnitudes based on shaking intensity reports, and several other earthquakes with reported magnitudes larger than 5.5 now have estimated magnitudes less than 5.5 based on felt areas. With the advent of portable seismographs in the early 1970s, multiple temporary seismograph network deployments revealed basic information about seismicity along the ISB and in Yellowstone National Park. The temporary nature and spatial variability of these early network deployments precluded systematic cataloging of small-magnitude seismicity until the Montana Bureau of Mines and Geology (MBMG) established a permanent regional seismic monitoring network in the early 1980s. The Montana Regional Seismic Network (MRSN) has expanded during the past four decades and now provides basic monitoring coverage of most of western Montana and adjacent areas. The MBMG uses MRSN data to determine hypocenters and magnitudes for thousands of earthquakes annually and has recorded the aftershock sequences of two magnitude 5.5+ earthquakes that occurred within the network. The final sections of this chapter review advances in our understanding of Montana seismicity and tectonics gleaned from MRSN data.

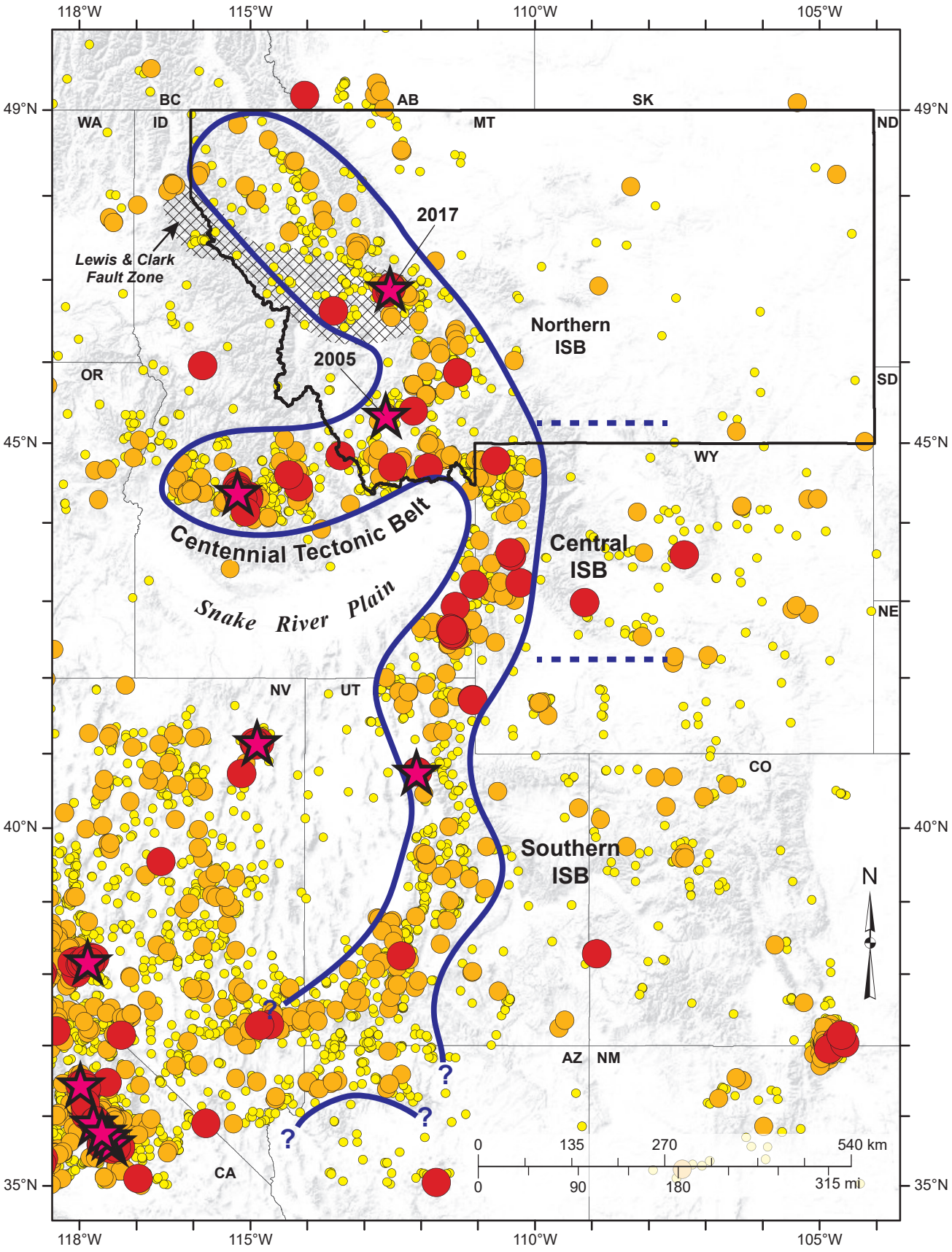

Figure 1. Intermountain west region earthquakes with magnitudes of 2.5 or larger from 2000 through 2020 illuminate the Intermountain Seismic Belt (ISB). The northern, central, and southern ISB sections shown as in Smith and Arabasz (1991). Yellow, orange, and red circles show earthquake epicenters with magnitudes of 2.5–3.4, 3.5–4.4, and 4.5–5.4, respectively. Magenta stars show epicenters with magnitudes of 5.5–7.1. The M_w 5.6 Dillon earthquake on July 26, 2005 and the M_w 5.8 Lincoln earthquake on July 6, 2017 are labeled with their respective years. Earthquake data are from the Montana Regional Seismic Network and the U.S. Geological Survey Composite Catalog.

HISTORICAL MONTANA EARTHQUAKES

In July 1805, the Lewis and Clark Expedition reported hearing loud booming sounds coming from northwest of their camp near the Great Falls of the Missouri River (Coues, 1893). The noises occurred at different times of day, often during clear weather. Some authors have interpreted these noises as evidence of earthquake activity (Anderson and Martinson, 1936; Ulrich, 1936). However, Qamar and Stickney (1983, appendix B) discussed difficulties with attributing these noises to earthquakes.

Accounts and descriptions of Montana's earthquake activity began 150 years ago, soon after permanent settlement with occupants who provided written records. The first unequivocal report of an earthquake came from Helena in 1869. Tuttle (1909) reported his experience on the morning of May 22: "there came a rumbling sound as of a heavy wagon dragged rapidly across a bridge. With it came a shaking of the house which threw down some pieces of furniture and some dishes in the pantry. Soon after, I went out on Main Street and discovered that the same disturbance had been noted everywhere. We were therefore sure the town had been visited by an earthquake." This account marks the beginning of Montana's documented earthquake history.

Numerous publications document historical earthquakes in Montana. The Seismological Society of America published accounts of global earthquakes, including those felt in Montana, as *Seismological Notes* from 1911 through 1969. After 1975, Seismological Notes reported only magnitude 6 or larger earthquakes, or those causing substantial damage, or those judged to be of special interest. *United States Earthquakes* was published annually by the U.S. Department of Commerce, Coast and Geodetic Survey from 1928 to 1968, the National Oceanic and Atmospheric Administration (NOAA) Ocean Survey in 1969, the NOAA Environmental Data Service from 1970 to 1972, and jointly by the NOAA Environmental Data and Information Service and the U.S. Geological Survey henceforth. Several publications compiled prominent earthquakes from these sources, most notably Coffman and others (1982), superseded by Stover and Coffman (1993), which compiled information on Montana's principal earthquakes—those with Modified Mercalli Intensities of VI or larger or magnitudes of 4.5 or larger—from 1872 through 1985. Qamar and Stickney (1983) pointed out that prior to 1963, the NOAA earthquake catalog contained no instrumental earthquake locations in Montana for seismic events less than magnitude 4.0. Qamar and Stickney (1983) and Wong and others (2005) also discussed important historical earthquakes in Montana. Smith and Arabasz (1991) presented a comprehensive review of the seismicity of the Intermountain Seismic Belt through 1985, which includes western Montana.

Below is a discussion and listing (table 1) of earthquakes with magnitudes of 5.5 or larger in western Montana (W of longitude 110°W) or magnitudes of 5.0 or larger in eastern Montana. Table 1 lists the type and source of reported magnitudes for these historical earthquakes. Stover and Coffman (1993) listed earthquakes in 1929, 1945, and 1952 with magnitudes of 5.6, 5.5, and 5.5, respectively, that are not included here because reanalysis of available data suggest they have magnitudes less than 5.5, as discussed at the end of the following section.

Major Historical Earthquakes 1897–1964

November 4, 1897, Southwest Montana

An earthquake was widely felt throughout western Montana, eastern Idaho, and northern Utah at about 2:30 a.m. on November 4, 1897. Dillon suffered the most severe effects; the courthouse walls cracked and plaster fell from the ceiling. The early date of this earthquake precedes seismographic recording in North America, and thus we only have felt reports from which to estimate the epicenter and magnitude. Contemporary newspaper accounts provide descriptions of the shaking severity that allowed Modified Mercalli Intensity (MMI; appendix A; Wood and Neumann, 1931) assignments at 16 locations. Bakun (written commun., 2005) used these MMI assignments according to the method of Bakun and Wentworth (1997, 1999) to estimate an epicenter (45.3°N, 112.3°W) about 30 km (19 mi) east of Dillon and an intensity magnitude (M_I) of 5.6 ± 0.35 for the 1897 earthquake (fig. 2). Because of the small number of MMI observations and their poor distribution with respect to the epicenter, there is a large uncertainty [at least 50 km (31 mi)] in this epicenter.

May 16, 1909, Northeast Montana

The May 16, 1909 earthquake is the largest historical earthquake in the northern Great Plains of the United States and Canada. Stover and Coffman (1993) did not list this earthquake because its initial epicenter

Table 1. Western Montana earthquakes of magnitude 5.5 or larger and eastern Montana earthquakes of magnitude 5.0 or larger, 1897 through 2020.

Origin						Hypocenter				Magnitude											
Date			Time							USGS											
yr	mo	d	h	min	s	Latitude (deg)	Longitude (deg)	Depth (km)	Location Reference	Mb	MS	Mfa	Other (M)	Moment (**M**)	Local (ML)	Intensity M (MI)	Preferred	Magnitude Reference	Intensity Maximum (MMI)	Felt Area ($1,000^2$ km)	Comment
1897	11	4	9	29		45.26	-112.27		This paper			6.4				5.6±0.35	5.6	This paper	VI	500	Location and magnitude from method of Bakun and Wentworth, 1997, 1999
1909	5	16	4	15		48.81	-105.38		Bakun and others (2011)							5.35	5.4	Bakun and others (2011)	VI	1,500	
1925	6	28	1	21	5	46.08	-111.51		This paper		6.75			6.6		6.55	6.6	Stover and Coffmann (1993)	VII	1,000	Location and magnitude from method of Bakun and Wentworth, 1997, 1999
1925	6	28	2	5	27	46.08	-111.51		AME								6.4	This paper	VII	518	Felt area from Pardee (1926)
1925	6	28	3	35		46.08	-111.51		AME								5.5	This paper		129.5	Felt area from Pardee (1926)
1925	6	28	4	20		46.08	-111.51		AME								5.5	This paper	VI	129.5	Felt area from Pardee (1926)
1925	7	10	14	42		46.08	-111.51		AME								5.5	This paper	V	129.5	Felt area from Pardee (1926)
1935	10	12	7	50	39	46.6	-112.0	5	Stover and Coffmann (1993)			5.9					5.8	Stover and Coffmann (1993)	VII	181	Modified Qamar and Stickney (1983) fig. 5 relation used to calculate magnitude
1935	10	19	4	48	2	46.6	-112.0		Stover and Coffmann (1993)		6.25						6.3	Stover and Coffmann (1993)	VIII	570	
1935	10	31	18	37	47	46.6	-112.0		Stover and Coffmann (1993)		6.0						6.0	Stover and Coffmann (1993)	VIII	315	
1947	11	23	9	46	3.3	44.82	-111.713	5	Stover and Coffmann (1993)		6.25			6.12			6.1	Doser, 1989	VIII	340	
1959	8	18	6	37	14	44.7925	-111.2001	12	Reference A	7.0	7.5		7.5	7.3	7.7		7.3	Doser & Smith (1989)	X	1,175	Doser and Smith (1989) calculate separate locations and magnitudes for 2 subevents
1959	8	18	7	56	16	44.7669	-110.8901		Reference A				6.5				6.5	Doser & Smith (1989)			
1959	8	18	8	41	47	44.8010	-111.0734		Reference A				6.0				6.0	Doser & Smith (1989)			
1959	8	18	11	3		44.94	-111.80		Doser & Smith (1989)				5.6				5.6	Doser & Smith (1989)			Magnitude type not specified
1959	8	18	15	26	6	44.8466	-110.8308		Reference A	6.5	6.3		6.5	6.3			6.3	Doser & Smith (1989)			
1959	8	19	4	4	0	44.76	-111.60	8	Doser & Smith (1989)	5.8	5.9		6.0				6.0	Doser & Smith (1989)			
1964	10	21	7	38	27	44.7732	-111.7434	9	Reference A	5.8	5.0			5.6			5.6	Doser & Smith (1989)	V	65	
2005	7	26	4	8	36	45.345	-112.615	10.5	MBMG	5.7	5.2			5.6			5.6	USGS ComCat	VI		
2017	7	6	6	30	16.89	46.8908	-112.5383	13.6	MBMG	5.8	5.6			5.8	6.2		5.8	USGS ComCat	VIII		

Note. Date, time (in Coordinated Universal Time), location, magnitude, maximum Modified Mercalli Intensity, and felt area reported when available. The number of decimal places reported for the epicenter latitude and longitude corresponds to that reported by the source listed in the Location Reference column. Various magnitudes reported from the USGS and other sources include: M_b, body wave; M_S, surface wave; M_{fa}, felt area; M, unspecified magnitudes from other sources; **M,** moment magnitude; M_L, local magnitude; M_I, intensity magnitude (Bakun and Wentworth,1997, 1999); Preferred, the preferred magnitude, **M** if available, with the source listed in the Magnitude Reference column. Additional information about the various magnitude types is available at: https://www.usgs.gov/natural-hazards/earthquake-hazards/science/magnitude-types?qt-science_center_objects=0#qt-science_center_objects. Note that two Hebgen Lake earthquakes (1959/8/18 at 07:56 and 15:26) at the eastern end of the aftershock zone lie slightly outside the Montana state border. AME, assumed mainshock epicenter. Reference A: https://www.sciencebase.gov/catalog/item/5af9a09fe4b0da30c1b82c9b.

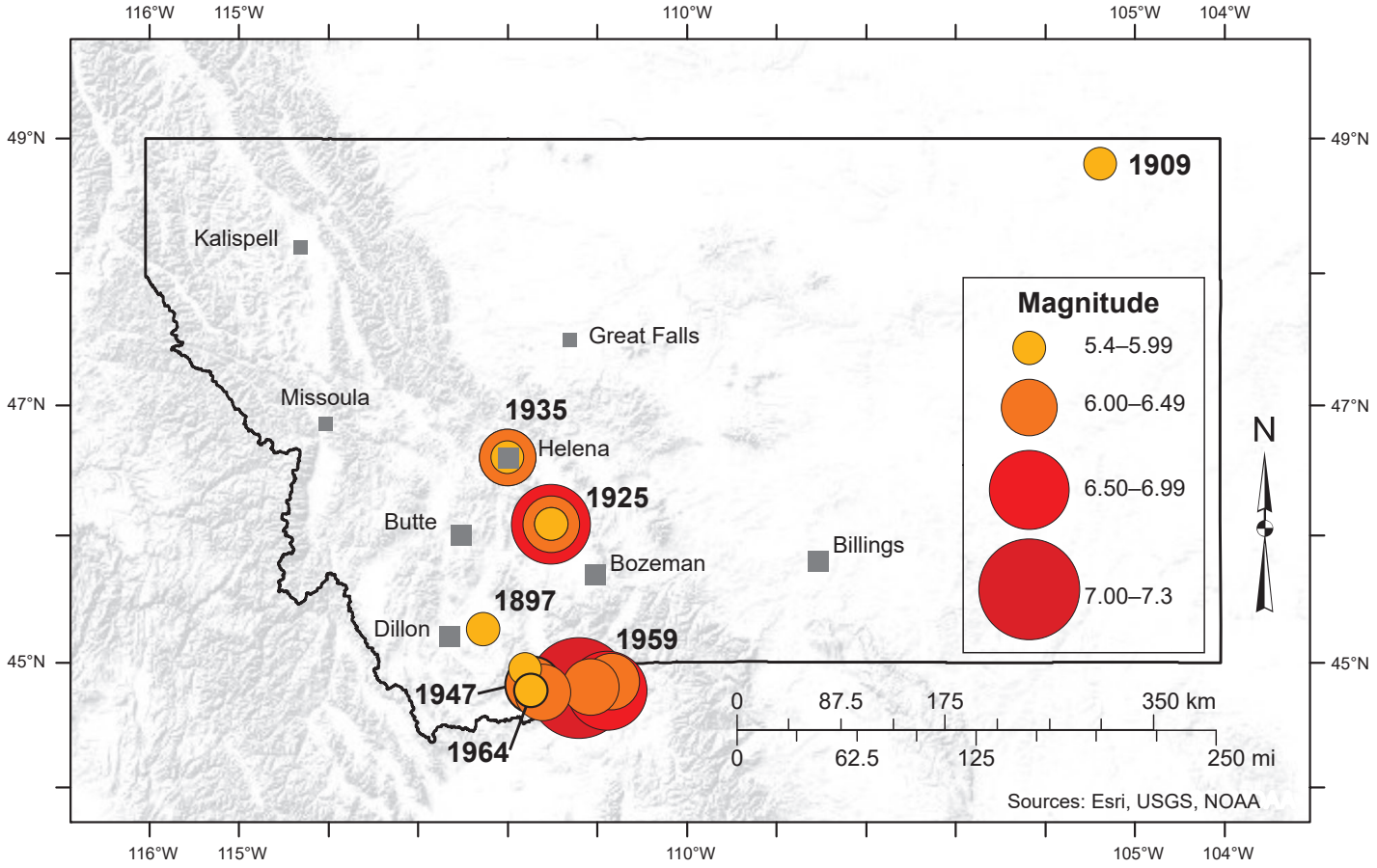

Figure 2. Earthquakes before 1965 with magnitudes of 5.5 or larger in western Montana and eastern Montana earthquakes larger than magnitude 5.0. Epicenters labeled with year of occurrence.

was estimated to lie in southern Saskatchewan. The 1909 earthquake shook eastern Montana, North Dakota, and parts of South Dakota, Wyoming, Minnesota, Alberta, Saskatchewan, and Manitoba. People felt the shaking over a region of more than 1,500,000 km^2 (579,153 mi^2), but the maximum MMI was only VI. With seismograph recording technology in its infancy, insufficient instrumental data were available with which to determine an epicenter. The initial estimate of an epicenter, based on MMI assignments, placed it in southern Saskatchewan (Heck, 1938; Heck and Eppley, 1958). Nuttli (1976) prepared an isoseismal map that showed the area of maximum shaking intensity in southern Saskatchewan and estimated an epicenter at 50°N, 104°W. Horner and Hasegawa (1978) placed the epicenter one degree (111.2 km or 69.1 mi) to the south at the common border of Montana, North Dakota, and Saskatchewan, based on the accounts published in the *Manitoba Free Press* of May 17, 1909.

To determine a more accurate epicenter for the 1909 earthquake, Bakun and others (2010) searched historical newspaper reports for descriptions of the shaking and used them to assign MMI at as many locations as possible. They combined these new MMI assignments with Nuttli's (1976) MMI assignments for a total of 90 observations. Bakun and others (2011) used these MMI assignments together with the intensity analysis method of Bakun and Wentworth (1997, 1999) to determine an epicenter (48.81°N, 105.38°W; fig. 2) near the town of Scobey, MT, about 100 km (62 mi) WSW of Horner and Hasegawa's (1978) estimated epicenter. One puzzling aspect of this analysis was the complete lack of any newspaper reports of the earthquake at the five closest towns, even though the earthquake shaking was felt for hundreds of kilometers in all directions and would have undoubtedly been perceptible at these locations close to the epicenter. Bakun and others (2011) speculated that the local newspapers chose not to report negative news that might discourage the planned construction of a new railroad spur line into the epicentral area and the commerce and settlers that would follow.

Seismologists have used several methods to estimate the magnitude of the 1909 earthquake. Agarwal (1962) reported that Dominion Observatory personnel in Ottawa determined a magnitude of 6.5

using a low-magnification, horizontal pendulum seismograph. A more robust analysis of these data by Horner and others (1973) determined that the limited instrumental data from Dominion Observatory were consistent with a magnitude of about 5½, which better agrees with a maximum reported shaking intensity of VI. Using a total felt area of 1,300,000 km^2 (501,933 mi^2) and felt area versus magnitude relation derived for the northern Rocky Mountains, Qamar and Stickney (1983) estimated a magnitude "as large as 6½." Using a felt area of 1,500,000 km^2 (579,153 mi^2) and a felt area versus magnitude relation developed for the central United States, Nuttli (1976) estimated a body-wave magnitude of 5.3. This magnitude agrees quite well with the surface-wave magnitude of 5.3 determined from seismograms recorded at two European observatories (Bakun and others, 2011). As part of their reanalysis of MMI data, Bakun and others (2011) determined an M_I of 5.3–5.4. The preponderance of data indicate that the 1909 earthquake had a magnitude of 5.3. It was felt over such a large region because of the intrinsically lower attenuation that characterizes the central and eastern U.S. as compared to the tectonically active western U.S., which includes western Montana.

June 28, 1925, Clarkston Valley, Montana

A strong earthquake in SW Montana at 6:21 pm on June 27, 1925 (June 28 at 01:21 Coordinated Universal Time; June 28 is used in this report) caused considerable damage to brick structures within a 600 mi^2 (1,554 km^2) area surrounding the epicenter. Strong shaking caused rock falls from railroad cuts and steep hillslopes and opened cracks in unconsolidated ground. A church in Three Forks, the school in Manhattan, and the jail at White Sulphur Springs—all masonry structures—were badly damaged. Residents felt shaking over an area of 310,000 mi^2 (802,896 km^2), stretching from Calgary, Alberta to Casper, WY, and from Spokane, WA to the Montana–North Dakota border. Maximum shaking intensity was 9+ on the 10-point (and now rarely used) Rossi–Forell intensity scale (fig. 3A). Stover and Coffman (1993) estimated intensities from this earthquake using the Modified Mercalli intensity scale and created the isoseismal map reproduced in figure 3B.

The epicenter of the June 28, 1925 earthquake has been a matter of some discussion in seismological literature. Pardee (1926) visited the epicentral area for 30 days in the summer of 1925 to interview residents and investigate the earthquake's effects. Based on the distribution of shaking intensities, he concluded that the earthquake occurred in the northern Clarkston Valley (46.08°N, 111.33°W) at unspecified depth along the Clarkston Fault (fig. 4). It is a W-dipping, valley-bounding fault that juxtaposes hanging-wall, Tertiary-aged basin deposits dipping up to 20° eastward against thrust and folded Paleozoic and Mesozoic rocks in the footwall of the Laramide-aged Lombard thrust fault. Geologists have failed to find evidence of Late Quaternary surface displacement along the Clarkston Fault (Stickney and others, 2000; Vuke and Stickney, 2013; USGS Quaternary Fault and Fold Database); however, Pardee (1926, plate 12) documented a linear zone of "shattered earth" near the surface trace of the Clarkston Fault. Vuke and Stickney (2013) tentatively identified the location of this zone of "shattered earth" but did not ascribe it to tectonic offset.

In an early attempt to locate the epicenter using instrumental data, Byerly (1926) used P-wave arrival times from seismograph stations at Victoria, Berkeley, and Pasadena (epicentral distances ranging from 935 to 1,479 km (581 to 919 mi) to calculate an epicenter at 46.40°N, 111.24°W (±0.8° latitude, ±0.10° longitude; fig. 4). This location places the epicenter over 30 km (19 mi) NNE of the Clarkston Valley, well north of the area of maximum shaking intensity. Subsequently, Dewey and others (1973) used Byerly's (1926) P-wave arrival times together with Herrin and other's (1968) P-wave travel times to compute an epicenter at 46.2°N, 111.4°W, approximately 15 km (9 mi) north of the Clarkston Valley (fig. 4). In addition, Dewey and others (1973) used P-wave first motions and S-wave polarization angles recorded at teleseismic distances to determine a strike-slip focal mechanism with a SSE-oriented T-axis. Coffman and others (1982) reported an epicenter located at 46.0°N, 111.2°W, about 12 km (7 mi) east of the Clarkston Valley. Qamar and Hawley (1979) used P_g-P_n time differences recorded by seismographs at Spokane [Δ = 490 km (302 mi)] and Saskatoon [Δ = 720 km (447 mi)] to determine a hyperbolic distribution of points along which the epicenter must lie. This locus of possible epicenters (fig. 4) touches the southern end of the Clarkston Valley, and the uncertainty zone that allows for ±0.5 s seismogram timing errors encloses most of the Clarkston Valley, supporting Pardee's (1926) original estimate of the epicenter within the Clarkston Valley. Qamar and Hawley's (1979) curve also closely approaches the epicenter of Dewey and others (1973).

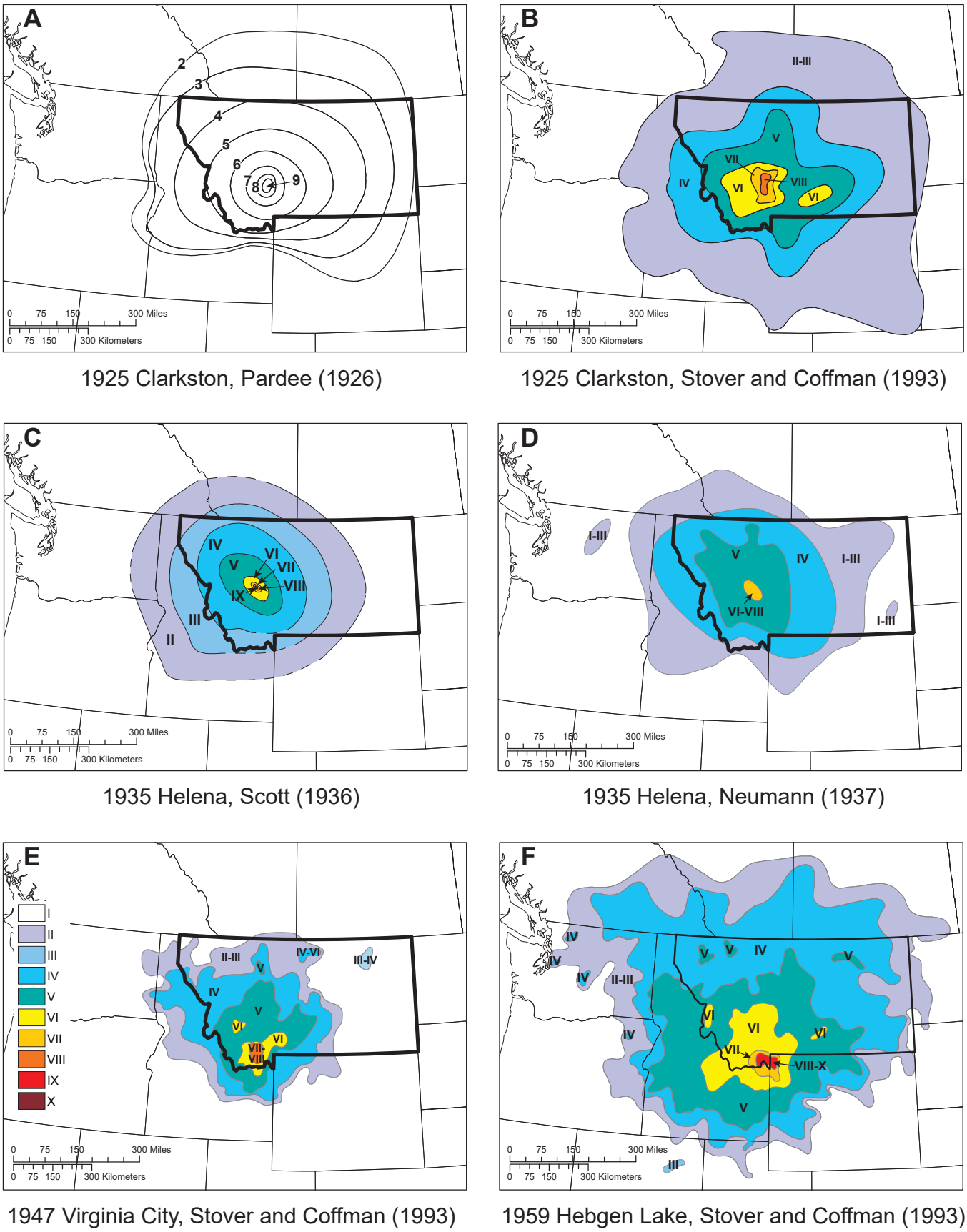

Figure 3. Isoseismal maps of historic Montana earthquakes. (A) Pardee's (1926) isoseismal map of the June 28, 1925 earthquake using the now obsolete Rossi–Forel intensity scale. All other isoseismal maps show shaking intensities using the Modified Mercalli Intensity scale (appendix A). (B) June 28, 1925 Clarkston Valley earthquake isoseismal map from Stover and Coffman (1993). (C) October 18, 1935 Helena earthquake from Scott (1936). (D) October 18, 1935 Helena earthquake from Neumann (1937). (E) 1947 Gravelly Range earthquake from Coffman and Stover (1993). (F) 1959 Hebgen Lake earthquake from Coffman and Stover (1993).

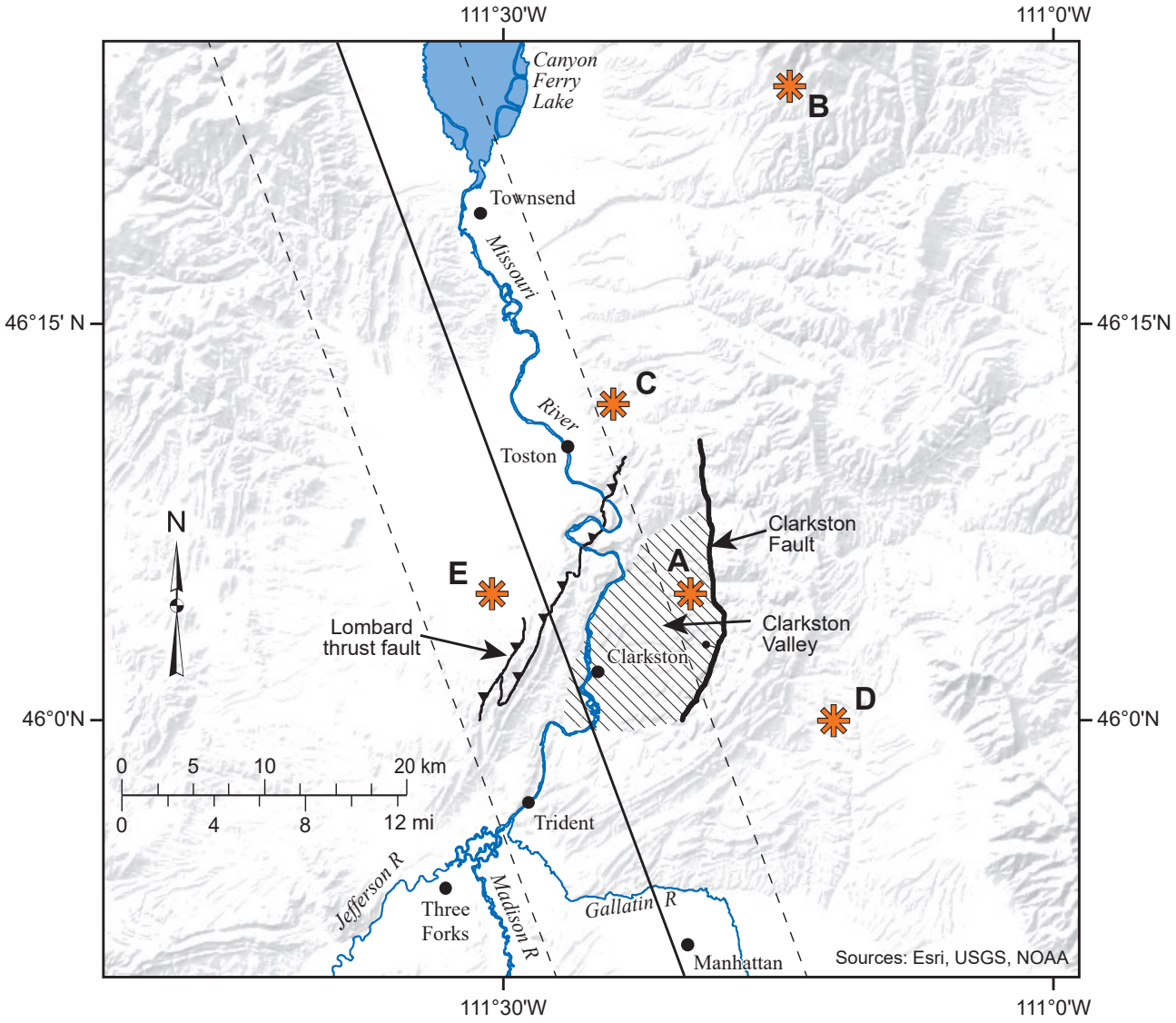

Figure 4. Asterisks show epicenters for the June 28, 1925 Clarkston earthquake reported by: (A) Pardee (1926); (B) Byerly (1926); (C) Dewey and others (1973); (D) Coffman and others (1982); and (E) Bakun (2005, written commun.). The solid NNW-trending line represents the locus of possible epicenters reported by Qamar and Hawley (1979) with dashed lines representing uncertainty range. The shaded area shows the Clarkston Valley, bounded on the east by the W-dipping Clarkston normal fault. The W-dipping Lombard thrust fault lies west of the Clarkston Valley.

Doser (1989) used teleseismic waveform modeling and first motion analysis to determine source parameters for the 1925 earthquake but apparently held the epicenter to Pardee's (1926) epicenter coordinates. Doser's (1989) focal mechanism indicates oblique normal faulting on a N-trending, N-dipping fault or on a NE-striking, NW-dipping fault with a SE-directed, nearly horizontal T-axis (minimum compressive stress direction). The Clarkston Fault (fig. 4) strikes north, similar to the N-trending nodal plane, but dips west, in the opposite direction of the nodal plane, suggesting that the 1925 earthquake did not occur on the Clarkston Fault.

Bakun (written commun., 2005) used Pardee's (1926) description of the earthquake's effects to assign MMI at 109 sites, which he then applied to the method of Bakun and Wentworth (1997, 1999) to estimate an epicenter west of the Clarkston Valley (46.08°N, 111.51°W), about 15 km (9 mi) west of the W-dipping Clarkston fault (fig. 4). The 95% confidence contour of this intensity center solution includes Pardee's (1926) epicenter in the Clarkston Valley. The intensity center is also consistent with Qamar and Hawley's (1979) locus of possible epicenters where they cross the Clarkston Valley. M_I is 6.55 at the intensity center, which agrees well with Doser's (1989) instrumental moment magnitude of 6.6.

Pardee (1926) interviewed five observers who reported feeling a slight earthquake—a possible foreshock—on May 31 at 7:55 a.m. A vigorous af-

tershock sequence immediately followed the June 28 mainshock. The strongest aftershock followed 49 min after the mainshock. Some witnesses reported that the shaking was nearly as strong as the initial shock, but the shaking duration was shorter. The strong aftershock was perceptible over an area of about 200,000 mi^2 (517,998 km^2) and caused additional rock falls and chimney damage, which is consistent with a magnitude of about 6.4, as estimated from the felt area versus magnitude relation in figure 5. Near the epicenter, witnesses reported that "the ground was in almost continuous tremble during the night" (Pardee, 1926). At Trident, residents felt an average of 4 aftershocks each day for the first month and 2 per day during the second month after the mainshock. A Trident resident chronicled 52 aftershocks that occurred through September 3, 1925. From the towns at which the larger aftershocks were felt, Pardee (1926) estimated the size of the disturbed area for 10 of these shocks. Using an updated version of Qamar and Stickney (1983, fig. 5), felt area versus magnitude relation (fig. 5), it appears that 4 of these aftershocks had magnitudes in the 5.5 to 5.2 range, 5 had magnitudes in the 4.9 to 4.4 range, and the smallest was 3.2. The two largest of these aftershocks occurred 2 h and 14 min and about 13 days after the mainshock, and both had estimated felt areas of 50,000 mi^2 (129,499 km^2). Later aftershocks included a magnitude 5.4 on December 12, 1926 and a magnitude 5.6 on February 2, 1929 (Stover and Coffman, 1993). This later event likely had a significantly smaller magnitude, as discussed below.

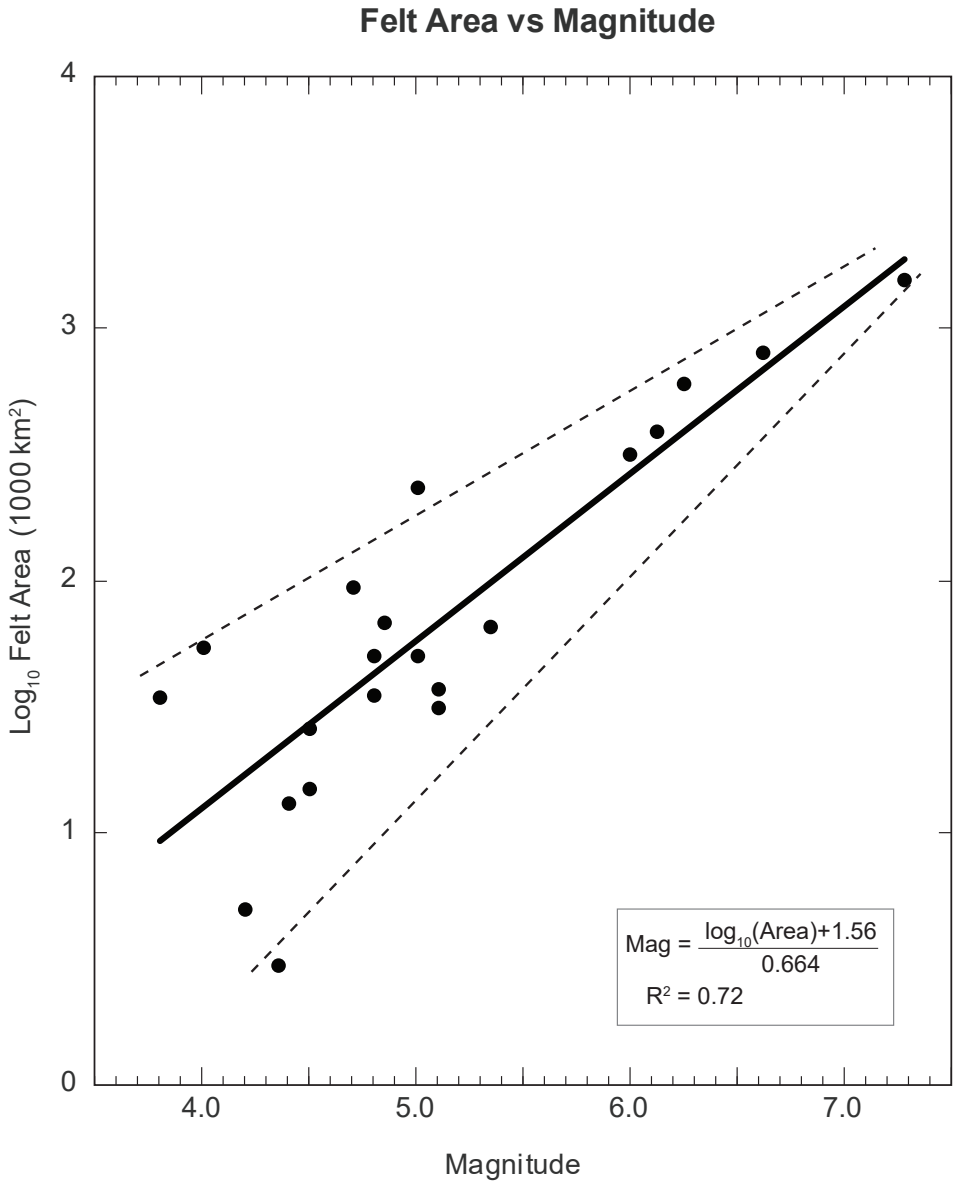

Figure 5. An empirical relation between the total felt area of an earthquake and magnitude, modified after figure 5 of Qamar and Stickney (1983). The solid line is a linear regression to the data with regression equation and r-squared (goodness of fit) at lower right. The dashed lines show the approximate range of uncertainty in the relation.

1935 Earthquake Sequence near Helena, Montana

Prior to 1935, only four U.S. earthquakes (Charleston, SC, 1886; San Francisco, CA, 1906; Santa Barbara, CA, 1925; and Long Beach, CA, 1933) were more destructive than the 1935 Helena earthquakes (Neumann, 1937). The 1935 Helena earthquake sequence included Montana's first deadly earthquakes and caused extensive damage to the capital city. Two weeks of foreshock activity preceded the two largest shocks, with magnitudes of 6¼ and 6, and more than 2,500 felt aftershocks followed during the next 3 yr. The combined shaking from the two largest quakes caused structural damage to approximately 60 percent of the buildings in Helena and an estimated $4 million in damages (~$76 million in 2020 dollars). Two people died in each of the two largest shocks—all as a result of falling building debris. Hundreds of residents left homeless sheltered in railroad cars, shelters operated by the Red Cross and the Salvation Army, and in a tent city dubbed Camp Cooney (fig. 6). The earthquakes rendered several Helena schools unusable and the Helena Board of Education set up temporary classrooms in 18 railroad coaches that the Northern Pacific and Great Northern railroad companies provided free of charge (Anderson and Martinson, 1936).

The Helena sequence began on October 3, 1935 with an earthquake that only Helena residents felt, marking the beginning of a 15-day foreshock sequence. A larger earthquake followed on October 12 that was felt over 70,000 km^2 (27,027 mi^2), with a maximum MMI of VII. The largest shock occurred October 18 with an estimated magnitude of 6¼ and was felt over 230,000 km^2 (88,804 mi^2) with a maximum intensity of VIII (figs. 3C, 3D), resulting in extensive damage (fig. 6) and two deaths. A slightly smaller earthquake of estimated magnitude 6 on October 31 caused additional damage, two additional deaths, and was felt over 140,000 km^2 (54,054 mi^2), also with maximum intensity of VIII. Additional earthquakes with maximum intensities of VI occurred on October 27, November 22, and November 28. The Helena earthquake sequence included 1,880 felt earthquakes from October 3, 1935 through April 30, 1936 (Scott, 1936). The two largest earthquakes caused structural damage to about 60 percent of the buildings in Helena. Phenomena resulting from the strong shaking included toppling and rotation of cemetery monuments and chimneys, liquefaction of alluvial sediments manifesting as sand blows, area streets with "rippled" pavement, changes to springs (Scott, 1936), and damage to the Helena water system totaling about $30,000 (Lupien, 1936).

The 1935 Helena earthquake sequence resulted in four deaths and an estimated $4 million in damages (Scott, 1936). Heck (1935) reported a damage estimate of $3 million, 40 residences demolished, 200 damaged, and that 80 percent of all buildings in Helena suffered some damage. Two deaths occurred during the October 18 earthquake, both a result of falling building debris along city streets (fig. 6). Two workers died during the October 31 earthquake when a large smoke stack at the Kessler Brewery collapsed upon them. Between October 12 and November 21, 1935, six additional deaths were directly or indirectly attributed to nervous shock according to an unpublished U.S. Coast and Geodetic Survey earthquake report submitted by W.E. Maughan, the meteorologist stationed in Helena; however, Scott (1936) reported that reliable sources claim that not more than two of the six deaths could be directly attributed to the earthquake. The exact number of injuries is not known with certainty, but estimates suggest that not more than 50 persons were treated for major and minor cuts and bruises (Scott, 1936). The lack of greater casualties is credited to the fact that the first severe shock occurred during the evening when schools were empty and few people were on the streets and that "far-sighted authorities" had closed the schools prior to the second major shock (Scott, 1936).

The proximity of this seismic sequence to the city of Helena and systematic documentation by the personnel at the Federal Weather Bureau in Helena and several volunteers resulted in an earthquake list that includes 2,535 felt earthquakes from October 3, 1935 through November 30, 1938. In addition to the dates and times of earthquake occurrence, the list includes estimates of shaking strength and duration, and for many events, comments about the direction or character of ground shaking and accompanying earth noises. In his report dated November 4, 1935, W.E. Maughan, Assistant Meteorologist at the Federal Weather Bureau in Helena, classified the listed events as weak, moderate, strong, very strong, or violent, and correlated these classifications in terms of Mercalli intensities as I or II; III, IV, or V; VI or VII; and VIII or IX, respectively. According to this classification, 2,221 earthquakes were weak, 231 were moderate, 78 were strong, 3 were very strong, and 2 were violent.

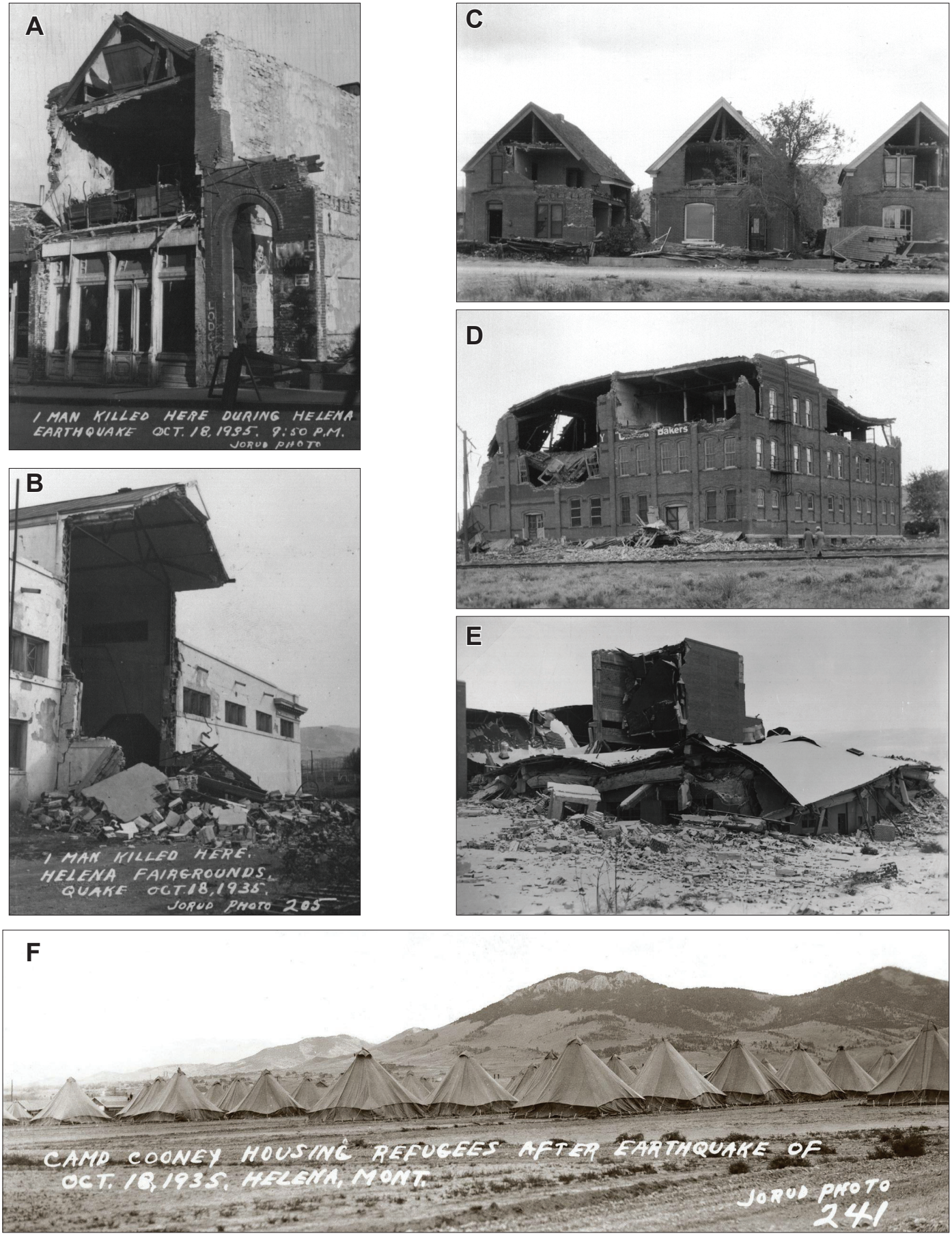

Figure 6. Photos of damage from the 1935 Helena earthquakes. (A and B) Falling building debris resulted in fatalities; (C) damage to single-family homes of masonry construction; (D) damage to the Nabisco Bakery; (E) collapsed wing of the Helena High School as seen after the October 31 earthquake; (F) tent city set up to accommodate Helena citizens left homeless by the October 18 earthquake.

Helena experienced at least one perceptible shock for 185 consecutive days beginning with the very strong shock of October 12, 1935. According to Maughan, noise accompanied almost any shock of consequence and the 3 most severe shocks produced loud roaring sounds. A comparison of felt earthquakes and their instrumentally determined magnitudes since 1982 suggests that Helena area earthquakes of magnitude 2.5 and larger in populated areas are usually reported as felt (Stickney, 2015).

The descriptions of shaking and earth noises contained in the listing are consistent with seismicity distributed over a zone extending from the northwest of Helena to the north or northeast of Helena (fig. 7). Observers described the initial shock of the sequence on October 3, 1935 in Helena as a slight rumbling noise followed by a severe vertical jolt (perhaps a heard P-wave and a felt S-wave) while people at Fort Harrison, 5 mi (8 km) northwest of Helena, reported the strongest shaking, consistent with an epicenter northwest of Helena closer to Fort Harrison. Following the severe October 12 earthquake at 12:51 a.m., Mr. Greenfield at the Greenfield Ranch, about 6 mi (9.7 km) northwest of Helena, reported feeling 38 tremors in the first 25 min after the mainshock and 75–100 tremors in all, many more than were noted in Helena during the same period. A significant aftershock 41½ min after the largest shock was described in Helena as: "This shock best since the first one. Heavy rumble seemed to be from the northwest and faded with less noise to the southeast." Many of the earthquake descriptions for the October 13 to 18 period include descriptions of motion, direction, or movement as northwest to southeast. All these observations are consistent with sources located to the northwest of Helena.

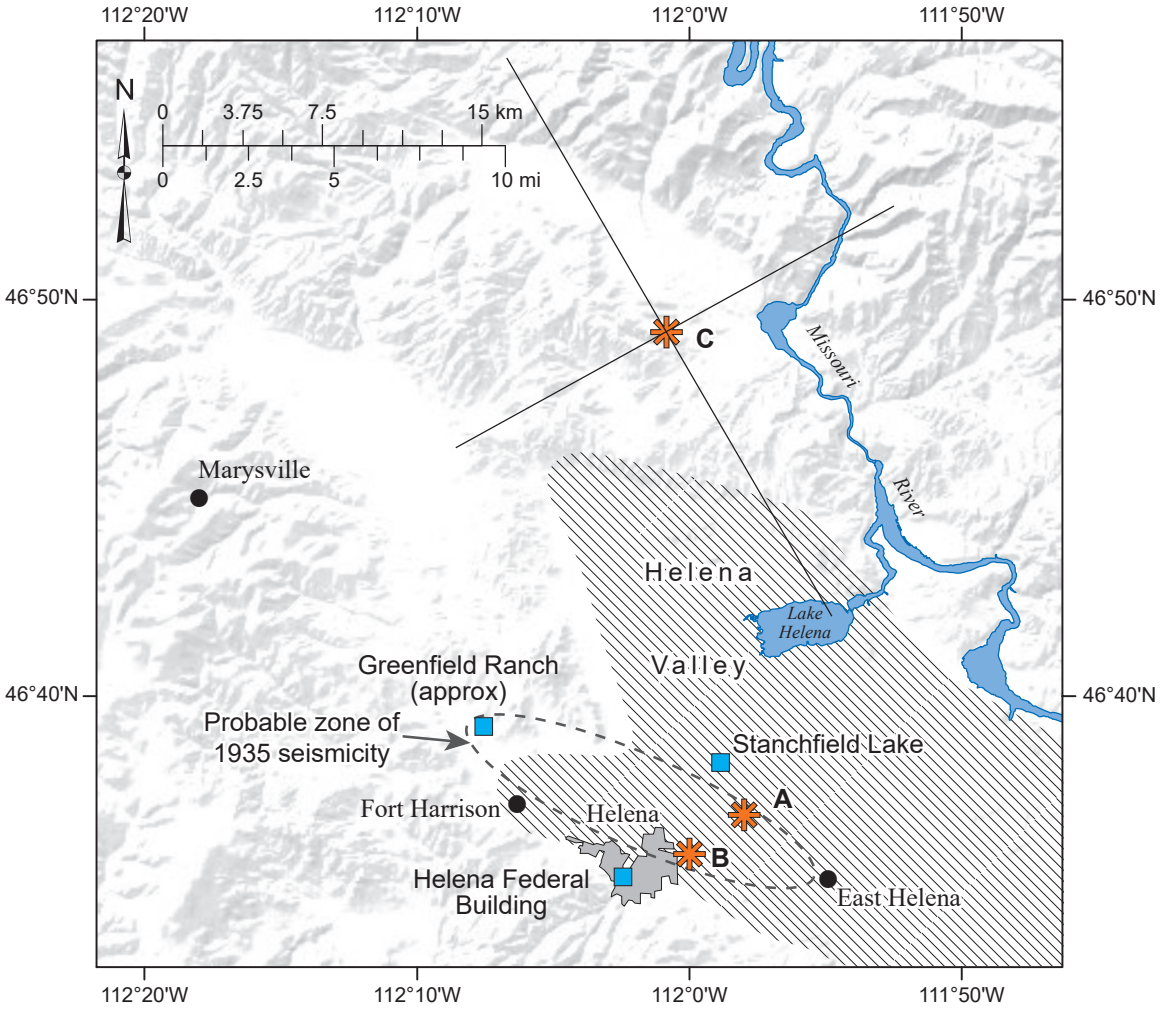

Figure 7. Map showing geographic features in the Helena region and October 18, 1935 earthquake epicenters as orange asterisks reported by: (A) Neumann (1937); (B) Stover and Coffman (1993); and (C) Dewey and others (1973). The error bars centered on C show epicenter uncertainty with respect to October 31, 1935 epicenter (Dewey and others, 1973). The shaded area shows the topographic extent of the Helena Valley. The dashed oval shows the possible extent of the 1935 earthquake sequence inferred from felt reports and Neumann's (1937) estimates of aftershock epicenters from strong motion records. Blue squares show geographic features mentioned in text.

Following the second major earthquake on October 31, one volunteer Weather Bureau reporter in Helena observed, "I might have been mistaken but most of temblors in this series seemed to come from a different direction than the previous series before this date." In support of this observation, Dean S. Carder, Assistant Magnetic and Seismic Observer with the U.S. Coast and Geodetic Survey, stationed in Helena to operate a seismic instrument installed on October 21, reported in a *Supplement to Report on the Helena Earthquakes with Special Emphasis on the Earthquake of October 31, 1935* that he was sitting in a parked car facing north outside the Federal Building when the October 31 earthquake occurred at 11:37 a.m. He described a sharp blow coming from the northeast and deep underground, followed a second later by violent side to side rocking, consistent with an epicenter a short distance northeast of downtown Helena.

A great variety of earthquake descriptions from later in the sequence hint at both nearby and more distant sources. Of course, earthquake sizes strongly influence how observers report earthquakes. However, descriptions for earthquakes classified as weak, such as "long rolling rumble," "quivering, no noise," "long rolling rumble and quivering," and "easy rumble and quiver" suggest small earthquakes at some distance from the observers. In contrast, descriptions for earthquakes also classified as weak, such as, "deep explosion," "heavy blast," "jar and rumble," "loud bumping rumble ending in slight vertical jar," and "jolt" suggest small earthquake sources very close to the observers. The wide variety of descriptions suggest earthquakes coming from a variety of locations near Helena (fig. 7).

Following the October 18 earthquake, U.S. Coast and Geodetic Survey personnel removed a strong motion instrument operating at Golden Gate Park in San Francisco, CA and installed it in the basement of the Helena Federal Building on October 21, 3 days after the destructive October 18 earthquake (Heck, 1935). This instrument utilized a pendulum to sense significant ground motion, which triggered recording of three components of ground acceleration on photographic paper for about 1 min. Because this instrument sensed ground motion of the P-wave arrival to trigger recording, it never recorded the beginning of P-arrival of the triggering earthquake. Despite this shortcoming, the October 31 earthquake recorded horizontal ground motions of 14.5 percent of the acceleration of gravity (fig. 8), for many years the closest on-scale recording of ground motion near the epicenter of a destructive earthquake and an important record for structural engineers.

Neumann (1937) analyzed the seismograms (fig. 8) recorded by the Helena strong motion instrument. He identified 10 aftershocks that were recorded after a preceding earthquake triggered the instrument and thus recorded the arrivals of both P- and S-waves. The measured S minus P intervals ranged from 0.8 to 1.3 s, from which he inferred epicentral distances of 3 to 6 km (1.9–3.7 mi) from the Federal Building and focal depths of 2 to 5 km (1.2–3.1 mi) below the surface. Using relative amplitudes of the P-waves recorded on the horizontal components, Neumann (1937) estimated that the azimuths from the Federal Building to the 10 completely recorded aftershocks ranged from N20°W to N70°E and were "rather widely distributed" and consistent with a concealed, WNW-trending fault zone passing about 4 km (2.5 mi) north of Helena (fig. 7). The average bearing of the 10 aftershocks is approximately N55°E from the Federal Building. Lacking precise information on the earthquake locations, Neumann (1937) adopted an epicenter at 46° 37′ N, 111° 58′ W (**A** in fig. 7) for the earthquake series and acknowledged that "any shock of the series may have easily originated several kilometers from this point." Stover and Coffman (1993) reported epicenters for all of the principal earthquakes of the 1935 sequence at 46.6°N, 112.0°W (**B** in fig. 7), apparently rounding Neumann's (1937) reported epicenter to the nearest 0.1 degree.

Dewey and others (1973) located the October 18 earthquake (**C** in fig. 7) with respect to the October 31 earthquake using the master event method and determined that the earlier event lay approximately 22 km (13.7 mi) north of the later event. This result is consistent with Scott's (1936) report that almost everyone in Helena described the October 31 event as a sharper and more pronounced jolt than the quake on October 18 despite the slightly smaller magnitude of the later earthquake. However, this location of the October 18 event more than 20 km (12 mi) north of Helena seems to contradict some of the felt reports described above. Using teleseismic waveform modeling and first motions, Doser (1989) determined dextral strike-slip mechanisms with NE–SW-trending T-axes for both the October 18 and 31 earthquakes.

In response to the Helena earthquake sequence, a large group of Helena citizens met and drew up a pro-

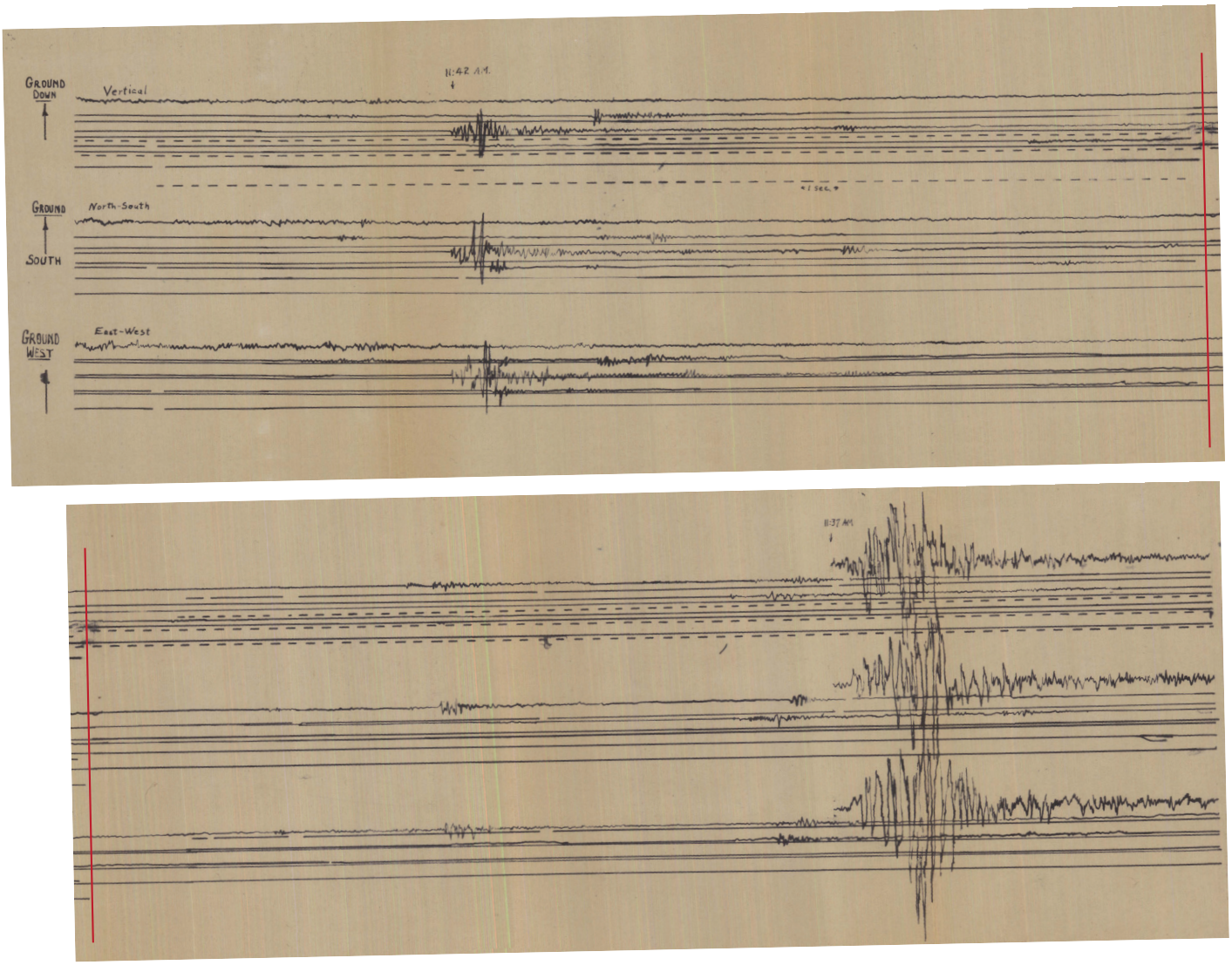

Figure 8. Strong motion seismogram recorded in the basement of the Helena Federal Building October 31, 1935. The three groups of traces show (from top to bottom) the vertical, N–S, and E–W ground motions. The seismogram is split into two parts at the vertical red line. Time increases from left to right along each trace and, after reaching the right edge of the seismogram, continues on each subsequently lower line, similar to lines of text on a page. The dashed line indicates 1-s timing intervals. The main shock (lower right) triggered recording for 4.6 min. Subsequent aftershocks triggered the instrument several additional times.

gram for future earthquake investigations in Montana (Scott, 1936). The stated purpose of this program was to gather facts about the Helena earthquakes and use this information to estimate the possibility of future damage and outline effective and economical ways to repair recent earthquake damage. Partners in this effort included U.S. Coast and Geodetic Survey personnel, U.S. Senator James E. Murray, who requested funding from the Public Works Administration, the Montana Bureau of Mines and Geology, and the Civil Engineering Department of the State College (now Montana State University). Six projects proposed under this program included continued operation of seismic instruments in Helena and Bozeman, establishment of a seismic monitoring station at the School of Mines in Butte, and analysis of instrumental and macroseismic data. The citizens' task force also proposed geodetic surveys to investigate crustal movements, a damage survey, a reconstruction survey, a detailed geological survey, and an investigation of the depth to bedrock throughout the Helena Valley. The continuous operation of the Butte seismograph on the Montana Tech campus, since August 1936, is a legacy of this program, and is Montana's longest continuously operating station.

The 1935 Helena earthquake sequence demonstrates that moderate-magnitude earthquakes can cause extensive damage and casualties when proximal to cities. The causative fault, or faults, are not known with certainty, but Doser's (1989) fault plane solutions are consistent with right-lateral slip on a westerly trending fault, which is compatible with regional bedrock faults

in the Lewis and Clark Zone (fig. 1), a 400-km-long (240-mi-long) zone that includes at least 12 major faults extending from Helena to Coeur d'Alene, ID (Wallace and others, 1990).

November 23, 1947, Southwest Montana

A strong earthquake shook southwest Montana at 2:46 a.m. on November 23, 1947. Gutenberg and Richter (1954) reported a surface-wave magnitude of 6¼ for this earthquake, but later work by Doser (1989) reported a moment magnitude of 6.1. Shaking was perceptible over an area of 340,000 km^2 (131,275 mi^2; fig. 3E) and was felt from the Canadian border south to Idaho Falls, ID, and from Ritzville, WA east to eastern Montana (Stover and Coffman, 1993). Intensity VIII shaking occurred in the area around Virginia City and Ennis, where newspaper articles reported damaged chimneys, fallen plaster, and broken windows (http://quake.utah.edu/wp-content/uploads/1947-Virginia-City-MT-News-Articles.pdf). The lack of significant damage from such a sizable earthquake is primarily due to its location remote from populated areas and infrastructure, and a time of year when the seasonal tourist population was absent.

Stover and Coffman (1993), citing Murphy (1950), reported an instrumental epicenter for this earthquake at 44.820°N, 111.713°W within the southern part of the Gravelly Range (**A** in fig. 9). Dewey and others (1973) relocated the 1947 epicenter (44.92°N, 111.53°W) in the Madison Range (**B** in fig. 9), just

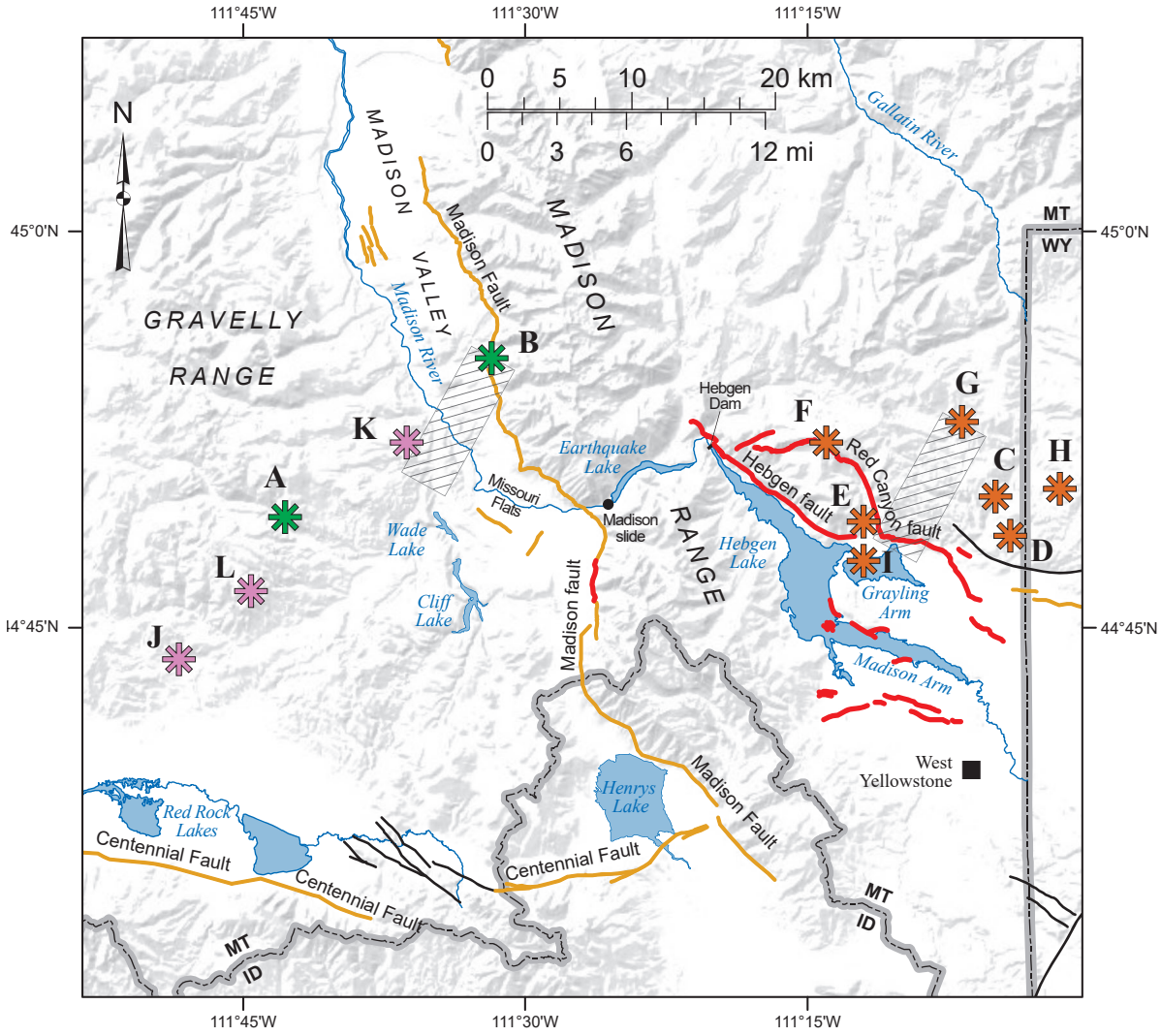

Figure 9. Hebgen Lake region epicenters. Green asterisks (A–B) show epicenters for the 1947 earthquake reported by: (A) Stover and Coffman (1993); and (B) Dewey and others (1973). Orange asterisks (C–I) show 1959 earthquake epicenters reported by: (C) the U.S. Coast and Geodetic Survey; (D) least-squares method Ryall (1962); (E) systematic deviations method Ryall (1962); (F) compensating station-pairs method Ryall (1962); (G) Doser (1985); (H) subevent 5.1 s after initial event Doser (1985); and (I) USGS Global Catalog of Calibrated Earthquake Locations. Pink asterisks (J–L) show epicenters for the 1964 earthquake reported by: (J) Stover and Coffman (1993); (K) Dewey and others (1973); and (L) USGS Global Catalog of Calibrated Earthquake Locations. The shaded rectangles extending southwest from B and G show Doser's (1985) estimate of epicenter bias. Faults with surface rupture in 1959 are shown as red line segments. Late Quaternary and mid- to early Quaternary faults shown by orange and black line segments, respectively.

east of the trace of the Madison Fault. Doser (1989) used Dewey and other's (1973) epicenter when determining the focal depth, moment magnitude, and focal mechanism of the 1947 earthquake. Recognizing a 10 km (6.2 mi) N to NE bias of early instrumental epicenters from this region, Doser (1989) inferred that the 1947 epicenter actually lay near the north edge of Missouri Flats in the southern Madison Valley, west of the Madison Fault (fig. 9), in an area of high modern seismicity. Using P-wave first motions and S-wave polarization angles, Dewey and others (1973) determined two possible focal mechanisms for the 1947 earthquake, one normal and the other strike-slip. Doser (1989) inverted waveforms of the 1947 earthquake to determine a focal depth of 8 ± 2 km (5 ± 1.2 mi) and a focal mechanism that is a combination of strike-slip and normal faulting. She observed that the nodal plane trending 104° and dipping 48° ± 6° S has a similar orientation to the seismologically determined fault plane (93° ± 5°) of the 1959 Hebgen Lake earthquake (discussed below). Doser (1989) further speculated that the 1947 earthquake may have ruptured a subsurface portion of the Madison Fault trending 130° just north of Madison Canyon, thus loading a short section of the Madison Fault south of Madison Canyon for surface rupture during the 1959 earthquake. One puzzling aspect of Doser's (1989) 1947 earthquake focal mechanism is the 63° ± 4° T-axis trend. Other researchers report a predominant NNE–SSW extension direction for this region using fault plane solutions (Stickney and Bartholomew, 1987; Stickney and Smith, 2009) and deformation measured with a trilateration network (Savage and others, 1993).

August 18, 1959, Hebgen Lake

The magnitude 7.3 Hebgen Lake earthquake occurred at 6:37 UTC on August 18, 1959 (11:37 pm August 17 local time) and is the largest historical Montana earthquake. It produced surface rupture along two major faults and numerous smaller faults (fig. 9), and coseismic subsidence extended well beyond the surface faulting (fig. 10), suggesting a deeper E–W-trending seismogenic fault. The strong seismic shaking triggered landslides and rockfalls over a wide region and seriously damaged—but did not destroy—the Hebgen Dam, a large earthfill dam built very close to the Hebgen Fault. Tectonic tilting generated large waves that overtopped Hebgen Dam and did considerable damage along the shores of Hebgen Lake, washing several cabins off their foundations. A vigorous aftershock sequence included earthquakes as large as any historical earthquakes in the State. The earthquake caused 29 deaths and dozens of injuries despite its location remote from large population centers, demonstrating that popular tourist areas may have significant seismic risk. Had the 1959 earthquake occurred during the winter months, it is likely that no casualties would have resulted. Landslides and rockfall blocked highways, stranding earthquake survivors in Madison Canyon, who self-organized and retreated to a safe location where they tended the injured until outside help arrived the following morning. The 1959 Hebgen Lake earthquake triggered a full emergency response involving Federal, State, and local agencies and officials who responded to treat the injured and rescue survivors, assess damages, and begin repairs. A congressional delegation visited the region 5 days after the mainshock, and the Army Corps of Engineers oversaw the excavation of a new spillway through the Madison Slide, which dammed the Madison River to form Earthquake Lake. Despite the primitive state of seismographic recording at the time, the 1959 earthquake provided important new information about a major surface-rupturing earthquake in the intermountain west. Surface fault displacements exceeding 6 m together with downwarping measurements from post-earthquake shorelines provided new insights into basin development in an extensional tectonic setting. The 1959 earthquake serves as a stark reminder that even areas with small permanent populations—which typifies many areas of western Montana—may suffer dramatic impacts from future major earthquakes. Aspects and effects of the 1959 earthquake are discussed in more detail below.

Shaking Intensity and Felt Area

The Hebgen Lake earthquake generated shaking over an area of about 1,554,000 km^2 (600,003 mi^2) (Coffman and others, 1982) but Stover and Coffman (1993) reported a felt area of 1,100,000 km^2 (424,712 mi^2), which they attributed to Coffman and others (1982). Perceptible ground shaking extended over nine U.S. states and three Canadian provinces (fig. 3F). Shaking was perceptible from Calgary, Alberta south to Salt Lake City, UT and from Seattle, WA east to Dickinson, ND. Steinbrugge and Cloud (1962) compiled data on the Hebgen Lake mainshock shaking effects to determine MMI in the epicentral region. The dramatic surface faulting and Madison Slide justified assignments of MMI X and IX, respectively. Howev-

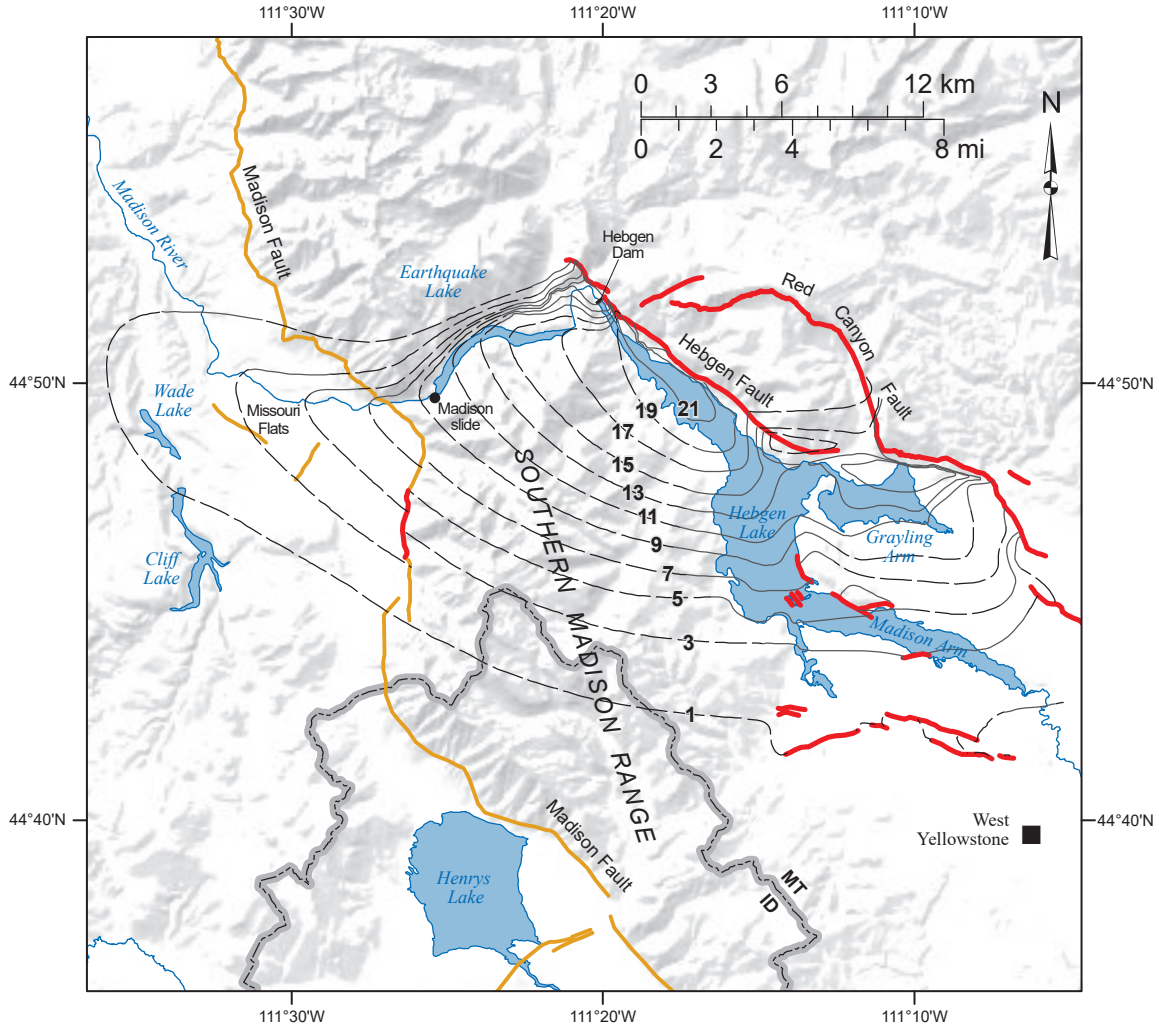

Figure 10. Map modified after Stickney (2012), showing Quaternary faults in the Hebgen Lake region and contours of coseismic subsidence (in feet) from Myers and Hamilton (1964) that accompanied the 1959 earthquake. Red line segments show faults with 1959 surface rupture from Myers and Hamilton (1964). Orange line segments show Late Quaternary faults.

er, the shaking effects at nearby locations (sometimes within a few feet of the scarps), as evidenced by building damage, did not exceed MMI VIII. The region of MMI VIII shaking extended about 50 km (31 mi), from west of Wade and Cliff Lakes eastward to the Norris Junction area in Yellowstone National Park (Steinbrugge and Cloud, 1962). As observed from isoseismal maps of previous large Montana earthquakes (fig. 3), the perceptible limit is distinctly lopsided. From the epicenter, shaking extended about 170 mi (274 km) southeastward into central Wyoming but extended more than 590 mi (950 km) northwestward into southern British Columbia (fig. 3F). The diminished distance of shaking perceptibility southeast and south of the epicenter implies greater attenuation of seismic waves propagating southward through the Yellowstone–Snake River Plain volcano-tectonic system and Basin and Range Province as compared to propagation through more typical northern Rocky Mountains paths to the north and northwest of the epicenter.

Human Impacts

The Madison Slide detached from the south canyon wall and cascaded into the Madison River Canyon (fig. 11A), where it buried the lower part of Rock Creek campground and claimed the lives of 26 people encamped there. Rock fall claimed the lives of two other campers near Cliff Lake, west of the Madison Valley (Witkind, 1964a). Rock fall likely claimed the life of a lone mountaineer on Granite Peak some 75 mi (120 km) ENE of Hebgen Lake, whose partial remains were discovered at the toe of the Granite Peak glacier 40 years after the earthquake (Morris, 2016, and http://www.bozemandailychronicle.com/articles/2000/08/21/news13496.txt). The Madison Slide and landslides along the shore of Hebgen Lake trapped some 250 survivors in Madison Canyon. Fearing that Hebgen Dam could fail at any moment and flood the canyon above Madison Slide, the survivors gathered on the highest accessible ground and self-organized to care for the

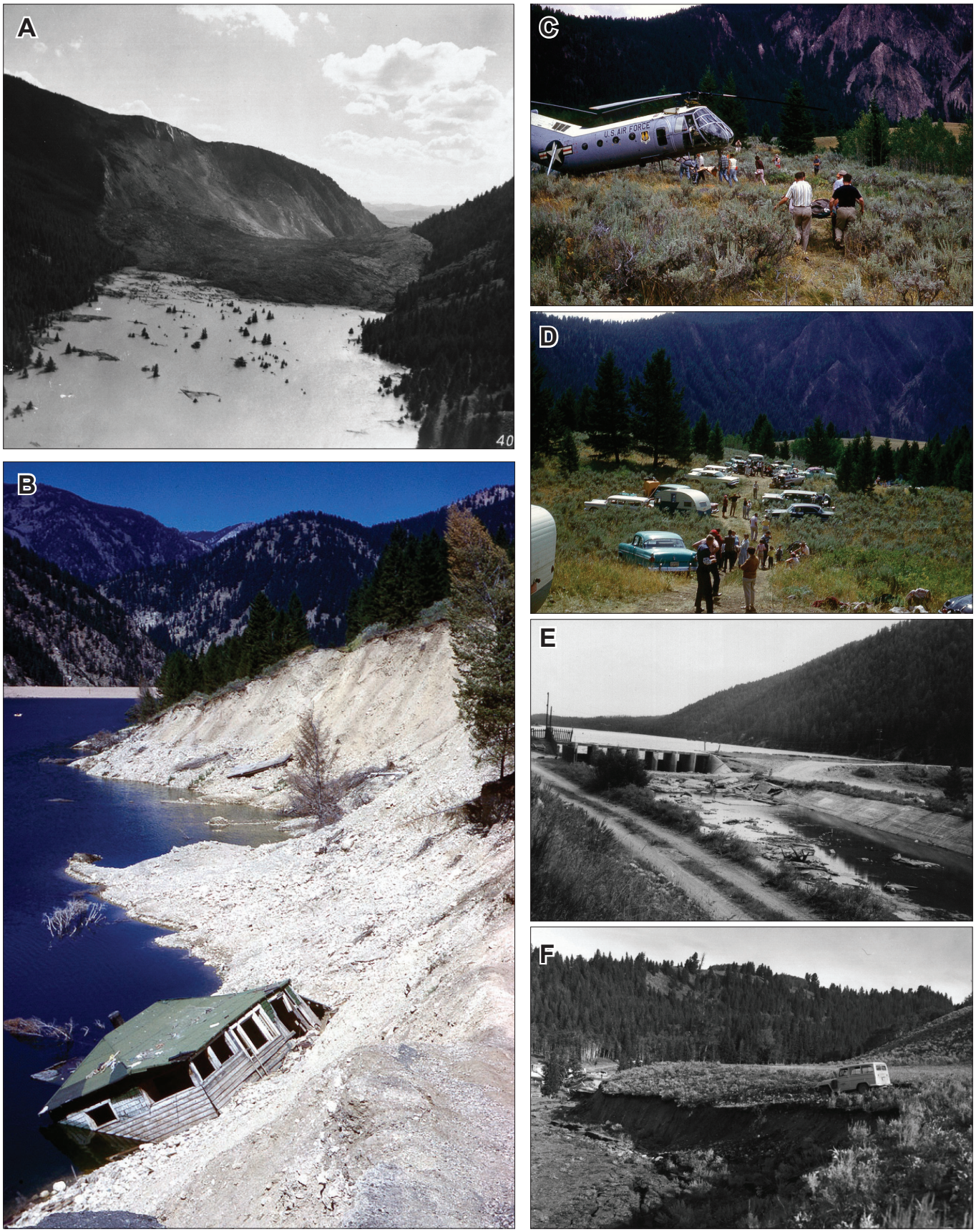

Figure 11. Photos of damage from the 1959 Hebgen Lake earthquake. (A) Madison Slide dams Madison Canyon, impounding the newly forming Earthquake Lake. (B) A cabin washed into Hebgen Lake floated ashore on fresh landslide scar. Hebgen Dam is visible at upper left. (C) A U.S. Air Force helicopter evacuates injured survivors the following morning. (D) Survivors trapped in Madison Canyon assembled on Refuge Point awaiting assistance. (E) Hebgen Dam emergency spillway damaged by strong shaking and seiche waves that overtopped the dam. (F) New fault scarp on the Blarneystone Ranch near the east end of the Red Canyon Fault.

injured (fig. 11D). Early the next morning a team of 12 U.S. Forest Service Smoke Jumpers parachuted onto what became known as Refuge Point to render first aid to the injured and prepare them for U.S. Air Force helicopter evacuation (figs. 11C).

Surface Faulting

The 1959 Hebgen Lake earthquake is the only historical Montana earthquake that produced surface faulting. The distribution and pattern of surface faulting is complex and involves significant displacements along two major faults and minor offsets along a host of lesser faults (fig. 10; Myers and Hamilton, 1964). The 8-mi-long (13-km-long) Hebgen Fault lies parallel to the northeast shore of Hebgen Lake and extends from about 1.4 mi (2.3 km) below Hebgen Dam southeastward to just north of the "narrows" where the Grayling Arm of Hebgen Lake joins the main body of the lake. Scarps up to 21 ft (6.4 m) high formed along the Hebgen Fault during the 1959 earthquake. The second major fault is the 11-mi-long (18-km-long) Red Canyon Fault, which extends from the western border of Yellowstone National Park northwestward along the mountain front north of Grayling Arm to Red Canyon. At Red Canyon, the Red Canyon Fault bends northward, following the eastern valley wall of Red Canyon in a southwestward concave arc through mountainous topography to within 2 km (1.2 mi) of the Hebgen Fault. Scarps up to 19 ft (5.8 m) high formed along the Red Canyon Fault. At least 18 shorter fault scarps with offsets less than 3 ft (1 m) formed, primarily in the southern end of Hebgen Basin and along the south shore of the peninsula formed between the Grayling and Madison Arms of Hebgen Lake. A 2-mi-long (3.2-km-long) section of the Madison Fault, which lies at the western front of the Madison Range, west of Hebgen Lake, ruptured with up to 3 ft (1 m) of displacement. Myer and Hamilton (1964) presented a detailed description and interpretation of fault scarps that formed in the 1959 Hebgen Lake earthquake.

Coseismic Deformation

The fault scarps are just part of a larger picture of coseismic subsidence that extends from the west edge of Yellowstone National Park, 40 km (25 mi) westward to the vicinity of Cliff and Wade Lakes. Highway 287 passes through the epicentral area, along which the U.S. Coast and Geodetic Survey had surveyed a second-order level line. A post-earthquake, first-order resurvey of this level line together with deformed shorelines along Hebgen, Cliff, and Wade Lakes allowed coseismic deformation measurements. Myers and Hamilton (1964) used the measured deformation data together with fault scarp heights (Witkind, 1964b) to create an isobase map (fig. 10), which displayed contours of earthquake-related deformation of the Hebgen Lake Basin, southern Madison Range, and across the southern Madison Valley—known as Missouri Flats. The isobase map pattern reveals an asymmetric downwarp with steep southward gradient of subsidence, primarily along the faults north of Hebgen Lake but extending westward through Madison Canyon into Missouri Flats. In contrast, the south flank of this downwarp extends from the southern part of the Hebgen Lake Basin as a more gradual region of subsidence, with the amount of subsidence increasing northward along the Madison Arm of Hebgen Lake towards the northeast shore. Isobase measurements are lacking within the southern Madison Range and limited in Missouri Flats, but the available data indicate an elongate subsidence zone extending 25 mi (40 km) from the border of Yellowstone National Park westward to just west of Cliff and Wade Lakes. The N–S extent of the subsidence zone in the Hebgen Lake Basin is 12 mi (20 km), extending approximately from south of Hebgen Lake to the Red Canyon fault scarp on the north (fig. 10). The area of maximum subsidence—21 ft (6.4 m)—measures 3.7 mi (6 km) long by 0.4 mi (0.65 km) wide and coincides with the northwest one-third of Hebgen Lake. An area of about 60 mi^2 (155 km^2) subsided more than 10 ft (3 m) and about 200 mi^2 (518 km^2) subsided more than 1 ft (0.3 m; Myers and Hamilton, 1964). By including subsidence measurements near Gibbon River Rapids in Yellowstone National Park, Myers and Hamilton (1964, p. 81) stated that "the basin of proved subsidence is 43 miles (69 km) long, from Norris Junction to Cliff Lake, and trends N78°W."

In the view of Myers and Hamilton (1964), large scarps along parts of the Hebgen and Red Canyon Faults formed most readily where favorably oriented, near-surface bedrock bedding planes existed. In areas lacking favorably oriented bedding planes, minor faulting and warping accommodated coseismic deformation. Because near-surface bedding planes in complexly folded and faulted Paleozoic sedimentary rocks are unlikely to extend to seismogenic depths, "the surface fault pattern must accordingly differ from the pattern of deeper, and more fundamental, displacements" (Myers and Hamilton, 1964, p. 87).

This idea of a deeper, more fundamental displacement is the key concept that distinguishes two competing interpretations of the primary mechanisms controlling coseismic deformation. Witkind and others (1962) and Myers and Hamilton (1964) interpreted the subsidence pattern extending from Missouri Flats through Madison Canyon and into the Hebgen Lake Basin as the result of an E–W-trending structure at depth that affected the southern Madison Range and the basins on each side more or less equally. They viewed the spectacular scarps north of Hebgen Lake as having formed along near-surface, favorably oriented, pre-existing zones of weakness to accommodate tectonic displacement that propagated upward from deeper movement along a concealed primary structure. This interpretation became known as the single-basin concept.

In contrast, Witkind and others (1962) and Frasier and others (1964) argued for the dual-basin concept to explain observed deformation in the epicentral region. The dual-basin concept posited that Missouri Flats and the Hebgen Lake Basin both subsided along adjacent range-bounding faults but the intervening southern Madison Range did not subside during the 1959 earthquake. Lacking subsidence measurements within the southern Madison Range, the crux of the single-basin versus dual-basin concepts comes down to the interpretation of subsidence data from within Madison Canyon between the Madison Range Front on the west and Hebgen Dam on the east. The U.S. Coast and Geodetic Survey conducted a leveling survey along this reach of Highway 287 (State Highway 499 in 1959) in 1934 and repeated the leveling survey in September and October of 1959, following the earthquake. The difference in measured highway profiles ranged from 6 to 22 ft (1.8 to 6.7 m) and varied smoothly along the profile except where obvious signs of landslides disrupted the road surface. Myers and Hamilton (1964) argued that this smoothly varying subsidence supports the single-basin concept of tectonic subsidence extending across the southern Madison Range. However, Frasier and others (1964) argued that the subsidence data cannot be trusted because most of it was collected across unconsolidated deposits (glacial till and alluvium) and the reported subsidence reflects seismically generated compaction of these deposits. As discussed below, other lines of evidence seem to favor the single-basin concept.

Hebgen Lake Seiche and Damage to Hebgen Dam

The sudden and differential subsidence of the Hebgen Lake Basin during the earthquake generated large and complex waves, which oscillated back and forth across the lake for up to 12 h. Four of the initial waves overtopped Hebgen Dam (Witkind, 1964a; Stermitz, 1964), badly damaging the emergency spillway (fig. 11E). The highest—and presumably first—wave, as indicated by swash marks and stranded debris, was 10 ft (3 m) above the post-earthquake water line near Hebgen Dam, thus overtopping the dam with 1.5 ft (0.45 m) of water (Myers and Hamilton, 1964). Along the northeast shore, the waves swept several cabins off their foundations and into the lake (fig. 11B). Intense seismic shaking damaged Hebgen Dam, causing the earth fill material on either side of a concrete core wall to settle by as much as 5 ft (1.5 m). Additional damage resulted from downslope movement of the alluvial fan material in the hanging wall of the Hebgen Fault, on which the northeast abutment of the dam rested. This downslope movement shifted the emergency spillway works up to 1.8 ft (0.5 m) horizontally towards the southwest with respect to the concrete core wall which, anchored on bedrock for most of its 700-ft (213-m) length, remained stationary. Scratches on the core wall resulting from rock fragments entrained in the shifting earthfill revealed these movements (Hadley, 1964).

Effects on Water

Stermitz (1964) attributed increased flows in the Madison, Gallatin, and Henrys Fork Rivers, and other streams within 75 mi (120 km) of Hebgen Lake, to the strong ground shaking produced by the mainshock and several strong aftershocks. Swenson (1964) documented both increases and decreases in spring discharge and increased water turbidity at numerous springs along with dramatic effects on wells throughout the epicentral region. Da Costa (1964) documented well water fluctuations throughout the conterminous United States and beyond due to the seismic shaking.

Madison Landslide

The strong ground shaking generated by the mainshock triggered numerous landslides in an area 20 mi (32 km) N–S and 50 mi (80 km) E–W of Hebgen Lake (Hadley, 1964). A landslide 0.6 mi (1 km) southeast of Hebgen Dam disrupted Highway 287 and blocked the only southeastward egress from the epicentral area. The spectacular Madison Slide blocked Madison Canyon just above where it opens into the Madison Valley

about 6 mi (10 km) below Hebgen Dam. The Madison Slide is the largest seismically triggered North American landslide during historic times. It originated about 1,300 ft (400 m) up on the south canyon wall and cascaded northward into the canyon, deposited 37 million yd^3 (28 million m^3) of broken rock, and formed a landslide dam nearly 0.9 mi (1.5 km) long and covering the pre-slide river channel up to 220 ft (67 m) deep (Hadley, 1964). Before the earthquake, a steeply dipping buttress of Precambrian dolomite near the base of the south canyon wall held canyonward-dipping, deeply weathered gneiss and schist in place. The Madison Slide slid as a broken-up but coherent mass such that the remnants of the dolomite buttress came to rest at the slide's leading edge up to 417 ft (127 m) above the canyon floor, and trees growing on the forested canyon wall came to rest on top of the slide—evidence of the lack of churning during slide movement.

Earthquake Lake

The Madison Slide dammed the Madison River, behind which Earthquake Lake began to fill (fig. 11A). The elevation of the low point in the Madison Slide dam was close to the same elevation as the foot of Hebgen Dam, raising the possibility that if Earthquake Lake filled to its maximum possible level, Hebgen Dam could be compromised. The Madison Slide also represented another danger; if allowed to fill completely, Earthquake Lake would overtop the dam and uncontrolled downcutting of a new outlet channel might result in catastrophic flooding downstream in the Madison Valley. To alleviate both of these potential problems, the Army Corps of Engineers (ACE) began excavating a new spillway in the crest of the Madison Slide shortly after the earthquake. After 22 days of work, the ACE had created a new spillway 30 ft (9 m) lower than the natural low point in the slide, and Earthquake Lake began to flow through the modified spillway on September 10, 1959 (Johnson and Omang, 1972). Rapid downcutting of the channel motivated the ACE to excavate the outlet channel an additional 60 ft (18 m) deeper. Between 1960 and 1971, the Madison River incised the outlet an additional 19 ft (8 m; Johnson and Omang, 1972). The maximum level of Earthquake Lake is still visible along the south shore, marked by a ring of dead trees and regrowth of younger trees approximately 50 ft above the current lake level.

Aftershocks

A powerful aftershock sequence began immediately after the Hebgen Lake mainshock. Victims near the epicenter described the ground as in a near-constant state of shaking. However, Stover and Coffman (1993) listed only seven aftershocks during the 11 weeks following the mainshock, four of which had magnitudes ranging from 5.0 to 4.4, three had no reported magnitudes, and none of these seven aftershocks had reported felt areas. The incomplete reporting of aftershock activity is no doubt attributable to the early state of regional seismic monitoring.

Doser and Smith (1989) reported five Hebgen Lake aftershocks during the first 24 h, with moment magnitudes ranging from 5.6 to 6.5. These aftershocks are discussed further in the Seismographic Studies section below.

Seismographic Studies

The 1959 Hebgen Lake earthquake occurred before the advent of regional seismic network monitoring and routine use of modern hypocenter-location computer software. Only three permanent seismograph stations operated in Montana, which employed photographic paper recordings and used station chronometers requiring daily time corrections. Determining epicenters was a laborious process that required collecting seismograms, manually reading seismic phase arrivals from paper seismograms, and manually locating epicenters using graphical methods. These factors together with the lack of detailed seismic velocity models yielded epicenters with uncertainties on the order of ±10 km (6.2 mi) under the best of circumstances and virtually no focal depth control. The seismographic studies of the 1959 Hebgen Lake earthquake sequence are discussed chronologically below.

The U.S. Coast and Geodetic Survey determined epicenters for the Hebgen Lake mainshock and eight aftershocks through August 19, 1959 (USCGS, 1959). The mainshock and two aftershocks have epicenters quoted to the nearest minute of latitude/longitude "for which the data are in very good agreement," three aftershocks have epicenters quoted to the nearest 0.1 degree of latitude/longitude that are "well located but have some scatter in the data," and three aftershocks had epicenters quoted to the nearest ½ degree of latitude/longitude "where agreement is poor." To this list, Murphy and Brazee (1964) added eight aftershock locations through October 6, 1959, seven of which "had to be determined graphically because of a paucity of readings." These preliminary epicenters lie within an area extending 85 km (53 mi) in the E–W direction and 40 km (25 mi) in the N–S direction, with one

graphically determined epicenter lying another 23 km (14 mi) northward on the east side of the Emigrant Valley (Murphy and Brazee, 1964). Only six of the instrumentally determined earthquakes had magnitudes assigned; a magnitude of 7.1 determined by Pasadena for the mainshock, which persisted in the literature for many years, with aftershock magnitudes ranging from 6½ to 5½, quoted to the nearest quarter magnitude unit. Although only 17 earthquakes in the 1959 sequence had published epicenters, Murphy and Brazee (1964) estimated that the Butte and Bozeman seismograph stations recorded more than 1,300 aftershocks through October 15, 1959. The Butte and Bozeman seismograph stations—the closest to the epicentral region—recorded no recognized foreshocks (Murphy and Brazee, 1964).

The U.S. Coast and Geodetic Survey (1959) used P-wave arrivals from 27 seismograph stations to determine the preliminary 1959 mainshock epicenter (44°50′N, 111°05′W; **C** in fig. 9). Fifteen of these stations operated in California and Nevada. A problematic aspect of the instrumentally determined 1959 mainshock epicenter is that it lies 3.3 mi (5.3 km) northeast of the closest part of the Red Canyon fault scarp. Clearly, it is impossible for the epicenter to lie north of the trace of the S- or SW-dipping fault(s) that slipped in 1959, so the preliminary epicenter must include a northward bias.

The U.S. Geological Survey deployed two seismograph stations that operated for about 2½ days beginning 3½ days after the mainshock. One station operated about 55 km (34 mi) southwest of the mainshock, on the south flank of the Centennial Range. The other station operated at two different sites about 135 km (84 mi) south of the mainshock, near Victor, ID. The closer, Centennial Range station recorded more than 600 aftershocks with magnitudes ranging from 0.4 to 3.7 (Stewart and others, 1964). Using a graphical method that utilizes the S minus P times at each station and the difference in P-arrival times, Stewart and others (1964) estimated epicenters for 30 aftershocks with magnitudes ranging from 1.8 to 3.5. Epicentral uncertainties estimated from the graphical location method ranged from 0 to 13 km (8 mi), with an average of about 5 km (3.1 mi; Stewart and others, 1964). Most of these epicenters form an inverted "L" shape with arms about 45 km (28 mi) long. One arm trends westward from the western margin of Yellowstone National Park through Hebgen Lake to the southern Madison Valley. Nearly all of the epicenters in the Hebgen Lake Basin lie south of the Hebgen and Red Canyon Faults. The other arm of the inverted "L" extends southward, more or less along the Montana–Wyoming border. Stewart and others (1964) noted that this northerly epicenter alignment "has no known relation to surface geological features…[and]…is interpreted to be the result of a major regional-stress distribution at depth." An alternate explanation for this northerly epicenter alignment, particularly the epicenter cluster at the south end, near the intersection of the Montana, Wyoming, and Idaho borders, is epicenter mislocation. The station operated near Victor, ID at a distance of about 135 km (84 mi) from the mainshock is sufficiently distant that it should record both the direct and mantle-refracted P- and S-waves for aftershocks occurring at typical focal depths. Misidentification of any of these phases could result in erroneous epicentral distance determinations and hence epicenter mislocation. The two-station epicenter-location method employed in this study provides only crude epicenter estimates at best, so it is problematic to infer tectonically active features from these epicenters.

Ryall (1962) conducted the first detailed study of the 1959 Hebgen Lake hypocenter using P-waves recorded at 125 global seismograph stations. Using the method of least-squares, Ryall (1962) revised the mainshock epicenter to a position 3.5 km (2.2 mi) SSE of the U.S. Coast and Geodetic Survey preliminary location (44°48.5′N, 111°04.2′W; **D** in fig. 9), but still well within the footwall block of the Red Canyon Fault. By analyzing systematic P-wave travel time residuals with respect to the Jeffeys and Bullen (1940) travel time tables, Ryall (1962) recognized errors in the epicenter and origin time and then applied two graphical methods to compensate for these errors. The method of systematic deviations adjusted the original U.S. Coast and Geodetic Survey epicenter 9 km (5.6 mi) WSW (44°49′N, 111°12′W; **E** in fig. 9) and the method of compensating station-pairs adjusted the epicenter 12 km (7.5 mi) WNW (44°52′N, 111°14′W; **F** in fig. 9). Both of these adjustments place the epicenter just south of the Red Canyon fault scarp and within the region of surface faulting. Ryall (1962) does not specify which of these adjusted epicenters may best represent the true epicenter.

The absence of local seismograph stations in the Hebgen Lake region made the determination of the

depth of focus difficult. Ryall (1962) used P-wave travel times from three Montana seismograph stations—Bozeman, Butte, and Hungry Horse—together with a regional crustal structure profile (Steinhart and Meyer, 1961) to place constraints on the focal depth of the 1959 earthquake. This analysis yielded depth estimates between a surface focus and 25 km (16 mi): "the depth of 25 km might be considered as the best estimate; it represents at least an upper limit on the depth of focus" (Ryall, 1962). A search of the seismograms for a pP depth phase was inconclusive. However, on many seismograms, a large clear seismic phase arrives 5–8 s after the P-wave. An analysis of this second seismic phase suggested that, rather than a pP depth phase, it was a P-wave from a second, larger fault rupture that occurred south of the initial rupture (Ryall, 1962)—the first recognition that the Hebgen Lake mainshock had a complex mechanism consisting of at least two subevents.

Dewey and others (1973) conducted the next seismological analysis of the 1959 earthquake and its aftershocks. Using Ryall's (1962) least-squares epicenter as the calibration event, Dewey and others (1973) applied the joint epicenter determination method to the 17 most widely recorded earthquakes occurring from 1925 to 1971 in the Montana/Idaho/Wyoming region. This analysis computed epicenters relative to the calibration event and also determined "source-station adjustments," which reduce network bias of the computed epicenters. They then applied these source-station adjustments to single-event locations for all other earthquakes recorded by at least 10 seismograph stations. Finally, they computed confidence ellipses for each epicenter and discarded those events with confidence ellipse semi-major axes that exceeded 20 km (12 mi), thereby retaining only the best-quality epicenters. They did not attempt to determine focal depths and fixed them at sea level. This procedure resulted in epicenters for 22 aftershocks for the first year after the 1959 mainshock, with magnitudes ranging from 4 to 6½. The aftershocks define a 90-km (56 mi) E–W zone with most aftershocks—including the largest—clustered at each end. The aftershock zone roughly centers on the zone of surface faulting but extends well beyond it in both directions.

Using seismograms recorded at regional and teleseismic distances, Doser (1985) modeled body waves and inverted their amplitudes to determine seismic moment tensors for the 1959 Hebgen Lake mainshock and several large aftershocks. Doser (1985) attempted to more accurately locate the mainshock epicenter (44°52.80′N, 111°06.78′W; **G** in fig. 9) but quantified a systematic north to northeast bias of up to 10 km (6.2 mi) in the 1959 epicenters, probably due to lateral velocity heterogeneities along southwestward ray paths to regional stations. As Ryall (1962) originally suggested, the 1959 mainshock consisted of two subevents that occurred 5 s apart. The first m_b 6.3 subevent initiated at a depth of 10 ± 2 km (6.2 ± 1.2 mi) and the second m_b 7.0 subevent (**H** in fig. 9) initiated 5–8 km (3.1–5.0 mi) to the southeast at a depth of 15 ± 3 km (9.3 ± 1.9 mi). Both subevents occurred on a single or parallel fault planes dipping 60° ± 5° S. The second subevent initiated near the base of the seismogenic zone and ruptured upward towards the surface (Doser, 1985).

During the first 24 h of the aftershock sequence five earthquakes with magnitudes greater than 5.5 occurred in northwest Yellowstone National Park. After 24 h, aftershock activity shifted to the western end of the aftershock zone with a magnitude 6.0 earthquake in the southern Gravelly Range. Nearly all subsequent aftershocks occurred within 10 km (6.2 mi) of aftershock epicenters that occurred during the first 48 h (Doser, 1985), indicating that the aftershock zone did not expand appreciably beyond the dimensions established early in the sequence. Using mainshock subevent focal mechanisms and focal depths derived from her study, Doser (1985) presented two possible models relating seismically determined slip at depth to mapped geological structures and the surface faulting observed along the Hebgen and Red Canyon Faults. These faulting models, together with more recent seismic monitoring studies covering the 1959 aftershock zone (Smith and others, 1977; Trimble and Smith, 1975; Smith and Arabasz, 1991), strongly suggest that 1959 seismicity must have occurred southward of the surface ruptures, earlier epicenters to the contrary notwithstanding.

The U.S. Geological Survey has recently relocated important global earthquake clusters, including seismicity in the Hebgen Lake area (U.S. Geological Survey Global Catalog of Calibrated Earthquake Locations). These relocations indicate that the 1959 mainshock epicenter (44.7925°N, 111.2001°W; **I** in fig. 9) lies beneath the Grayling Arm of Hebgen Lake, south of the surface ruptures as would be expected for slip on a S-dipping fault. Four large aftershocks included in this reanalysis also lie in positions that are

more reasonable with respect to the fault scarps and the distribution of modern seismicity.

Fault Plane Solutions

Ryall (1962) used P-wave first motions measured from 71 seismic stations to construct a fault plane solution for the 1959 mainshock. His analysis indicated a fault plane with a strike of N80°W ± 10°, dipping 54° SW ± 8°.

Dewey and others (1973) computed focal mechanisms for the 1959 mainshock and two large aftershocks. The mainshock focal mechanism is not significantly different from Ryall's (1962). However, the fault plane inferred from seismological data has a distinctly different trend than the Hebgen fault scarp observed at the surface, leading Dewey and others (1973) to suggest that the initial rupture on a N80°W-trending fault preceded near-surface, N50°W-trending rupture—perhaps the second subevent Ryall (1962) observed—that formed surface scarps along the Hebgen and Red Canyon Faults.

Dewey and others (1973) determined that the August 18 aftershock at 15:26 UTC (magnitude 6½, Berkeley) occurred near the east end of the aftershock zone in northwest Yellowstone National Park, with a focal mechanism indicating dextral oblique slip on a N70°E, S-dipping fault plane. The August 19 aftershock at 04:04 UTC (magnitude 6¼, Berkeley) occurred near the west end of the aftershock zone in the southern Gravelly Range west of Missouri Flats with a poorly constrained focal mechanism indicating either normal slip on an E-trending, S-dipping fault, or strike-slip movement on a NW- or a NE-trending fault. An m_b 5.2 earthquake occurred on October 21, 1964 near the west end of the 1959 aftershock zone with a strike-slip focal mechanism (Dewey and others, 1973) and is likely a late aftershock. The T-axes are nearly horizontal and oriented south for the mainshock and all three aftershocks. The 80-km-long (50-mi-long) E–W aftershock zone that extends well beyond surface faulting, clustering of largest aftershocks at ends of the aftershock zone, and fault plane solutions favor Myers and Hamilton's (1964) single-basin concept but do not conclusively reject Fraser and others' (1964) dual-basin concept (Dewey and others, 1973).

Doser's (1985) moment tensors confirmed Ryall's (1962) and Dewey and others' (1973) mainshock focal mechanism, provided focal depths, and focal mechanisms for four additional large aftershocks. Doser (1985) determined fault plane solutions for four additional aftershocks that occurred with the first 5 h of the mainshock. All occurred within the eastern end of the aftershock zone in northwest Yellowstone National Park and exhibited oblique-normal, strike-slip, and oblique reverse faulting, most having E–W or NW–SE T-axes. This variety of aftershock focal mechanisms and the oblique-normal focal mechanism with northeast–southwest T-axis for the June 30, 1975 Yellowstone Park earthquake (M_L 6.1, M_s 5.9; Pitt and others, 1979) near Norris Junction suggest rapidly varying stress orientations near the Yellowstone caldera boundary (Doser 1985). Two large aftershocks at the western end of the aftershock zone and earthquakes in the central part of the aftershock zone all have N–S-oriented T-axes, regardless of whether they are normal, strike-slip, or some combination thereof.

October 21, 1964 Southern Gravelly Range

The October 21, 1964 earthquake occurred within the western part of the 1959 Hebgen Lake earthquake aftershock zone and is likely a late aftershock. The magnitude of this earthquake is problematic. Stover and Coffman (1993) reported a variety of magnitudes, including an m_b 5.8 which they attribute to the USGS. This value apparently came from U.S. Earthquakes, 1964 (von Hake and Cloud, 1966), where an unspecified magnitude of 5.8 is reported. Nuttli and others (1979) calculated an m_b of 5.0 and an M_s of 4.9 for the 1964 earthquake. Stover and Coffman (1993) also reported moment magnitude of 5.22, attributed to Doser (1989), who reported a moment magnitude of 5.6.

Stover and Coffman (1993) reported a felt area of 65,000 km^2 (25,097 mi^2) with a maximum MMI of V. Stickney remeasured the felt area of the 1964 earthquake from the original isoseismal map of von Hake and Cloud (1966) and determined a value of 25,657 mi^2 (66,451 km^2), in good agreement with Stover and Coffman (1993). Using an expression derived from an updated version of Qamar and Stickney's (1983) figure 5 (fig. 5), a felt area of 66,451 km^2 predicts a magnitude of 5.1, which is consistent with the maximum MMI of V and in good agreement with Nuttli and others' (1979) reported magnitude values, the m_b of 5.2 attributed to the International Seismological Center (ISC; Dewey and others, 1973), and an m_b of 5.1 ± 0.1 in the ISC Bulletin (http://www.isc.ac.uk/). The discrepancy between Doser's (1989) 5.6 moment magnitude and several other magnitudes from various sources clustering near magnitude 5 remains enigmatic.

The USGS relocated the 1964 earthquake along

with a group of Hebgen Lake region events and published the results in the Global Catalog of Calibrated Events (U.S. Geological Survey Global Catalog of Calibrated Earthquake Locations). The revised location (44.7732°N, 111.7434°W) lies in the southern Gravelly Range (**L** in fig. 9), about 7 km (4.3 mi) northeast of the original epicenter and about 15 km (9.3 mi) southwest of Dewey and others' (1973) reported epicenter.

Earthquakes Previously Assigned Magnitudes of 5.5 or Larger

Stover and Coffman (1993) cited three historical Montana earthquakes with magnitudes ranging from 5.5 to 5.6 that are excluded from table 1. Reevaluation of original data indicate that all three earthquakes most likely had magnitudes less than 5.5.

February 15, 1929

The February 15, 1929 earthquake occurred northeast of Three Forks and produced MMI V shaking near the epicenter. This earthquake is likely a late aftershock of the 1925 Clarkston earthquake. Stover and Coffman (1993) reported a felt area of 161,000 km^2 (62,163 mi^2), attributed to Coffman and others (1982), and estimated a magnitude of 5.6 from this felt area. The original information for this earthquake came from Heck and Bodle (1931), where the felt area was reported as "at least 40,000 square miles" (103,600 km^2). This latter value is 35 percent smaller than the 161,000 km^2 (62,163 mi^2) reported by Stover and Coffman (1993). To resolve this difference in reported felt areas, Stickney remeasured the felt area from the original isoseismal map (Heck and Bodle, 1931) and using ArcMap, determined an area of 23,353 mi^2 (60,484 km^2), significantly smaller than Heck and Bodle's (1931) estimate of 40,000 mi^2 (103,600 km^2). Using an expression derived from an updated version of Qamar and Stickney's (1983) figure 5 (fig. 5), a felt area of 60,484 km^2 (23,353 mi^2) predicts a magnitude of 4.2, which is consistent with the maximum MMI of V and the lack of serious damage that would likely accompany a nearby M 5.6 earthquake. Even if one accepts Heck and Bodle's (1931) estimate of "at least 40,000 square miles" (103,600 km^2), the above felt area versus magnitude relation predicts a magnitude of 4.7, still significantly smaller than the magnitude 5.6 reported by Stover and Coffman (1993).

September 23, 1945

The September 23, 1945 earthquake occurred in northwest Montana on the west side of Flathead Lake near the town of Lakeside and produce maximum MMI VI shaking. Stover and Coffman reported a felt area of 95,000 km^2 (36,680 mi^2), attributed to Bodle and Murphy (1947), and estimated a magnitude of 5.5 based on this felt area. Bodle and Murphy (1947) reported a felt area of "approximately 36,000 square miles" (93,240 km^2), in reasonable agreement with Stover and Coffman's (1993) reported value. To confirm the felt area, Stickney remeasured the felt area from the original isoseismal map (Bodle and Murphy, 1947) and using ArcMap, determined an area of 37,276 mi^2 (96,544 km^2). Using an expression derived from an updated version of Qamar and Stickney's (1983) figure 5 (fig. 5), a felt area of 96,544 km^2 (37,276 mi^2) predicts a magnitude of 5.3.

April 1, 1952

The April 1, 1952 earthquake occurred in northwest Montana and produced maximum MMI VII shaking at one location along the east shore of Flathead Lake. Stover and Coffman (1993) reported a felt area of 77,000 km^2 (29,730 mi^2), attributed to Murphy and Cloud (1954), and estimated a magnitude of 5.5 based on this felt area. However, Murphy and Cloud (1954) reported a felt area of "approximately 35,000 square miles" (90,650 km^2), 18 percent larger than the value reported by Stover and Coffman (1993). To resolve this difference in reported felt areas, Stickney remeasured the felt area from the original isoseismal map (Murphy and Cloud, 1954) and using ArcMap, determined an area of 28,667 mi^2 (74,247 km^2), 36 percent smaller than Murphy and Cloud's (1954) estimate of 35,000 mi^2 (90,650 km^2), but comparable to the value of 77,000 km^2 (29,730 mi^2) reported by Stover and Coffman (1993). Using an expression derived from an updated version of Qamar and Stickney's (1983) figure 5 (fig. 5), a felt area of 74,247 km^2 (28,667 mi^2) predicts a magnitude of 5.2.

Recent Significant Earthquakes 1970–2020

Virtually all of Montana experienced MMI shaking of V or greater before 1960, whereas after 2000, most of western Montana has not experienced MMI shaking greater than IV (fig. 12). The frequency of magnitude 5.5+ earthquakes is substantially smaller during the 60 years following the 1959 Hebgen Lake earthquake than it was for a similar period preceding the 1959 earthquake (fig. 13). Only two earthquakes with magnitudes larger than 5.5 have occurred in Montana since the 1959 earthquake and its major aftershocks, and no

Montana earthquakes in the past 60 yr have exceeded magnitude 6.0 (fig. 13).

July 26, 2005 Dillon

The July 26, 2005 Dillon earthquake, with M_w 5.6, was the largest Montana earthquake in at least 41 years. The Dillon earthquake occurred 16 km (9.9 mi) north of Dillon in a region of unremarkable previous seismicity (fig. 1) that lacks recognized nearby Quaternary faults. The Dillon earthquake produced MMI VI shaking in Dillon, and a USGS strong motion instrument on the University of Montana Western campus recorded ground acceleration of 12.7% g, which caused damage to several schools and 60% of the older masonry chimneys in Dillon. Ground cracks unrelated to primary faulting formed in the epicentral area resulting from strong shaking in weak soils, and shaking caused minor damage to an I-15 overpass

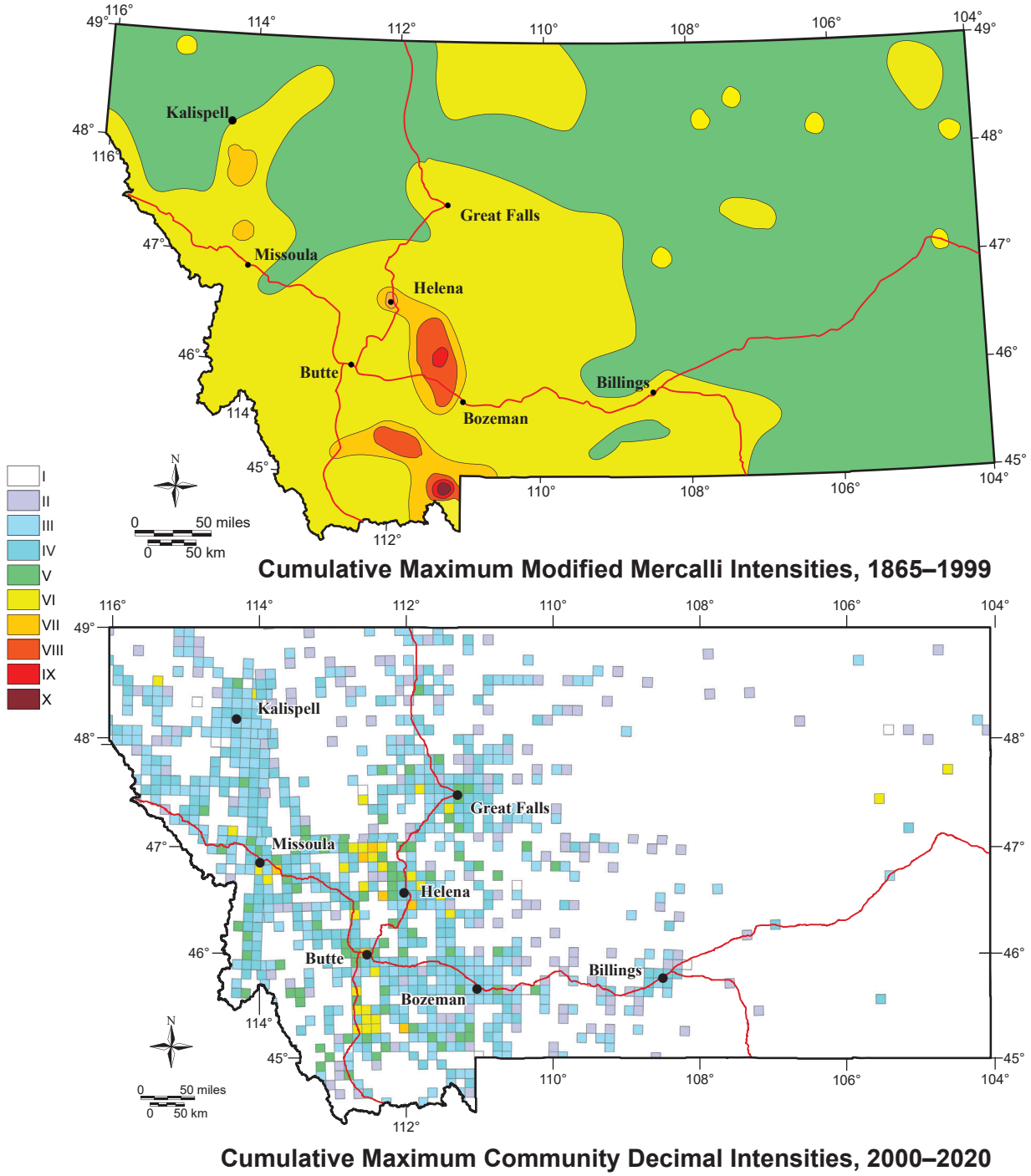

Figure 12. Top: Cumulative maximum Modified Mercalli Intensities from Montana isoseismal maps from 1909 to 1999, modified from Qamar and Stickney (1983). Note that the entire state experienced at least MMI V shaking during this period. Bottom: Cumulative maximum Community Decimal Intensities (CDI) 2001 through 2020 collected through the USGS Did You Feel It? (DYFI) system (https://earthquake.usgs.gov/data/dyfi/). CDI values are an aggregation of DYFI reports received from 10 x 10 km areas.

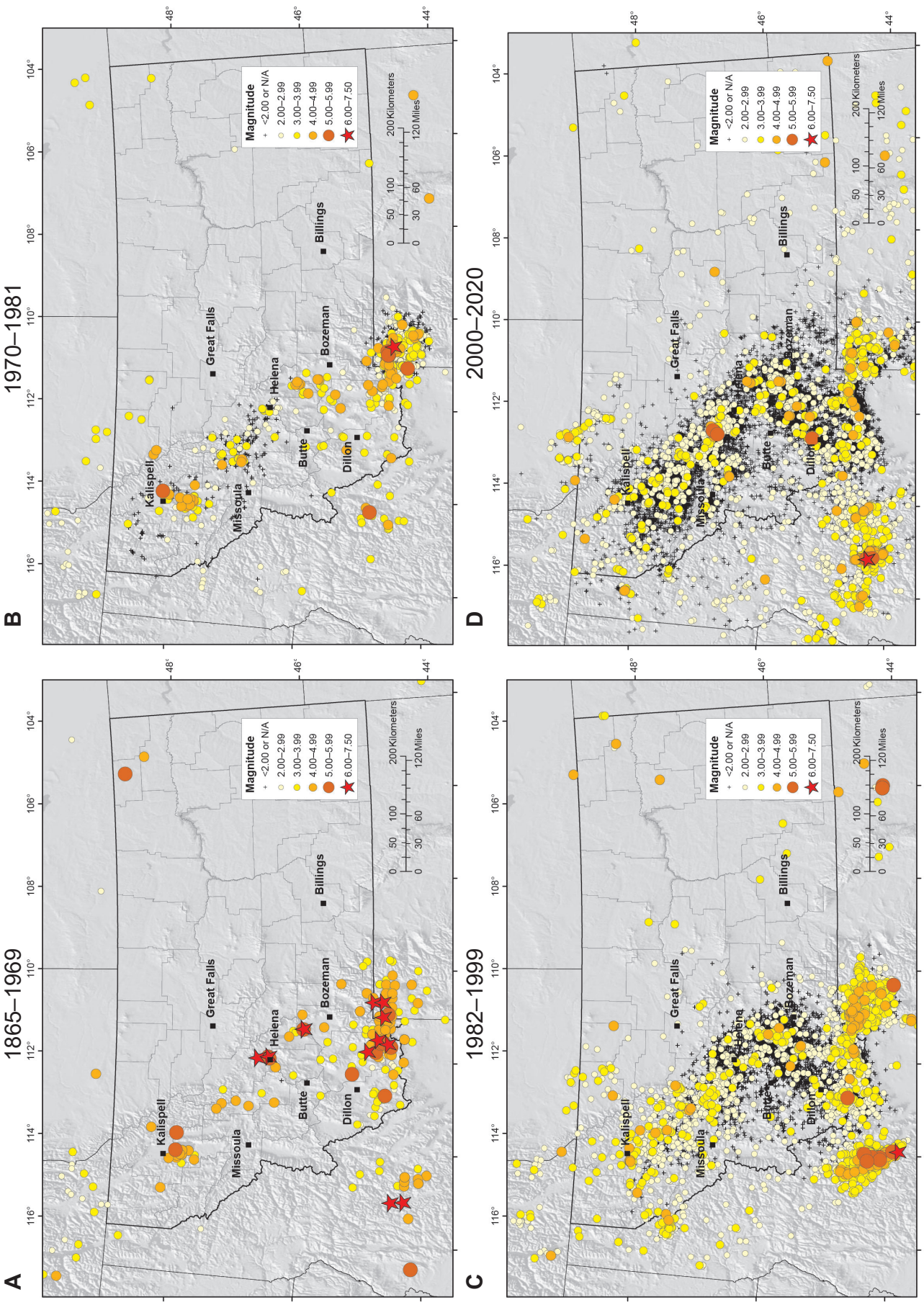

Figure 13. Seismicity in Montana and surrounding areas. (A) 1865–1969 (105 yr): historical seismicity, most epicenters prior to 1940 estimated from intensity reports, and later from very sparse regional seismographic coverage. All of Montana's magnitude 6.0 and larger earthquakes occurred during this period. (B) 1970–1981 (12 yr): epicenters determined from sparse regional seismographic coverage and the advent of temporary and telemetered networks. (C) 1982–1999 (18 yr): early permanent telemetered networks provide better coverage for limited areas. (D) 2000–2020 (21 yr): permanent regional networks provide at least minimally adequate monitoring coverage of most seismically active areas, and software tools together with the Internet allow real-time incorporation of data from regional stations.

north of Dillon. No detectable foreshocks occurred in the impending epicentral area for 22 mo prior to the mainshock. A vigorous aftershock sequence included 2 magnitude 4+ earthquakes, 41 magnitude 3+, and at least 1,450 locatable earthquakes during 22 mo. Aftershocks in the first few days formed a 6.5 by 3.5 km (4.0 b y 2.2 mi) NNE-trending elliptical zone roughly centered on the mainshock. The mainshock occurred 10.5 ± 1.0 km (6.5 ± 0.6 mi) below the surface, and a significant portion of the aftershocks with hypocenters deeper than 10 km (6.2 mi) occurred during the first 24 h. Two months after the mainshock, aftershocks concentrated north and south of the mainshock epicenter, and the extent of the aftershock zone had slightly expanded. The mainshock focal mechanism determined from P-wave first motion and from waveform inversions indicated normal slip on a N- or NW-trending fault. Stickney (2007) suggested a N-trending fault dipping 44° to 58° E as the seismic source. Most aftershock hypocenters occurred no shallower than 7 km (4.4 mi) below the surface (Stickney, 2006b) and occupy a wedge-shaped volume above the inferred fault plane. Fault plane solutions for the two largest aftershocks indicated strike-slip movement. T-axes from fault plane solutions are consistent with the regional northeast–southwest extensional stress field. The 2005 Dillon earthquake is a classic example of a moderate-magnitude ISB earthquake on a blind fault in an area lacking Quaternary faults with unremarkable previous seismicity.

July 6, 2017, Lincoln

The largest Montana earthquake in 53 years occurred 13 km (8.1 mi) ESE of Lincoln on July 6, 2017 (fig. 1). The largest earthquake in the lower 48 states during 2017, this M_w 5.8 earthquake produced MMI VI shaking in the epicentral area. Perceptible shaking extended from Seattle, WA to western South Dakota and from Edmonton, Alberta to Salt Lake City, UT. The shaking knocked items from shelves within 100 km (62 mi) of the epicenter and residents of Lincoln, the nearest town, experienced a power outage. No serious injuries occurred nor were reports of serious damage received, due in part to the sparse population in the immediate epicentral area. This earthquake occurred within the MRSN, and the MBMG located the mainshock hypocenter at a depth of 13.4 ± 0.5 km (8.3 ± 0.3 mi) below sea level. A vigorous aftershock sequence followed immediately, with magnitude 5.0 and 5.1 aftershocks occurring 5 min, 18 s, and 87 min after the mainshock, respectively. The mainshock moment tensor solution indicates strike-slip faulting, either sinistral (left-lateral) slip on a fault striking N13°E or dextral (right-lateral) slip on a fault striking N75°W. The latter nodal plane matches the orientation and slip sense of nearby Lewis and Clark Zone faults, but more than 400 aftershocks that occurred through September 30, 2017 formed an 8-km-long (5-mi-long) NNE-trending zone, implying that the NNE-striking nodal plane represents the fault plane (McMahon and others, 2017, 2018). The USGS deployed three temporary broadband stations in the epicentral area shortly after the mainshock, and the MBMG used these data together with MRSN data to locate more than 3,800 aftershocks through December 2020. A subset of aftershocks extends up to 20 km (12 mi) ESE and 30 km (19 mi) WNW of the mainshock epicenter, parallel to the primary structural grain of the Lewis and Clark Zone. Smith and others (2021) used data from a temporary aftershock deployment together with MRSN station data to determine precise aftershock locations and concluded that the aftershock clusters extending primarily westward from the mainshock resulted from bookshelf faulting along a series of N-trending, left-lateral strike-slip faults within the WNW–ESE Lewis and Clark Zone. The 2017 Lincoln earthquake occurred at least 25 km (16 mi) from the nearest recognized Quaternary fault, demonstrating yet again that most areas of western Montana are vulnerable to significant ground shaking resulting from moderate magnitude earthquakes on blind faults.

SEISMOGRAPHIC MONITORING

Early Seismograph Stations, 1931–1970

Piecemeal instrumental seismic monitoring began relatively late in Montana as compared to other regions of the U.S. In Montana, only three seismograph stations opened before 1960 and only five operated by 1970 (fig. 14A). Smith and Arabasz (1991) provide a brief overview of early instrumentation along the ISB. Below is a brief description of seismic monitoring efforts in Montana.

The earliest seismograph station in Montana was operated by the Montana State University Physics department with funding from the U.S. Coast and Geodetic Survey. Station BZM began operating in May 1931 in the basement of Roberts Hall on the campus of Montana State University in Bozeman and closed in March 1968. The MSU Physics department also operated a World Wide Standardized Seismograph Sta-

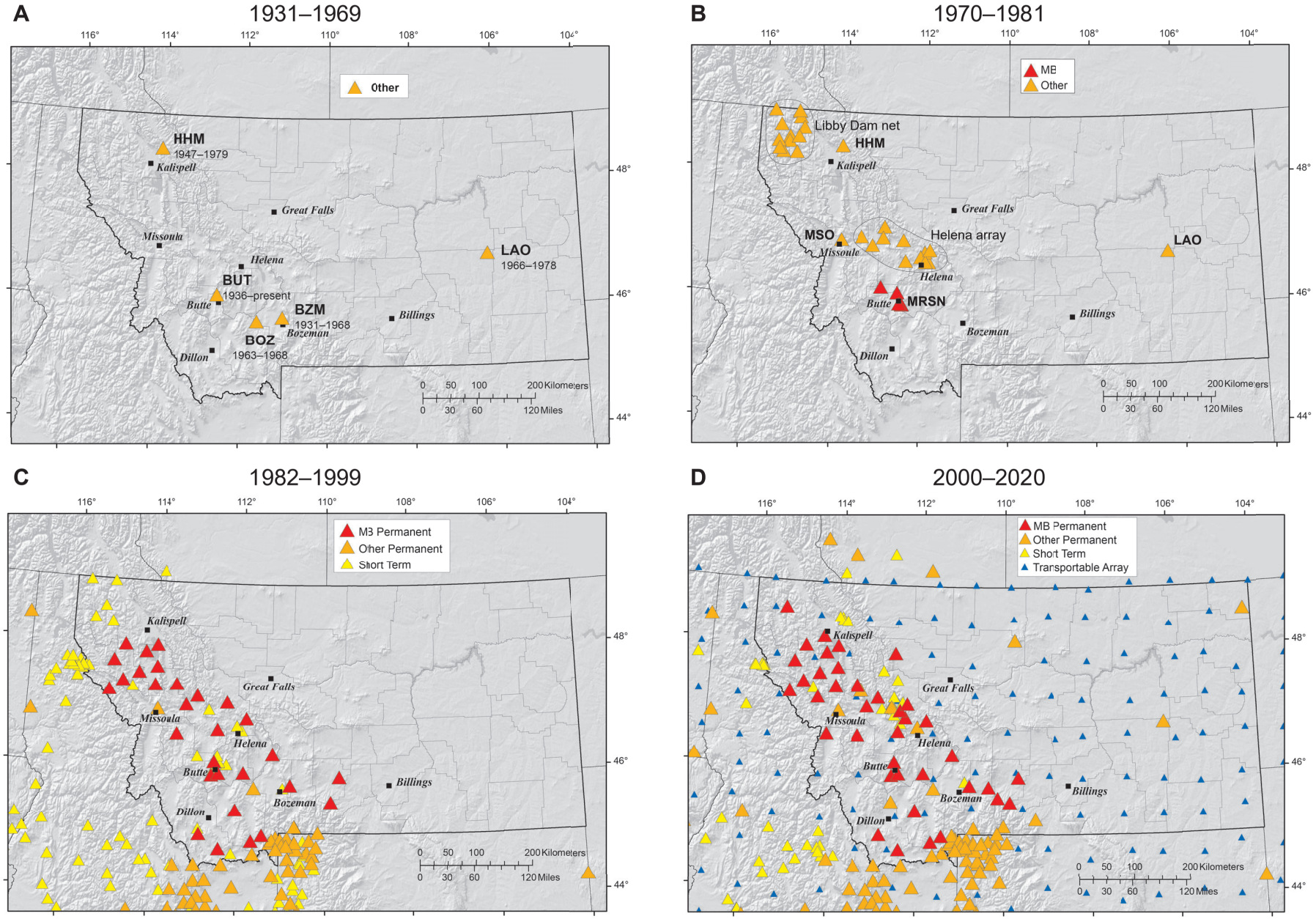

Figure 14. Evolution of seismic monitoring in Montana. Note that not all seismograph stations operated for the full duration of the time periods shown. (A) Early Montana seismographs (1931–1969) labeled with their station codes and dates of operation. Data were recorded on-site on photographic drum recorders except for LAO, which had analog telephone-based telemetry. (B) Early telemetered networks and continuing early stations (1970–1981). Red triangles are MBMG Montana Regional Seismograph Network stations (MB network code) and orange triangles are Montana stations operated by other institutions. Temporary seismograph deployments not shown. (C) Seismograph stations used by the MBMG to locate Montana and surrounding seismicity (1982–1999). Red triangles are MBMG stations (MB network code), orange triangles are permanent stations operated by other institutions, yellow triangles are seismograph stations that operated for limited periods (months to a few years), mainly by other institutions, but includes a few MB stations that were relocated to new sites. Initially, most of these stations were recorded on drum recorders but later transitioned to triggered digital recording. (D) Recent seismograph stations used to locate Montana and surrounding seismicity (2000–2020). Red, orange, and yellow triangles as in C. Small blue triangles are IRIS Transportable Array (TA) stations that operated for about 2 yr at each site and migrated from west to east between 2006 and 2012. Almost all of the data produced by these stations were collected by the MBMG as continuous, near real-time digital data streams, except for TA stations for which just event seismograms were collected.

tion (WWSSN) in an underground seismic vault about 45 km (28 mi) west of Bozeman (BOZ) from 1963 to 1968. Following the closure of BOZ, the equipment was moved to a new surface vault near Missoula and opened as WWSSN station MSO in November 1973, where the University of Montana Geology department operated it with USGS support through 1980. After losing USGS funding, the Geology department continued to operate MSO with declining reliability until its closure in 1987. MSO reopened as a USGS backbone network station in August 2002 and BOZ reopened as a USGS backbone network station in 1999.

Following the 1935 Helena earthquakes, the U.S. Department of Commerce funded the Montana School of Mines Physics department to operate the Butte seismograph (BUT), which opened in August 1936 in the basement of the Metallurgy Building on the Montana School of Mines campus. The U.S. Geological Survey funded the Butte station from 1944 through December 1979, after which the MBMG took over its operation. The Butte station has undergone several generations of instrumentation and was moved about 45 m from the Metallurgy Building to the basement of the Museum Building, but continues operation to present, making it the longest continuously operating station in Montana.

The U.S. Bureau of Reclamation opened the Hungry Horse seismograph station (HHM) in November 1947, ahead of the 1953 completion of the nearby Hungry Horse Dam. The USGS took over operation of the station about 1960 and closed the station in December 1979.

The Ford Aerospace and Communications Corporation operated an array of seismograph stations in eastern Montana for the U.S. Air Force Advanced Research Projects Agency beginning in 1966. The Large Aperture Seismic Array (LASA) consisted of 525 seismometers arranged in 21 star-shaped subarrays distributed over a 200 km diameter (124 mi diameter; Green and others, 1965; Hedlin and others, 2000). LASA was designed and operated to detect and discriminate distant underground nuclear explosions but provided some data for earthquakes in Montana (Bakun and others, 2011). Eight of LASA's subarrays closed in 1974 and the central station (LAO) apparently operated through February 1978. Two stations in the D ring (LD1 and LD3) continued operating through at least December 1980. LAO reopened as a U.S. Geological Survey national backbone network station in July 2004.

The U.S. Army Corps of Engineers opened the Libby Dam station (LDM) in February 1970 about 4 mi (6.4 km) upstream from the newly constructed Libby Dam. This station operated until 1986. The site sat abandoned and slated for demolition when the MBMG adopted the seismic vault and reopened LDM in 2003. Information about the instrumentation at these early Montana seismograph stations is available in Poppe (1980).

Early Seismographic Network Studies, 1970–1981

Introduction

The early 1970s saw the advent of battery-powered, portable seismograph stations, which enabled the first reconnaissance seismic surveys to reveal background seismicity patterns and faulting styles in Montana. At least 15 temporary seismic network deployments are reported in the literature between 1970 and 1982. This period also saw the first telemetered networks in Montana (fig. 14B), which included five networks variously operated by the U.S. Geological Survey, the University of Montana, the U.S. Army Corps of Engineers, and the U.S. Air Force Technical Applications Center (the LASA described above). None of these telemetered networks operated for more than 10 yr; however, the USGS Yellowstone network (which provides some monitoring coverage for Montana) formed the basis of the modern Yellowstone network. The MBMG also began installing stations of the MRSN in 1980 (fig. 14B), discussed below in the *Early Permanent Network Monitoring* section.

These early instrumental monitoring efforts identified seismically active areas along the northern ISB (fig. 13B), established that earthquake swarms occur in western Montana, and provided the first evidence that earthquake focal depths are typically shallow, with depths of less than 15 km (9.3 mi) below the surface. Most early portable network deployments lasted from days to weeks and comprised 6 to 12 stations; thus few earthquakes were sufficiently well recorded to determine fault plane solutions. To compensate for this shortcoming, P-wave first motions for groups of earthquakes were combined to produce composite fault plane solutions, under the assumption that multiple earthquakes in a region occurred on the same or similarly oriented faults in response to a uniform stress field. Despite the uncertainty of the underlying assumption, composite fault plane solutions began to reveal the nature of active faulting and the basic ori-

entation of the regional stress fields along the northern ISB. Below, some results of these early networks are discussed by geographic region, beginning in northwest Montana, then moving to west-central Montana, into southwest Montana, and finally to northeast Montana.

Northwest Montana

The ISB in northwest Montana (north of 47°N) is historically active, with reports of felt earthquakes going back to 1924. An energetic earthquake swarm centered southwest of Flathead Lake began in April 1969 and proceeded in fits and starts through December 1971. This swarm included 36 earthquakes with magnitudes ranging from 4.0 to 4.9. The two earliest temporary network deployments in northwest Montana targeted the Flathead earthquake swarm. As part of an end-to-end ISB survey Sbar and others (1972) deployed six seismograph stations in the Swan and Flathead Valleys from August 29 to 31, 1969. During this brief deployment, they located 10 earthquakes clustered in Big Arm Bay of Flathead Lake and recorded over 30 other small earthquakes with similar S minus P intervals. A composite fault plane solution for the earthquakes forming this cluster suggested slip on a N-trending, W-dipping normal fault. Several other microearthquakes detected during this deployment "were located near enough to known recently active faults to suggest that they may be associated with these faults" (Sbar and others, 1972).

Stevenson (1976) analyzed data from a nine-station seismic network deployed around Flathead Lake from October 13 through November 29, 1971 and located 259 earthquakes with magnitudes ranging from 0.1 to 3.3. Most epicenters formed two clusters—a southern cluster, comprised of 173 earthquakes, with dimensions of 11 by 5 km (6.8 by 3.1 mi) centered 8 km (5 mi) northwest of Polson, and a northern cluster, comprised of 54 earthquakes, about 4 km (2.5 mi) in diameter centered 21 km (13 mi) northwest of Polson, just north of Big Arm Bay. Thirty-two additional earthquakes occurred in the surrounding area, including five epicenters that form a weak northerly alignment near the center of the northern half of Flathead Lake. A cross-section of hypocenters in the southern cluster from October 29 through November 13, 1971 formed a distinct planar zone dipping 70°NE and striking N30°W. During the preceding and following 15-day periods, hypocenters did not form an obvious planar zone. This temporal variability of hypocenter distributions seems compatible with the variety of fault plane solutions Stevenson (1976) reported, which included strike-slip, normal, and reverse mechanisms. Six of the 10 fault plane solutions have first motion patterns that are compatible with two different mechanisms and 6 of the 10 are composites of two to four individual earthquakes. However, one unambiguous, single-event fault plane solution shows normal slip on an NNW-trending fault, but the dip of the NE-dipping nodal plane is about 45° shallower than the NE-dipping zone observed on the cross-section. Stevenson (1976) suggested that most of the focal mechanisms are consistent with N–S compression, but E–W extension appears equally plausible.

Stickney (1980) studied earthquakes that occurred in the Kalispell Valley north of Flathead Lake from August 1974 through September 1979 using data from regional and local seismograph stations. An earthquake sequence began in late December 1974, intensified in January and February 1975, when a magnitude 5.0 earthquake occurred on February 4, before gradually dying out in April 1975. Intermittent activity continued through October 1976. Four seismograph stations near Libby Dam, four stations in central Idaho, nine stations between Missoula and Helena, and a single station near Hungry Horse Dam provided data with which to study the Kalispell Valley seismicity. Data from a 4-day deployment of five portable seismograph stations in August 1976 and a 28-day deployment of six portable stations in August–September 1979 supplemented the earthquake dataset. Stickney (1980) found that most epicenters formed a 20-km-long (12-mi-long), NE–SW-trending zone that crossed the Kalispell Valley between the towns of Creston and Big Fork. The orientation of the NE–SW epicenter zone coincided with the direction of greatest epicentral uncertainty, but he argued that other data supported the zone of epicenter distribution and that it was not simply an artifact of sub-optimum station distribution. Fault plane solutions suggested that the largest earthquakes resulted from oblique-normal slip on a NE-trending, NW-dipping normal fault (the Creston Fault) identified using gravity data.

Qamar and others (1982) examined the location and timing of earthquakes in the Flathead Lake area of northwest Montana. They noted that instrumentally located epicenters occurred north and west of Flathead Lake, typically well separated from the bold range fronts of the Swan and Mission Mountains, which are

bounded by Quaternary—but apparently dormant—faults. Swarms of earthquakes have occurred near Flathead Lake in 1945, 1952, 1964, 1969, 1971, and 1975, leading Dunphy (1972) to suggest that 3 m seasonal lake level changes may have triggered seismicity. To test whether seismicity correlated with seasons, Qamar and others (1982) performed a statistical analysis of seismicity from 1930 through 1979 and concluded that they could not reject the hypothesis that earthquakes occur randomly during the year. Qamar and others (1982) also used acoustic subbottom profiling equipment to examine lake bottom sediments, which revealed areas of disturbed sediments but no clear evidence of young faulting offsetting the sediments. They concluded that the disturbed sediments were more likely due to the retreat of the Cordilleran ice sheet that occupied the lake basin about 10,000 years ago rather than from seismic shaking resulting from a large, local earthquake. The trenching results of Ostenaa and others (1995) identified evidence for a magnitude ~7.5 earthquake 7,700 ± 200 yr ago that ruptured the southern section of the Mission Fault, which provides a plausible nearby source of strong seismic shaking (10–20% g, USGS Scenario Earthquake Catalog) for generating sediment disturbance and slumping in Flathead Lake.

West-Central Montana

West-central Montana (the ISB between latitudes 47°N and 45.5°N) includes the source areas of the 1925 Clarkston Valley earthquake (M 6.6) and the 1935 Helena earthquakes (M 6.3, 6.0, and over 2,500 felt aftershocks), and numerous other earthquakes larger than M 3.8 (Stover and Coffman, 1993). Several early monitoring efforts provided initial information on the distribution, depth, and style of seismicity in this region.

Sbar and others (1972) deployed six seismographs with an aperture of about 120 km (75 mi) in the Three Forks–Townsend region from August 24 to 27, 1969. They located 11 earthquakes, 6 of which occurred up to 100 km (62 mi) outside the network. Four of the earthquakes located inside the network occurred in the general vicinity of the M 6.6, 1925 Clarkston Valley earthquake. No focal depths were greater than 15 km (9.3 mi). A composite fault plane solution suggesting oblique-reverse faulting was ambiguous.

Freidline and others (1976) operated six portable seismograph stations in three configurations in the Helena region from June 25 through August 18, 1973 to investigate a heat-flow anomaly near Marysville. They detected no seismicity in the immediate vicinity of the heat-flow anomaly but did locate 97 earthquakes during the survey. The seismicity occurred diffusely through a broad NW-trending zone mostly northwest of Helena. Clusters of epicenters with dimensions of about 7 km (4.4 mi) occurred near Marysville and about 10 km (6.2 mi) northwest of Helena. Hypocenters in the latter zone constitute a zone dipping 60° to 70° S, extending to a depth of 12 km (7.5 mi) below the surface. Composite fault plane solutions from the Scratchgravel Hills and Marysville area indicate both strike-slip and normal faulting, with similar NE–SW-oriented T-axes. Earthquake magnitudes during this survey ranged from 0.0 to 3.0 and a cumulative recurrence analysis of these data indicate a b-value of 0.7 ± 0.2. No earthquakes had focal depth greater than 17 km (10 mi). Friedline and others (1976) speculated that the seismicity between Marysville and Helena may represent the source zone of the 1935 earthquake sequence.

Stickney (1978) summarized 2 yr of data collected by the telemetered eight-station Helena array operated by the University of Montana (UM) Geology department. From October 1974 through September 1976, Helena array data yielded 441 earthquake locations with magnitudes ranging up to 3.9. Seismicity was diffuse and widely distributed throughout the 50 by 130 km (31 by 81 mi) array, with most hypocenters in the 5 to 15 km (3.1 to 9.3 mi) depth range and none deeper than 30 km (24 mi). Several seismicity concentrations in the eastern half of the array yielded composite fault plane solutions and hypocenter alignments interpreted as seismogenic faults. In the Scratchgravel Hills north of Helena, composite fault plane solutions suggested both strike-slip and normal faulting. A cross-section through the seismicity cluster in the southern Scratchgravel Hills, where a fault plane solution indicated normal faulting, revealed a near-vertical zone of hypocenters from 7 to 12 km (3.5 to 7.5 mi) deep, dipping steeply northeast. However, hypocenter uncertainty precluded conclusive identification of a fault plane. In the northern Scratchgravel Hills, hypocenters form a vertical zone from 1 to 18 km (0.62 to 11 mi) deep, suggesting that the NNE-trending nodal plane represents a left-lateral strike-slip fault. These results are quite similar to the seismicity patterns that Freidline and others (1976) observed in the Scratchgravel Hills. Stickney (1978) also discussed an earthquake swarm comprised of 56 earthquakes in the Avon

Valley, which yielded two composite fault plane solutions: an E–W-trending reverse fault for hypocenters 15 to 26 km (9.3 to 16 mi) deep and a NW-trending normal fault for hypocenters 6 to 15 km (3.7 to 9.3 mi) deep. Cross-sections of the hypocenter provide no useful information. A composite fault plane solution and hypocenter cross-section for seismicity in the Nevada Creek area suggested left-lateral movement on a NE-trending strike-slip fault. Finally, a composite fault plane solution for distributed seismicity in the Lincoln–Ovando area suggested normal slip along NW-trending faults.

Qamar and Hawley (1979) summarized the results of three microearthquake surveys in the Three Forks Basin plus seismicity recorded by the University of Montana's telemetered Helena array, deployed primarily northwest of Helena. A magnitude 4.4 earthquake occurred in the western Three Forks Basin on July 16, 1974 and prompted deployment of a three-station network of portable stations in the epicentral area. Over 48 h, the portable network recorded 29 locatable earthquakes, 19 of which had reasonably well-constrained focal depths with an average of 6 km (3.7 mi) below the surface. A composite fault plane solution using first motions from the mainshock and aftershocks suggested a strike-slip mechanism with a near-horizontal E–W-trending T-axis. A 5-day aftershock survey following the March 10, 1977 magnitude 4.8 earthquake revealed a cluster of over 40 aftershocks concentrated primarily in the southwest part of the Clarkston Valley. Several possible foreshocks were observed on a seismograph operating about 45 km (28 mi) to the southeast and the aftershock sequence was described as having "relatively few aftershocks," including three with magnitudes ranging from 2.7 to 3.2 during the first 32 h. A fault plane solution for the mainshock and two composite fault plane solutions for the aftershocks indicated normal faulting on N- and NW-trending normal faults with E–W-oriented T-axes, which is consistent with other fault plane solutions determined for recent earthquakes.

Qamar and Hawley (1979) also compared epicenters for nine earthquakes in the Three Forks region from 1974 through 1977 reported in the U.S. Geological Survey's Preliminary Determination of Epicenters (PDE) with epicenters determined by the University of Montana using data from all seismograph station data within 500 km (311 mi), including those in UM's Helena array and the USGS's Yellowstone network. They found that the PDE epicenters were mislocated 10 to 25 km (6.2 to 16 mi) generally northward of Qamar and Hawley's (1979) epicenters, by amounts ranging from two to five times the PDE epicenter uncertainty estimates. They explain this systematic epicenter mislocation as the result of the USGS not routinely using data from the Helena array and the Yellowstone network stations, and possibly, low upper mantle seismic velocities beneath Yellowstone and the Snake River Plain, which would affect P-wave travel times to stations farther south.

Southwest Montana

Southwest Montana [the ISB and the Centennial Tectonic Belt (CTB) south of 45.5°N latitude] is the most seismically active region of Montana. This region includes the 1959 M 7.3 Hebgen Lake earthquake and most of its aftershocks on the western flank of Yellowstone National Park and the persistent zone of seismicity corresponding to the CTB, extending 140 km (87 mi) WSW from Hebgen Lake westward into central Idaho.

Smith and others (1977) and Smith (1978) summarized the results of seismic surveys within and around Yellowstone National Park that lasted from 3 to 6 weeks involving 5 to 12 stations. Surveys in the summers of 1972, 1975, and 1976 included station deployments in Montana to the west, north, and northeast of Yellowstone. The most seismically active region near Yellowstone is the 75-km-long (47-mi-long) zone of seismicity extending from the northwest margin of the Yellowstone caldera westward to the southern Gravelly Range, which coincides with the aftershock zone of the 1959 earthquake. The 1975 survey provided the first detailed monitoring of the SW-trending seismicity band extending from the southern Madison Valley through the southern Gravelly Range, which cuts obliquely across the Centennial Valley, and on westward through central Idaho. Smith and Sbar (1974) termed this zone of diffuse earthquake epicenters the Idaho seismic zone. Stickney and Bartholomew (1987) used the distribution of epicenters together with late Quaternary faults to define the CTB, which largely coincides with the part of the Idaho seismic zone in Montana. Smith and others (1974) presented fault plane solutions for the northwest corner of the Yellowstone and Hebgen Lake area that define an E–W zone of N–S extension that coincides with the 1959 aftershock zone. An epicenter map summarizing seismicity from the first 5 yr of the Yellowstone network

(Pitt, 1979) illustrated the high level of seismicity in the northwest corner of Yellowstone National Park that extends westward into the Hebgen Lake Basin and the southern Madison Valley.

Smith and Sbar (1974) hypothesized that the seismicity along the northern ISB and the Idaho seismic zone, which extended westward from the Hebgen Lake region, defined the margins of the "Northern Rocky Mountain subplate." They argued that this subplate moves westward relative to stable North America and northward relative to the "Great Basin subplate," perhaps driven by a mantle plume beneath Yellowstone.

As mentioned above, Qamar and Hawley (1979) demonstrated that nine Clarkston Valley area earthquakes (magnitudes 3.0 to 4.4) from 1974 to 1977 reported in the U.S. Geological Survey Preliminary Determination of Epicenters were systematically mislocated an average of 18 km (11 mi) north or northwest of their true epicenter positions. Dewey (1987) documented a similar effect when relocating early instrumental events in central Idaho, and Doser (1985) recognized a bias of up to 10 km (6.2 mi) to the NNE for the 1959 Hebgen Lake earthquake and its aftershocks. This systematic mislocation likely reflects a bias in the regional seismic monitoring coverage prior to 1980, when seismic ray paths to many regional seismograph stations crossed velocity heterogeneities associated with the Yellowstone–Snake River Plain volcano-tectonic province (Xiaohua and Humphreys, 1998) and slower upper mantle velocities of the Basin and Range province to the south (Herrin and Taggart, 1962; Tesauro and others, 2014). Earlier instrumental epicenter determinations for the 1925 earthquake (Byerly, 1926; Dewey and others, 1973) most likely also suffered from this same bias. Pardee (1926) observed the "abrupt and abnormal decline of intensity" that "coincides suggestively" with the northern edge of the Snake River Plain.

Northeast Montana

Although most Montana earthquakes occur along the ISB or the CTB in western Montana, northeast Montana does exhibit some seismicity (figs. 1, 2). The largest and earliest northeast Montana earthquake occurred in 1909 as discussed above in the *Historical Seismicity* section. Marcuson and Krinitzsky (1976) reviewed historical seismicity in northeast Montana as part of a dynamic analysis of Fort Peck Dam. The second largest northeast Montana earthquake occurred on June 25, 1943 and generated MMI VI shaking at several towns (Bodle, 1945), cracked a "well-constructed" granary at Froid, and damaged chimneys and plaster at Homestead, Redstone, and Reserve (Coffman and Von Hake, 1982). Horner and Hasegawa (1978) estimated a magnitude of "about 4" for the 1943 event. Bakun and others (2011) compiled a list of instrumental earthquake locations, most of which were recorded by the Large Aperture Seismic Array, in northeast Montana and adjacent Saskatchewan and argue that they are consistent with slip along two NE-trending basement fault zones. The early dates of the two largest northeast Montana earthquakes precede extensive oil and gas field activities in the adjacent Williston Basin, and thus indicate that they are natural tectonic earthquakes characteristic of central U.S. seismicity. Although recent years have seen extensive oil and gas development activities in northeast Montana, there has been no concomitant increase in seismicity in contrast to what is observed elsewhere in the central U.S.

Summary

These early temporary network campaigns primarily used analog drum recorders that included stand-alone chronometers with significant daily drifts that required time corrections. The various institutions that conducted these temporary deployments and analyzed the data they recorded used a variety of crustal velocity models and differing methods for determining earthquake locations, in some cases utilizing graphical methods. The intermittent operation of these early networks and their spatial variability precluded a uniform and coherent earthquake catalog at magnitude less than about 4.0 during this period. The original seismograms from these deployments are scattered, and by in large, lost to history. Also, most hypocenter information was not published or archived (with several notable exceptions), so figures showing epicenter maps from the original publications are the only representations of these early epicenters. Despite these limitations, these early studies revealed many of the seismological characteristics of the northern ISB (fig. 13B), including the shallow nature of seismicity, swarm activity in some areas, background seismicity that does not coincide with mapped Quaternary faults, and the northerly oriented T-axes in the Hebgen Lake region reoriented to more E–W orientations in west-central and northwest Montana.

Montana Regional Seismic Network Monitoring, 1982–1999

Early in 1980, the U.S. Geological Survey ended funding to support three permanent seismograph stations operating in Montana, which required daily site visits to change and develop photographic paper on which seismograms were written. The Hungry Horse station (HHM) closed, the University of Montana continued to operate the Missoula station (MSO) on an *ad hoc* basis through 1987, and the MBMG took over operation of the Butte station (BUT) from the Montana College of Mineral Science and Technology (now Montana Technological University). The MBMG also opened the Earthquake Studies Office in 1980 and began establishing telemetered seismograph stations near Butte and Anaconda (fig. 14C). This marked the beginning of the MRSN, although sufficient instrumentation for routine earthquake locations was still 2 yr in the future. The closure of the Berkeley Pit open-pit copper mine in Butte and its subsequent flooding spurred State support for monitoring possibly induced seismicity in the Butte area, and by 1982, a sufficient number of stations existed to locate earthquakes (fig. 13C) and begin publishing an annual earthquake catalog. During the late 1980s and early 1990s, the MBMG expanded its seismic monitoring capabilities in southwest Montana. During the mid-1990s, a USGS grant and collaboration with University of Idaho researchers allowed expanded monitoring in west-central Montana along the Lewis and Clark Zone, and a cooperative agreement with the Confederated Salish and Kootenai Tribes of the Flathead Reservation allowed expanded monitoring in northwest Montana. Initially, analog seismograms were recorded on paper records and read by hand, a laborious and time-consuming process. Early triggered digital recording began in 1994, and continuous digital recording with Earthworm software began in 1999.

From 1982 through 1994 the MBMG published annual earthquake catalogs using data from all available local and regional seismograph stations (Stickney, 1984, 1985, 1986, 1987, 1988, 1989, 1991, 1993, 1994, 2006a). The MBMG discontinued printed seismicity catalogs after they became available online and contributes seismicity data (including data from the earlier printed catalogs) to the USGS Comprehensive Earthquake Catalog (ComCat) in addition to its own catalog/viewer (MBMG Mapper). After collecting earthquake data for 15 yr, primarily in southwest Montana, Stickney (1997) reanalyzed seismic data collected by the MRSN up to that time. He began by developing a new crustal velocity model using measured travel time from 13 mining and construction blasts, supplemented with arrival time data from 1,174 well-recorded earthquakes with locations widely distributed around southwest Montana. Using this improved velocity model, he relocated over 12,400 earthquakes that made up the catalog up to that time. Stickney (1997) then determined 390 fault plane solutions from earthquakes having sufficient P-wave first motion data and systematically discussed the seismicity and faulting for 17 subregions in southwest Montana that cover the northern Intermountain Seismic Belt between Hebgen Lake and Helena, and the eastern Centennial Tectonic Belt from Hebgen Lake westward to the Montana–Idaho border. This study confirmed that most of southwest Montana is under the influence of NE–SW-directed extensional tectonic forces, except for an E–W zone extending from Hebgen Lake through the Centennial Valley (corresponding to the eastern CTB), which is experiencing N–S-directed extension. A subset of fault plane solutions from this latter area suggests E–W compression as indicated by at least 20 predominately reverse faulting mechanisms. Stickney's (1997) analysis indicated that relatively few well-located hypocenters with accompanying fault plane solutions are associated with mapped Quaternary faults—even in cases where the hypocenters are proximal to faults. The dataset included seismicity from two areas with significant earthquake swarms, the 1987 Norris swarm and three swarms in the Red Rock Valley (1984, 1985, 1995–1996). During these periods of intensified seismicity, the fault plane solutions exhibited a greater diversity of T-axis orientations as compared to general background seismicity in the surrounding regions.

Norris Swarm

The Norris earthquake swarm began May 27, 1987 with a magnitude 3.2 event and numerous aftershocks. This swarm occurred outside of the MRSN as it existed at that time, so Stickney (1997) deployed a temporary network of five portable seismographs for 48 h, which allowed accurate hypocenters for 57 earthquakes. The epicenters formed a tight cluster about 1 km (0.6 mi) south of Beartrap Hot Springs (now known as Norris Hot Springs) with focal depths 3 to 6 km (1.9 to 3.7 mi) below the surface. Seismicity near Norris continued at the rate of one locatable

event per 2 days through mid-July, when seismicity increased to over 10 events per day. This increased seismicity motivated a second deployment of three portable seismographs on July 19. The largest shock of the swarm occurred July 22 with a magnitude of 4.1, which local residents felt with a maximum MMI of V. The portable seismographs recorded approximately 1,000 microearthquakes per day July 22–23. Continuing high seismicity levels prompted the deployment of five additional seismographs on August 18 and four more on August 21, for a total of 11 stations operating at 15 sites in the 10 by 10 km (6.2 by 6.2 mi) region surrounding the swarm. The full network operated for 8 days and recorded over 700 locatable earthquakes. The Norris swarm included 20 events with magnitudes of 3.0 or larger (Stickney, 1988). The better-located epicenters form an elongate, NW-trending zone about 8 km (5 mi) long and 5 km (3.1 mi) wide with focal depths ranging from 3.5 to 7 km (2.2 to 4.4 mi) below the surface. Fault plane solutions indicate that the earthquakes resulted from normal and oblique-normal faulting. Only 3 of 61 fault plane solutions indicate strike-slip faulting. A variety of fault plane solutions indicate that multiple faults slipped during the Norris swarm, but the average T-axis orientation of N57°E is consistent with the regional extension direction (Stickney, 1988). Focal mechanisms for earthquakes shallower than 4.5 km (2.8 mi) typically had steeply NE-dipping nodal planes (interpreted as the fault plane), and earthquakes deeper than 5.5 km (3.4 mi) typically had steeply SW-dipping nodal planes, leading Stickney (2007) to infer that a conjugate set of faults accommodated slip during the swarm. The maximum concentration of seismicity occurred in the 4.5 to 5.5 km (2.8 to 3.4 mi) depth range where these inferred faults intersect or overlap.

The Bradley Creek Fault is a N30°W-trending, NE-dipping Quaternary fault about 5 km (3.1 mi) southwest of Norris. Kennelly and Stickney (2000) used a planar regression to fit the Norris swarm hypocenters to a poorly fitting, NW-trending, NE-dipping plane that is similar to the surface trace of the Bradley Creek Fault. They speculated that slip at depth along the Bradley Creek Fault may account for some of the Norris swarm seismicity, but the poor spatial fit and numerous fault plane solutions lacking nodal planes compatible with the mapped fault indicate that the Bradley Creek Fault is not solely responsible for the 1987 Norris earthquake swarm.

Red Rock Valley Seismicity

Three earthquake swarms have occurred in the Red Rock Valley, northwest of Lima, since the inception of the MRSN. The Red Rock Valley is a NW-trending, 50-km-long (31-mi-long) graben bounded on the southern half of its southwest margin by the Red Rock Fault and bounded on the northern half of its northeast margin by the Monument Hill Fault. The southern half of the Red Rock Valley is historically aseismic, with most seismicity concentrating near the midpoint of the valley between the adjacent end points of the two valley-bounding faults. Stickney and Lageson (2002) interpreted the seismicity concentration near where valley-bounding fault geometry changes as a structural crossover zone. The 1984 and 1985 Red Rock Valley earthquake swarms occurred when the MRSN lacked good monitoring coverage for this region. By the time the 1996–1997 swarm occurred, the MRSN included two stations near the Red Rock Valley, and the Idaho National Engineering and Environmental Laboratories had expanded their seismic monitoring coverage to the south and west of the Red Rock Valley, enabling significantly improved hypocenters. Each of the three earthquake swarms included from over 80 to 120 locatable earthquakes, with 4 to 7 earthquakes in the magnitude 3.0 to 3.8 range. Fault plane solutions for the 1996–1997 swarm indicate primarily normal faulting on faults striking NW–SE to E–W. The magnitude 3.8 earthquake on December 28, 1996 (the largest of the swarm) has a fault plane solution indicating normal slip on a NW-trending fault, possibly compatible with slip at depth on the northern end of the Red Rock Fault. However, magnitude 3.5 and 3.7 earthquakes on January 17, 1996 and March 10, 1996 both indicate normal slip on an E–W fault(s), clearly incompatible with slip at depth on either the Red Rock or Monument Hill Faults (Stickney, 1997).

A magnitude 5.3 earthquake occurred on August 20, 1999 in the central Red Rock Valley, about 6 km (3.7 mi) west of the 1996–1997 swarm center. The largest Montana earthquake for 25 yr and the first magnitude 5.0+ Montana earthquake since establishment of the MRSN, the Red Rock Valley earthquake produced perceptible shaking over a region of 108,000 km^2 (41,699 mi^2) with a maximum MMI of V in the epicentral area (Stickney and Lageson, 2002). A vigorous aftershock sequence motivated deployment of a four-station temporary network surrounding the mainshock epicenter to complement the closest MRSN

permanent station, positioned just 8.5 km (5.3 mi) northwest of the epicenter. The temporary network detected nearly 200 aftershocks during the 3-day deployment—we chose 45 aftershocks recorded on all five local stations for further analysis. The largest aftershock, with a magnitude 4.0, occurred less than 6 h after we deployed the temporary network. We used the hypocenter and origin time of this large aftershock to compute station delays for permanent stations in the surrounding region. We then used these station delays to locate the aftershock hypocenters and relocate seismicity in the Red Rock Valley area for the previous 10 yr. The mainshock and largest aftershock both occurred 12.5 km (7.8 mi) below the surface. Aftershock epicenters form a tight cluster about 3 km in diameter, with the mainshock epicenter near the center of the cluster. Viewed in cross-section, the mainshock and largest aftershock are the two deepest events at 12.5 km and the other aftershocks occupy a V-shaped volume 12 to 8.5 km (7.5 to 5.2 mi) deep, directly above the mainshock hypocenter. The mainshock focal mechanism, determined from P-wave first motions and also from moment tensor inversion of waveforms, indicates normal slip on a fault striking about N70°W (Stickney and Lageson, 2002). We chose the S-dipping nodal plane as the probable fault plane. Although the 1999 Red Rock Valley earthquake occurred on a normal fault, down-dip from the adjacent Red Rock Fault, Stickney and Lageson (2002) suggested that the 30° discrepancy between the strike of the fault plane solution nodal planes and the surface fault trace precludes this event from having occurred at depth on the Red Rock Fault. Rather, they think this earthquake occurred on a blind fault that is part of a structural crossover between the north end of the Red Rock Fault and the south end of the Monument Hill Fault. This structural crossover zone is marked by frequent seismicity, including a magnitude 5.0 earthquake on January 6, 1965 (Dewey, 1987) that occurred close to the 1999 epicenter. Earthquake epicenters since 1988 relocated with the station delays surround, but largely avoid, the down-dip projection of the southern Red Rock Valley adjacent to the Holocene segment of the Red Rock Fault, providing yet another example of recent background seismicity occurring near, but not along, active range front faults.

Northwest Montana Seismicity

Lageson and Stickney (2000) reviewed historic seismicity in northwest Montana and used MRSN-recorded seismicity and fault plane solutions to construct a seismotectonic model for northwest Montana and adjacent areas. The review of northwest Montana seismicity revealed that ISB seismicity extends across the east half of the Lewis and Clark Zone and extends north of Kalispell. There are also earthquakes that occur outside the ISB, east of the Rocky Mountains in the Cut Bank area. Earthquakes in this region generally have poorly determined hypocenters because they are well outside the MRSN and distant from seismograph stations.

The largest earthquake in northwest Montana for the 1982–2000 period discussed by Lageson and Stickney (2000) was a magnitude 4.9 in the southern Swan Range on April 1, 1985. This earthquake exhibited a strike-slip fault plane solution, as do most other recent earthquakes with fault plane solutions in northwest Montana. A significant earthquake swarm occurred southwest of Kalispell near the town of Kila. During May and June of 1995, the Kila swarm included 13 events with magnitudes ranging from 2.5 to 4.5, with 10 events having magnitudes greater than 3.0 and four events having magnitudes greater than 4.0. The magnitude 4.5 event occurred May 2, 1995 and was strongly felt in the epicentral area but lacked reported damage. Unfortunately, the Kila swarm preceded the expansion of MRSN stations into northwest Montana, so there are insufficient data for accurate hypocenters and for fault plane solutions. Prior to the expansion of seismic monitoring stations in northwest Montana, the threshold for complete detection and location was magnitude 2.8 (Lageson and Stickney, 2000). Following expansion of the MRSN into northwest Montana, D'Alessandro and Stickney (2012) conservatively estimated a threshold of completeness in the Flathead Valley of magnitude 1.2. North-trending normal faults dominate the identified Quaternary faults in northwest Montana north of the Lewis and Clark Zone (Stickney and others, 2000), yet paradoxically, nearly all focal mechanisms from this area indicate strike-slip faulting in response to E to ENE extension and/or N to NNW compression.

The western half of the Lewis and Clark Zone (westward from Missoula) is dramatically less seismically active than the eastern half. Long-term seismic monitoring has defined two seismically active areas in the western Lewis and Clark Zone: the Coeur d'Alene mining district just west of the Montana border in northern Idaho, and the Alberton–Frenchtown seismic

zone (discussed below). Most seismicity in the Coeur d'Alene mining district is induced by deep underground metal mines (Sprenke and others, 1991; Stickney and Sprenke, 1993). However, a magnitude 4.1 earthquake with a depth of 10 ± 3.8 km (6.2 ± 2.4 mi) on August 1, 1988, centered in Montana about 15 km (9.3 mi) northeast of the Coeur d'Alene mining district, has a fault plane solution that shows strike-slip faulting (Sprenke and others, 1991). The nodal planes indicate either sinistral slip on a N-trending fault or dextral slip on a W-trending fault. Although lacking identified Quaternary offset, the nearby Thompson Pass and Osburn Faults exhibit dextral slip and trend E–W, leading Sprenke and others (1991) to interpret the E–W nodal plane as the fault plane.

Montana Regional Seismic Network Monitoring 2000–2020

This period saw dramatic improvements in data recording and analysis capabilities and also digital archiving of continuous seismic waveform data. A few additional seismograph station deployments provided improved coverage of previously under-monitored regions. Implementation of Earthworm software in 1999 allowed the MBMG to continuously record seismic data from all Montana seismograph stations at the Earthquake Studies Office along with numerous stations in Wyoming, Idaho, Washington, and Canada operated by other agencies (fig. 14D). Prior to the implementation of Earthworm software, seismic data collected from northwest Montana stations were recorded on a local computer and these data were mailed to the Earthquake Studies Office in Butte for later analysis and integration into the Montana earthquake catalog weeks or months later—a time-consuming and labor-intensive process.

In the early 2000s, cooperative efforts with the Spokane Research Center of the National Institutes of Health enabled expanded seismic monitoring in south-central Montana near active platinum–palladium mines. From 1999 through 2006, the U.S. Geological Survey, with assistance from MBMG personnel, established 6 broadband stations across Montana. These modern digital seismograph stations are part of the Advanced National Seismic System 100-station backbone array, which provides uniform coverage for magnitude 2.5–3.0 and larger earthquakes across the lower 48 states. The MBMG established a station in the Bitterroot Valley in 2004 and a broadband station near Libby Dam in 2013 to improve monitoring in areas lacking adequate coverage. In the immediate aftermath of the 2005 Dillon earthquake, the USGS established a broadband station near Dillon that now operates as part of their Intermountain West network.

Zeiler and others (2005) developed an improved crustal velocity model with which to locate earthquake hypocenters. From 2000 to 2015, MBMG personnel used Seismic Analysis Code (Goldstein and others, 2003) to measure seismic phase times, amplitudes, and coda durations from digital seismograms and HYPO71 (Lee and Valdes, 1985) to determine earthquake hypocenters and magnitudes. This analysis procedure proved vastly superior to previous techniques but still lacked the processing efficiency for routine regional network data analysis, especially during seismic crises such as the 2005 Dillon aftershock sequence. Beginning in September 2015, with extensive assistance from the University of Utah Seismograph Stations, the MBMG implemented AQMS and Jiggle software for routinely processing network data, marking a revolutionary improvement in seismic analyst efficiency and analysis completeness. The current network provides a completeness threshold of about magnitude 1.5 for most of the Montana portion of the ISB (D'Alessandro and Stickney, 2012). Since August 15, 2001, all seismic data collected by the MRSN have been archived at the IRIS Data Management Center with a network code of MB. Seismograph network data recorded and analyzed since 2000 provide the most complete characterization of Northern Rocky Mountain seismicity yet available (fig. 13D).

Southwest Montana Seismicity

Stickney (2007) summarized 12 southwest Montana earthquakes with magnitudes of 4.0 or greater recorded by the MRSN that occurred from 1987 through 2007. A magnitude 4.6 earthquake occurred May 8, 2007 in the Ruby Valley, 8 km (5 mi) southeast of Sheridan, in a region of very low historical seismicity. MMI V shaking damaged several masonry buildings in Sheridan. The Sheridan earthquake occurred 13.6 ± 0.4 km (8.5 ± 0.2 mi) below the surface. A weak aftershock sequence (27 events with magnitudes 0.5 to 2.7) formed a NW-trending zone 3 km (1.9 mi) long and 1 km (0.6 mi) wide. Twelve days after the mainshock, aftershock activity increased dramatically and included the largest aftershock (M 3.0). This later surge of aftershock activity defined a second NW-trending zone, subparallel and 2 to 3 km (1.2 to 1.9 mi) northeast of the initial zone, suggesting activa-

tion of a second fault (Stickney, 2008). The mainshock focal mechanism, as determined from a P-wave first motion fault plane solution and from waveform inversion, indicates normal slip along a NNW-trending fault dipping 55° to 65° northeast. Projected upward from the mainshock hypocenter, this plane daylights close to the Ruby Range northern border fault. This geometric relation and the northwest aftershock trend suggest that slip on a small, subsurface patch of the Ruby Range northern border fault caused the 2007 Sheridan earthquake (Stickney, 2007). This is one of only a handful of examples of small or moderate magnitude earthquakes in Montana that are plausibly associated with slip at depth along a mapped Quaternary fault.

Another example of a moderate-magnitude earthquake likely associated with a mapped Quaternary fault is the February 5, 2006, magnitude 4.6 Centennial Valley earthquake (Stickney, 2007). This earthquake occurred within the eastern Centennial Tectonic Belt (Stickney and Bartholomew, 1987) within a persistent belt of epicenters extending from the southern Madison Valley southwestward through the southern Gravelly Range, traversing obliquely across the Centennial Valley and into the western Centennial Range. The area within 10 km (6.2 km) of the mainshock epicenter experienced more than 340 earthquakes during the preceding 25 yr, including 7 earthquakes in the magnitude 3.5 to 4.6 range. An abbreviated aftershock sequence consisting of four events (maximum magnitude 2.2) occurred over 3 days—unusually weak given the mainshock size and significant level of previous seismicity. The mainshock hypocenter occurred 14.0 ± 0.5 km (8.7 ± 0.3 mi) below the surface. The focal mechanisms determined from P-wave first motions and from waveform inversion indicate normal slip with a small oblique component. The inferred fault plane strikes E–W and dips about 65° N. Three previous nearby earthquakes have similar focal depths and focal mechanisms. Projected upwards from the hypocenter, a plane passing near all four hypocenters with N-dipping nodal planes intersects the surface near the trace of the Centennial Fault with an angle of 57°, a reasonable dip for a range-front normal fault. Although the 2006 Centennial Valley earthquake and three smaller events have hypocenters and focal mechanism consistent with slip at depth along the Centennial Fault, the majority of earthquakes with fault plane solutions for this area are incompatible with slip on the Centennial Fault (Stickney, 1997).

Stickney (2007) reviewed seismological data for four other significant southwest Montana earthquakes: August 7, 1989 near Manhattan, M 4.2; October 28, 1998 near Waterloo, M 4.1; October 31, 2005, Beaverhead Mountains, M 4.6; and June 18, 2006 near Pony, M 4.0. Focal mechanisms for all four earthquakes indicate normal or oblique-normal faulting, although P-wave first motion data for the 1989 Manhattan event are also compatible with strike-slip faulting. The 1998 Waterloo epicenter is close to the Quaternary Tobacco Root fault, but the focal depth and fault plane solution are incompatible with slip at depth along this fault. Likewise, none of the other events are apparently associated with mapped Quaternary faults. Aftershock sequences for these events ranged from a single magnitude 1.4 earthquake 29 h after the Beaverhead Mountains event to elevated seismicity rates that lasted for years for the Waterloo event. The NE–SW T-axis orientations for all events are consistent with the regional stress fields (Stickney and Bartholomew, 1987).

Northwest Montana Seismicity

Stickney (2011) recognized the Alberton–Frenchtown seismic zone (AFSZ) on the basis of 191 epicenters clustered in an E–W-trending, 35 by 10 km (22 by 6.2 mi) zone. The towns of Alberton and Frenchtown lie near the west and east ends of this zone, respectively. The east end of the AFSZ terminates near the Ninemile Fault, a suspected Quaternary fault, but no compelling evidence suggests that slip at depth along this fault is responsible for any AFSZ seismicity. Most well-located earthquakes have focal depths 10 to 15 km (6.2 to 9.3 mi) below the surface, typical of seismicity elsewhere along the northern ISB. Most of the 11 fault plane solutions indicate N–S normal faulting plus some strike-slip faulting for AFSZ earthquakes. The spatial distribution of the fault plane solutions indicates that multiple faults must accommodate AFSZ seismicity. The average T-axis orientation for earthquakes with fault plane solutions is near horizontal at S78°W, similar to other areas in western Montana.

Stickney (2015) analyzed MRSN data from the northern ISB to investigate possible differences in seismicity occurring south, within, and north of the eastern Lewis and Clark Zone and possible relationships with mapped Quaternary faults. The analysis included more than 13,000 earthquake hypocenters and 157 well-determined fault plane solutions, and incorporated data from the IRIS Transportable Array

(IRIS, 2018), which operated stations in Montana from 2006 to 2010 (fig. 14D). Stickney (2015) discussed 19 seismicity groupings and clusters—most of which contained multiple fault plane solutions—extending 300 km (186 mi) along the northern ISB from the Clarkston Valley south of Townsend northwestward to the Flathead Lake area. Recent seismicity has a patchy distribution that is not clearly associated with Quaternary faults. Numerous seismicity clusters occur in areas remote from mapped Quaternary faults, while other clusters occur near the end points or within the footwall blocks of Quaternary faults. Also present are aseismic patches and areas of low seismicity, some of which exist near the subsurface extent of Quaternary faults, such as the Canyon Ferry and Mission Faults. Holocene or latest Pleistocene scarps along these faults demonstrate that these aseismic patches have not always been so, and at some future time will likely become active again.

Seismicity in the region east of the Mission Fault and north of the Lewis and Clark Zone includes a subset of earthquakes with atypically deep hypocenters. This region is near the northeast margin of the MRSN, so the reliability of these deeper hypocenter determinations is problematic. However, while the Transportable Array (fig. 14D) operated in this region of Montana, numerous temporary stations provided crucial data that confirmed 127 earthquake hypocenters 20 to 25 km (12 to 16 mi) deep, and in a few cases up to 32 km below the surface. Most of these uncharacteristically deep events occurred in a 40-km-wide (25-mi-wide) belt north of the Lewis and Clark Zone, but 7 occurred within the eastern Lewis and Clark Zone (Stickney, 2015). Deep hypocenters proximal to the Mission, Swan, and South Fork Flathead Faults raise the possibility that these faults may store elastic energy to depths about 25 percent greater than the typical 15 km (9.3 mi) assumed in hazard analyses, suggesting unexpectedly large earthquakes may occur along these faults. Seventeen fault plane solutions for the deep events have normal and strike-slip focal mechanisms, similar to nearby seismicity with more typical shallow depths. Earthquake fault plane solutions indicate normal, oblique-normal, and strike-slip faulting. Just a few strike-slip mechanisms include a component of reverse faulting. The average T-axis orientation for earthquakes within and south of the Lewis and Clark Zone strikes 68° and plunges 2°, while for earthquakes north of the Lewis and Clark Zone, this orientation strikes 87° and plunges 4°. The apical half angle (a measure of the scatter in data points) for both groups is about 30°. This apparent 25° change in the extension direction is consistent with the northerly trend of Quaternary faults north of the Lewis and Clark Zone compared to the more northwesterly fault trend within and south of the Lewis and Clark Zone. Stickney (2015) notes that recent seismicity forms a nearly continuous swath along the northern ISB, but there is a 60-km-long (37-km-long) gap in the recognized Quaternary fault distribution between Ovando and the Helena Valley (Stickney and others, 2000). The presence of Lewis and Clark Zone strike-slip faults with documented Tertiary and older offsets in this area and numerous fault plane solutions with strike-slip mechanisms suggest the possibility that unrecognized, active, strike-slip faults may exist in this part of the ISB.

SUMMARY

Montana has a long history of significant earthquakes, and the entire State has experienced MMI V or greater shaking at least once during the past 110 years (fig. 12). The epicentral regions of major western Montana earthquakes have experienced destructive shaking levels from at least four historic earthquake sequences. However, only during the past four decades have systematic seismic recording, analysis, reporting, and archival become standard practice. The current MRSN configuration includes 44 stations extending more than 500 km (311 mi) from near the western edge of Yellowstone National Park to far northwest Montana. The MRSN is capable of detecting and locating earthquakes of magnitude 1.5 and larger throughout most of western Montana (D'Alessandro and Stickney, 2012). From 2000 through 2020, the MBMG used MRSN data to locate more than 37,874 earthquakes within Montana (fig. 13D), an average of about 1,800 earthquakes annually but ranging from 829 earthquakes in 2000 to 4,594 earthquakes in 2017. Montana seismicity rates during the first half of the 20th century are most likely higher than current rates (fig. 15), but the lack of earlier instrumentation limits our knowledge to only the most basic information about the larger historical events. The fact that Helena residents felt over 2,500 during the 1935 earthquake sequence implies that perhaps 25,000 or more would have been large enough for today's network to record and locate. Despite the absence of major earthquakes since 1982 when the MRSN began cataloging seismicity, 66,618 earthquake hypocenters and associated data

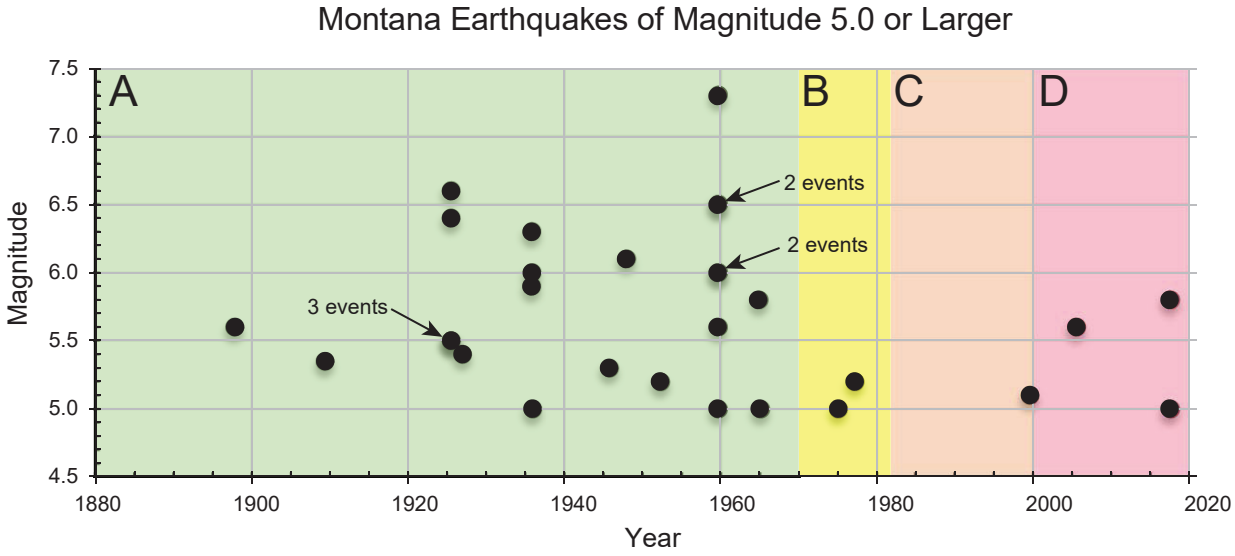

Figure 15. Montana earthquakes of magnitude 5.0 or larger from 1897 to 2020. The colored time blocks labeled A–D correspond to time ranges delineated in figures 13 and 14 (except that fig.14A begins in 1931). Incomplete written records prior to 1900 allow the possibility that M 5 earthquakes went undocumented. Note that there were three M 5.5 aftershocks of the 1925 Clarkston Valley earthquake, and two M 6.0 and two M 6.5 aftershocks of the 1959 Hebgen Lake earthquake. All of Montana's magnitude 6 or larger earthquakes occurred while seismic monitoring coverage was in its infancy (see fig. 14A) and only two earthquakes of magnitude 5.5 or larger have occurred since the inception of the Montana Regional Seismic Network (see figs. 14C, 14D).

have provided important insights into the relationships between seismicity and Quaternary faults, modern tectonic processes, and earthquake hazards along the ISB in Montana.

The vast majority of seismicity occurs within the ISB, and this belt, including the CTB, marks the zone of highest seismic hazard in Montana. The USGS National Seismic Hazard Map (https://www.usgs.gov/media/images/2018-long-term-national-seismic-hazard-map), which is based on historical and recent seismicity along with Quaternary fault information, reflect this fact. In many cases ISB seismicity occurs in the vicinity of mapped Quaternary faults. However, where sufficient hypocenter accuracy and focal mechanism data permit, there are only a few notable examples of plausibly relating small or moderate magnitude earthquakes to slip at depth on recognized Quaternary faults. The vast majority of ISB seismicity apparently occurs at depth along faults lacking recognized surface expression. Most major range-bounding Quaternary faults, including the Bitterroot and Emigrant Faults, which lie outside the ISB as defined by recent seismicity, show a virtual absence of seismicity during the historical record. Yet this cannot always be so—late Quaternary scarps along these faults that offset glacial deposits demonstrate that major earthquakes (and presumably aftershock sequences) have occurred on these faults in areas devoid of modern seismicity. We must infer that our current picture of seismogenic areas is only an incomplete snapshot of seismicity patterns that include long-term variations.

Fault plane solutions determined from P-wave first motions, supplemented with moment tensor solutions for larger earthquakes (generally M 4 or greater), indicate that extensional tectonic forces generate normal and strike-slip faulting in western Montana seismicity. The extension direction of these tectonic forces varies from approximately E–W in northwest Montana to NE–SW in southwest Montana, to about N15°E–S15°W in the Hebgen Lake Basin, southern Madison Valley, and Centennial Valley. The latter stress field is likely influenced by the Yellowstone–Snake River Plain volcanotectonic province.

CONCLUSIONS

Montana is a seismically active state with the potential for earthquakes as large as magnitude 7.5. The largest earthquakes are likely to occur on recognized faults, but moderate-magnitude earthquakes (M 5.5–6.5) may occur anywhere along the ISB, and still have the potential to cause significant damage if they occur near populated areas. Earthquake data collected with the MRSN, complemented by occasional temporary station deployments, have revolutionized our understanding of seismicity along the northern ISB. Ironically, the past 39 years—the period of the best seismic monitoring coverage in Montana's history—coincides with a period lacking destructive larger earthquakes in Montana and the occurrence of only three mainshocks

in the magnitude 5.0 to 5.8 range. Montana has high seismic hazard, and the risk of earthquake-related damage increases as the population and infrastructure of Montana continue to grow. We cannot prevent or predict earthquakes, so we must learn to live with them. A healthy seismic monitoring network that incorporates modern technology will continue to provide a better understanding and characterization of the seismic hazards facing the citizens of Montana.

ACKNOWLEDGMENTS

This paper benefited from comments on an early draft by Craig DePolo. Reviews by Bruce Presgrave and especially Walter Arabasz greatly improved this paper. The figures benefited from the cartographic skills of Susan Smith, MBMG. Layout and editing by Susan Barth, MBMG.

REFERENCES CITED

Agarwal, R.G., 1962, Earthquake of May 15, 1909: Journal of the Alberta Society of Petroleum Geologists, v. 10, no. 4, p. 198–202.

Anderson, C.R., and Martinson, M.P., 1936, Helena Earthquakes: Helena, Mont., Independent Publishing Company, 129 p.

Bakun, W.H., Stickney, M.C., Rogers, G., and Ristau, J., 2010, Modified Mercalli intensity assignments for the May 16, 1909, Northern Plains earthquake: U.S. Geological Survey Open-File Report 2010-1185, v. 1.1, 96 p., available at https://pubs.usgs.gov/of/2010/1185/ [Accessed 8/12/2021].

Bakun, W.H., Stickney, M.C., and Rogers, G.C., 2011, The 16 May 1909 northern Great Plains earthquake: Bulletin of the Seismological Society of America, v. 101, p. 3065–3071.

Bakun, W.H., and Wentworth, C.M., 1997, Estimating earthquake location and magnitude from seismic intensity data: Bulletin of the Seismological Society of America, v. 87, p. 1502–1521.

Bakun, W.H., and Wentworth, C.M., 1999, Erratum to Estimating earthquake location and magnitude from seismic intensity data: Bulletin of the Seismological Society of America, v. 89, p. 557.

Bodle, R.R., 1945, United States earthquakes 1943: U.S. Department of Commerce, Coast and Geodetic Survey, 49 p.

Byerly, P., 1926, The Montana earthquake of June 28, 1925, G.M.C.T.: Bulletin of the Seismological Society of America, 16, p. 209–265.

Coffman, J.L., von Hake, C.A., and Stover, C.W., 1982, Earthquake history of the United States: U.S. Department of Commerce, National Oceanic and Atmospheric Administration and U.S. Department of the Interior, Geological Survey, Publication No. 41-1, revised edition, [through 1980], 258 p.

ComCat, https://earthquake.usgs.gov/data/comcat/ [Accessed 8/12/2021].

Coues, E. (ed.), 1893, History of the expedition under the command of Lewis and Clark (1804–06): New York, Francis P. Harper, 4 vol., 1364 p.

D'Alessandro, A., and Stickney, M., 2012, Montana Seismic Network performance: An evaluation through the SNES method: Bulletin of the Seismological Society of America, v. 102, p. 73–87.

Da Costa, J.A., 1964, Effect of Hebgen Lake earthquake on water levels in wells in the United States: U.S. Geological Survey Professional Paper 435-O, p. 167–178.

Dewey, J.W., 1987, Instrumental seismicity of central Idaho: Bulletin of the Seismological Society of America, v. 77, p. 819–836.

Dewey, J.W., Dillinger, W.H., Taggart, J., and Algermissen, S.T., 1973, A technique for seismic zoning: Analysis of earthquake locations and mechanisms in northern Utah, Wyoming, Idaho and Montana: NOAA Technical Report, ERL267-ESL30, p. 28–48.

Doser, D.I., 1985, Source parameters and faulting processes of the 1959 Hebgen Lake, Montana, earthquake sequence: Journal of Geophysical Research, v. 90, p. 4537–4555.

Doser, D.I., 1989, Source parameters of Montana earthquakes (1925–1964) and tectonic deformation in the northern Intermountain seismic Belt: Bulletin of the Seismological Society of America, v. 79, p. 31–50.

Dunphy, G.J., 1972, Seismic activity of the Kerr Dam–S.W. Flathead Lake Area, Montana, *in* Earthquake Research in NOAA: U.S. Department of Commerce, NOAA Technical Report ERL 236-ESL 21, p. 59–61.

Friedline, R.A., Smith, R.B., and Blackwell, D.D., 1976, Seismicity and contemporary tectonics of the Helena, Montana area: Bulletin of the Seismological Society of America, v. 66, p. 81–95.

Green, P.E., Frosch, R.A., and Romney, C.F., 1965, Principles of an experimental large aperture seismic array (LASA): Proceedings of the IEEE, v. 53, no. 12, p. 1821–1833, doi: 10.1109/PROC.1965.4453.

Goldstein, P., Dodge, D., Firpo, M., and Minner, L., 2003, SAC2000: Signal processing and analysis tools for seismologists and engineers, *in* Lee, W.H.K., Kanamori, H., Jennings, P.C., and Kisslinger, C., The IASPEI International Handbook of Earthquake and Engineering Seismology, Academic Press, London.

Gutenberg, B, and Richter, C.F., 1954, Seismicity of the Earth and associated phenomena: New York, Hafner Publishing Inc., 310 p.

Hadley, J.B., 1964, Landslides and related phenomena accompanying the Hebgen Lake Earthquake of August 17, 1959: U.S. Geological Survey Professional Paper 435-K, p. 107–138.

Heck, N.H., 1935, U.S. Coast and Geodetic Survey field engineering bulletin, v. 9, p. 38–39.

Heck, N.H., 1938, Earthquake history of the United States: U.S. Department of Commerce, Coast and Geodetic Survey, Serial 609, 85 p.

Heck, N.H., and Bodle, R.R., 1931, United States earthquakes 1929: U.S. Department of Commerce, Coast and Geodetic Survey, Serial 511, 55 p.

Heck, N.H., and Eppley, R.A., 1958, Earthquake history of the United States, Part 1, continental U.S. and Alaska (exclusive of California and western Nevada), revised edition (through 1956): U.S. Department of Commerce, Coast and Geodetic Survey, Publication no. 41-1, 80 p.

Hedlin, M.A.H., Earle, P., and Bolton, H., 2000, Old seismic data yield new insights: Eos Transactions, American Geophysical Union, v. 81, no. 41, p. 469–480.

Herrin, E., and Taggart, J., 1962, Regional variations in Pn velocity and their effect on the location of epicenters: Bulletin of the Seismological Society of America, v. 52, p. 1037–1046.

Herrin, E., Tucker, W., Taggart, J., Gordon, D.W., and, Lobdell, J.L., 1968, Estimation of surface focus P travel times: Bulletin of the Seismological Society of America, v. 58, p. 1273–1291.

Horner, R.B., and Hasegawa, H.S., 1978, The seismotectonics of southern Saskatchewan: Canadian Journal of Earth Sciences, no. 15, p. 1341–1355.

Horner, R.B., Stevens, A.E., and Hasewaga, H.S., 1973, The Bengough, Saskatchewan, earthquake of July 26, 1972: Canadian Journal of Earth Science, v. 10, p. 1805–1821.

IRIS, 2018, Incorporated Research Institutions for Seismology website: http://ds.iris.edu/ds/nodes/dmc/earthscope/usarray/ [Accessed 8/12/2021].

Johnson, M.V., and Omang, R.J., 1972, Degradation of the Earthquake Lake outflow channel, southwestern Montana: U.S. Geological Survey Professional Paper 800-C, p. C253–C256.

Kanamori, H., and Jennings, P.C., 1978, Determination of local magnitude, ML, from strong-motion accelerograms: Bulletin of the Seismological Society of America, v. 68, p. 471–485.

Kennelly, P.J., and Stickney, M.C., 2000, Using GIS for visualizing earthquake epicenters, hypocenters, faults and lineaments in Montana, *in* Digital Mapping Techniques '00—Workshop Proceedings: U.S. Geological Survey Open-File Report 00-325, available at http://pubs.usgs.gov/openfile/of00-325/kennelly.html [Accessed 5/16/2018].

Lageson, D.R., and Stickney, M.C., 2000, Seismotectonics of northwest Montana, USA, *in* Schalla, R.A., and Johnson, E.H., eds., Montana Geological Society 50th anniversary symposium, Montana/Alberta thrust belt and adjacent foreland, v. 1, p. 109–126.

Lee, W.H.K., and Valdes, C.M., 1985, HYPO71PC: A personal computer version of the HYPO71 earthquake location program: USGS Open-File Report 85-749, 113 p.

Lupien, J.E., 1936, The earthquakes of 1935 and the Helena, Montana, water system: American Waterworks Association Journal, v. 28, p. 908–911.

Marcuson, W.F., III, and Krinitzsky, E.L., 1976, Dynamic analysis of Fort Peck Dam, U.S. Army Corps of Engineers Final Report, S-76-1, 298 p.

MBMG Mapper, http://data.mbmg.mtech.edu/mapper/mapper.asp?view=Quakes& [Accessed 8/12/2021].

McMahon, N.D., Stickney, M., Aster, R.C., Yeck, W., Martens, H.R., and Benz, H., 2017, Spatiotemporal analysis of the foreshock-mainshock-aftershock sequence of the 6 July 2017 M5.8 Lincoln, Montana earthquake: Abstract S21B-0098 presented at 2017 Fall Meeting, AGU, New Orleans, La., 11–15 Dec.

McMahon, N.D., Yeck, W.L., Stickney, M.C., Aster, R.C., Martens, H.R., and Benz, H.M., 2018, Spatiotemporal analysis of the foreshock-mainshock-aftershock sequence of the 6 July 2017 M5.8 Lincoln, Montana earthquake: Seismological Research Letters Early Edition, doi: 10.1785/0220180180.

Myers, W.B., and Hamilton, W., 1964, Deformation accompanying the Hebgen Lake earthquake of August 17, 1959: U.S. Geological Survey Professional Paper 435-I, p. 55–98.

Morris, L.E., 2016, The 1959 Yellowstone earthquake: Charleston, S.C., Arcadia Publishing, 192 p., ISBN 978.1.62585.782.8.

Murphy, L.M., 1950, United States earthquakes 1947: U.S. Coast and Geodetic Survey, Serial 730, 62 p.

Murphy, L.M., and Brazee, R.J., 1964, Seismological investigations of the Hebgen Lake earthquake: U.S. Geological Survey Professional Paper 435-C, p. 13–17.

Murphy, M.L., and Cloud, W.K., 1954, United States earthquakes 1952: U.S. Coast and Geodetic Survey, Serial 773, 112 p.

Neumann, F., 1937, United States earthquakes 1935: U.S. Coast and Geodetic Survey, Serial 600, 90 p.

Nuttli, O.W., 1976, Design earthquakes for Fort Peck, Montana (Appendix B), *in* Marcuson, W.F. III and Krinitzsky, E.L. (authors), Dynamic analysis of Fort Peck Dam: U.S. Army Corps of Engineers Final Report, no. S-76-1, 298 p.

Nuttli, O.W., Bollinger, G.A., and Griffiths, D.W., 1979, On the relation between Mercalli Intensity and body-wave magnitude: Bulletin of the Seismological Society of America, v. 69, p. 893–909.

Ostenaa, D.A., Levish, D.R., and Klinger, R.E., 1995, Mission Fault study: U.S. Bureau of Reclamation Seismotectonic Report 94-8.

Pardee, J.T., 1926, The Montana earthquake of June 27, 1925, *in* Shorter contributions to general geology 1926: U.S. Geological Survey Professional Paper 147, p. 7–23.

Pitt, A.M., 1979, Preliminary map of earthquake epicenters in Yellowstone Park and vicinity, 1973–1978: U.S. Geological Survey Open-File Report 79-717, scale 1:250,000.

Pitt, A.M., Weaver, C.S., and Spence, W., 1979, The Yellowstone Park earthquake of June 30, 1979: Bulletin of the Seismological Society of America, v. 69, p. 197–205.

Poppe, B.B., 1980, Directory of world seismograph stations: U.S. Department of Commerce Report SE-25, Part 1, v. 1, 465 p.

Qamar, A., and Breuniger, R., 1979, Earthquake hazard to the proposed Northern Tier Pipeline in Montana, Northern Tier Report No. 4: Montana Department of Natural Resources and Conservation, Helena, 54 p.

Qamar, A., and Hawley, B., 1979, Seismic activity near the Three Forks Basin, Montana: Bulletin Seismological Society of America, v. 69, p. 1917–1929.

Qamar, A., and Stickney, M.C., 1983, Montana earthquakes, 1869–1979; Historical seismicity and earthquake hazard: Montana Bureau of Mines and Geology Memoir 51, 80 p.

Qamar, A., Kogan, J., and Stickney, M.C., 1982, Tectonics and recent seismicity near Flathead Lake, Montana: Bulletin of the Seismological Society of America, v. 72, p. 1591–1599.

Savage, J.C., Lisowski, M., Prescott, W.H., and Pit, A.M., 1993, Deformation from 1973 to 1987 in the epicentral area of the 1959 Hebgen Lake, Montana, earthquake (MS-7.5): Journal of Geophysical Research, v. 98, no. B2, p. 2145–2153.

Sbar, M.L., Barazangi, M., Dorman, J., Scholz, C.H., and Smith, R.B., 1972, Tectonics of the Intermountain seismic belt, western United States: Microearthquake seismicity and composite fault plane solutions: Geological Society of America Bulletin, v. 83, p. 13–28.

Scott, H.W., 1936, The Montana earthquakes of 1935: Montana Bureau of Mines and Geology Memoir 16, 47 p.

Smith, E.M., Martens, H.R., and Stickney, M.C., 2021, Microseismic evidence for bookshelf

faulting in western Montana; Seismological Research Letters 92, p. 802–809, doi: 10.1785/0220200321.

Smith, R.B., 1978, Seismicity, crustal structure, and intraplate tectonics of the interior of the western Cordillera, *in* Smith, R.B., and Eaton, G.P., eds., Cenozoic tectonics and regional geophysics of the western Cordillera: Geological Society of America Memoir 152, p. 111–144.

Smith, R.B., and Arabasz, W.J., 1991, Seismicity of the Intermountain Seismic Belt, *in* Slemmons, D.B., Engdahl, E.R., Zoback, M.D., and Blackwell, D.D., eds., Neotectonics of North America: Boulder, Colo., Geological Society of America, Decade Map, v. 1.

Smith, R.B., and Sbar, M.L., 1974, Contemporary tectonics and seismicity of the western United States with emphasis on the Intermountain Seismic Belt: Geological Society of America Bulletin, v. 85, p. 1205–1218.

Smith, R.B., Shuey, R.T., Freidline, R.O., Otis, R.M., and Alley, L.B., 1974, Yellowstone hot spot: New magnetic and seismic evidence: Geology, v. 2, p. 451–455.

Smith, R.B., Shuey, R.T., Pelton, J.R., and Bailey, J.P., 1977, Yellowstone hot spot: Contemporary tectonics and crustal properties from earthquake and aeromagnetic data: Journal of Geophysical Research, v. 82, p. 3665–3676.

Sprenke, K.F., Stickney, M.C., Dodge, D.A., and Hammond, W.R., 1991, Seismicity and tectonic stress in the Coeur d'Alene mining district: Bulletin of the Seismological Society of America, v. 81, p. 1145–1156.

Steinbrugge, K.V., and Cloud, W.K., 1962, Epicentral intensities and damage in the Hebgen Lake, Montana, earthquake of August 17, 1959: Bulletin of the Seismological Society of America, v. 52, p. 181–234.

Steinhart, J.S., and Myer, R.P., 1961, Explosion studies of the continental structure: Carnegie Institution of Washington, Publication 622, 409 p.

Stermitz, F., 1964, Effects of the Hebgen Lake earthquake on surface water: U.S. Geological Survey Professional Paper 435-L, p. 139–150.

Stevenson, P.R., 1976, Microearthquakes at Flathead Lake, Montana: A study using automatic earthquake processing: Bulletin of the Seismological Society of America, v. 66, p. 61–80.

Stewart, S.W., Hofmann, R.B., and Diment, W.H., 1964, Some aftershocks of the Hebgen Lake earthquake: U.S. Geological Survey Professional Paper 435-D, p. 19–24.

Stickney, M.C., 1978, Seismicity and faulting of central western Montana: Northwest Geology, v. 7, p. 1–9.

Stickney, M.C., 1980, Seismicity and gravity studies of faulting in the Kalispell Valley: MS thesis, University of Montana, 82 p.

Stickney, M.C., 1984, Montana seismicity 1982: Montana Bureau of Mines and Geology Open-File Report 149, 11 p.

Stickney, M.C., 1985, Montana seismicity 1983: Montana Bureau of Mines and Geology Open-File Report 160, 30 p.

Stickney, M.C., 1986, Montana seismicity 1984: Montana Bureau of Mines and Geology OpenFile Report 164, 42 p.

Stickney, M.C., 1987, Montana seismicity 1985: Montana Bureau of Mines and Geology OpenFile Report 188, 52 p.

Stickney, M.C., 1988, The 1987 Norris Montana earthquake swarm: Seismological Research Letters, v. 59, p. 15–16.

Stickney, M.C., 1988, Montana Seismicity 1986: Montana Bureau of Mines and Geology OpenFile Report 204, 39 p.

Stickney, M.C., 1989, Montana seismicity 1987: Montana Bureau of Mines and Geology OpenFile Report 222, 42 p.

Stickney, M.C., 1991, Montana seismicity 1988: Montana Bureau of Mines and Geology Open-File Report 240, 35 p.

Stickney, M.C., 1993, Montana Seismicity 1989: Montana Bureau of Mines and Geology Open-File Report 263, 46 p.

Stickney, M.C., 1994, Montana and adjacent areas earthquakes 1986, *in* Stover, C.W., and Brewer, L., eds., U.S. Geological Survey Bulletin 2089, p. 189–192.

Stickney, M.C., 1995, Montana seismicity report for 1990: Montana Bureau of Mines and Geology Miscellaneous Contribution 16, 44 p.

Stickney, M.C., 1997, Seismic source zones in southwest Montana: Montana Bureau of Mines and Geology Open-File Report 366, 51 p.

Stickney, M.C., 2006a, Montana seismicity report for 2004: Montana Bureau of Mines and Geology Miscellaneous Contribution 20, 61 p.

Stickney, M.C., 2006b, The 26 July 2005 MW 5.6 Dillon, Montana Earthquake: Seismological Research Letters, v. 77, p. 209.

Stickney, M.C., 2008, The May 8, 2007 Sheridan, Montana Earthquake: Seismological Research Letters, v. 79, p. 294.

Stickney, M., 2012, Road log for the Hebgen Lake earthquake area: Northwest Geology, v. 41, p. 71–82.

Stickney, M., 2015, Seismicity within and adjacent to the Eastern Lewis and Clark Line, West-central Montana: Northwest Geology, v. 44, p. 19–36.

Stickney, M.C., and Bartholomew, M.J., 1987, Seismicity and late Quaternary faulting of the Northern Basin and Range Province, Montana and Idaho: Bulletin of the Seismological Society of America, v. 77, p. 1602–1625.

Stickney, M.C., and Lageson, D.R., 2002, Seismotectonics of the 20 August 1999 Red Rock Valley, Montana, earthquake: Bulletin of the Seismological Society of America, v. 92, p. 2449–2464.

Stickney, M.C. and Smith, D., 2009, Recent seismicity in the western part of the 1959 Earthquake Aftershock Zone: 2009 Annual Meeting Geological Society of America Abstracts with Programs, v. 41, no. 7, p. 54.

Stickney, M.C. and Sprenke, K.F., 1993, Seismic events with implosional focal mechanisms in the Coeur d'Alene mining district, northern Idaho: Journal of Geophysical Research, v. 90, p. 6523–6528.

Stickney, M.C., Haller, K.M., and Machette, M.N., 2000, Quaternary faults and seismicity in western Montana: Montana Bureau of Mines and Geology Special Publication 114, map scale 1:750,000.

Stover, C.W., and Coffman, J.L., 1993, Seismicity of the United States, 1568–1989 (Revised): U.S. Geological Survey Professional Paper, no. 527, 418 p.

Swenson, F.A., 1964, Ground-water phenomena associated with the Hebgen Lake Earthquake: U.S. Geological Survey Professional Paper 435-N, p. 159–165.

Tesauro, M., Kaban, M.K., Mooney, W.D., and Cloetingh, S., 2014, NACr14: A 3D model for the crustal structure of the North American Continent: Tectonophysics, v. 631, p. 65–86, https://doi.org/10.1016/j.tecto.2014.04.016 [Accessed 8/12/2021].

Trimble, A.B., and Smith, R.B., 1975, Seismicity and contemporary tectonics of the Hebgen Lake-Yellowstone Park region: Journal of Geophysical Research, v. 80, p. 733–741.

Tuttle, D.S., 1909, Reminiscences of a missionary bishop: New York, Thomas Whittaker, 498 p.

Ulrich, F.P., 1936, Helena earthquakes: Seismological Society of America Bulletin, v. 26, p. 323–339.

U.S. Coast and Geodetic Survey (USCGS), 1959, Preliminary report Hebgen Lake, Montana earthquakes, August 1959: U.S. Department of Commerce, 15 p.

U.S. Geological Survey Global Catalog of Calibrated Earthquake Locations, https://www.sciencebase.gov/catalog/item/59fb91fde4b0531197b16ac7 [Accessed 8/12/2021].

U.S Geological Survey Scenario Earthquakes Catalog, https://earthquake.usgs.gov/scenarios/eventpage/mt2016montana_699b_se#shakemap [Accessed 8/12/2021].

von Hake, C.A., and Cloud, W.K., 1966, United States earthquakes 1964: U.S. Coast and Geodetic Survey, 91 p.

Vuke, S.M., and Stickney, M.C., 2013, Geologic map of the Clarkston Valley, Broadwater and Gallatin Counties, west-central Montana: Montana Bureau of Mines and Geology Open-File Report 642, 17 p, map scale 1:24,000.

Wallace, C.A., Lidke, K.J., and Schmidt, R.G., 1990, Faults of the central part of the Lewis and Clark Line and fragmentation of the Late Cretaceous foreland basin in west-central Montana; Geological Society of America Bulletin, v. 102, p. 1021–1037.

Witkind, I.J., 1964a, Events on the night of August 17, 1959—The human story: U.S. Geological Survey Professional Paper 435, p. 1–4.

Witkind, I.J., 1964b, Reactivated faults north of Hebgen Lake: U.S. Geological Survey Professional Paper 435, p. 37–50.

Witkind, I.J., Myers, W.B., Hadley, J.B., Hamilton, W., and Fraser, G.D., 1962, Geologic features of the earthquake at Hebgen Lake, Montana, August 17, 1959: Bulletin of the Seismological Society of America, v. 52, p. 163–180.

Wong, I., Olig, S., Dober, M., Wright, D., Nemser, E., Lageson, D., Silva,W., Stickney, M., Lemieux, M., and Anderson, L., 2005, Probabilistic earthquake hazard maps for the state of Montana: Montana Bureau of Mines and Geology Special Publication 117, 72 p. plus CD.

Wood, H.O., and Neumann, F., 1931, Modified Mercalli intensity scale of 1931: Bulletin of the Seismological Society of America, v. 21, p. 277–283.

Xiaohua, P., and Humphreys, E.D., 1998, Crustal velocity structure across the eastern Snake River Plain and the Yellowstone Swell: Journal of Geophysical Research, v. 103, p. 7171–7186.

Zeiler, C.P., Stickney, M.C., and Speece, M.A., 2005, Revised velocity structure of western Montana: Bulletin of the Seismological Society of America, v. 95, p. 759–762.

APPENDIX A

MODIFIED MERCALLI INTENSITY SCALE

APPENDIX A

Modified Mercalli Intensity Scale of 1931 (abridged) from Wood and Neumann (1931).

I. Not felt except by a very few under especially favorable circumstances.

II. Felt only by a few persons at rest, especially on upper floors of buildings. Delicately suspended objects may swing.

III. Felt quite noticeably indoors, especially on upper floors of buildings, but many people do not recognize it as an earthquake. Standing motor cars may rock slightly. Vibration like passing of truck. Duration estimated.

IV. During the day felt indoors by many, outdoors by few. At night some awakened. Dishes, windows, doors disturbed; walls made cracking sound. Sensation like heavy truck striking building. Standing motor cars rocked noticeably.

V. Felt by nearly everyone; many awakened. Some dishes, windows, etc., broken; a few instances of cracked plaster; unstable objects overturned. Disturbance of trees, poles and other tall objects sometimes noticed. Pendulum clocks may stop.

VI. Felt by all; many frightened and run outdoors. Some heavy furniture moved; a few instances of fallen plaster or damaged chimneys. Damage slight.

VII. Everybody runs outdoors. Damage negligible in buildings of good design and construction; slight to moderate in well-built ordinary structures; considerable in poorly built or badly designed structures; some chimneys broken. Noticed by persons driving motor cars.

VIII. Damage slight in specially designed structures; considerable in ordinary substantial buildings with partial collapse; great in poorly built structures. Panel walls thrown out of frame structures. Fall of chimneys, factory stacks, columns, monuments, walls. Heavy furniture overturned. Sand and mud ejected in small amounts. Changes in well water. Disturbed persons driving motor cars.

IX. Damage considerable in specially designed structures; well-designed frame structures thrown out of plumb; great in substantial buildings, with partial collapse. Buildings shifted off foundations. Ground cracked conspicuously, underground pipes broken.

X. Some well-built wooden structures destroyed; most masonry and frame structures destroyed with foundations; ground badly cracked. Rails bent. Landslides considerable from river banks and steep slopes. Shifted sand and mud. Water splashed (slopped) over banks.

XI. Few, if any (masonry), structures remain standing. Bridges destroyed. Broad fissures in ground. Underground pipe lines completely out of service. Earth slumps and land slips in soft ground. Rails bent greatly.

XII. Damage total. Waves seen on ground surfaces. Lines of sight and level distorted. Objects thrown upward into the air.